THE INFLUENCE OF LOADING AND VOLTAGE SUPPLY CONDITIONS LV FEEDER ON HARMONIC EMISSION

BY

BANDAR S ALSHARIF

A Thesis Presented to the
DEANSHIP OF GRADUATE STUDIES

KING FAHD UNIVERSITY OF PETROLEUM & MINERALS

DHAHRAN, SAUDI ARABIA

In Partial Fulfillment of the
Requirements for the Degree of

MASTER OF SCIENCE

In

ELECTRICAL ENGINEERING

May 2016

KING FAHD UNIVERSITY OF PETROLEUM & MINERALS

DHAHRAN- 31261, SAUDI ARABIA

DEANSHIP OF GRADUATE STUDIES

This thesis, written by **Bandar S Alsharif** under the direction his thesis advisor and approved by his thesis committee, has been presented and accepted by the Dean of Graduate Studies, in partial fulfillment of the requirements for the degree of **MASTER OF SCIENCE IN ELECTRICAL ENGINEERING.**

Dr. Ibrahim M. El-Amin
(Advisor)

24/1/2017

Dr. Ali Ahmad Al-Shaikhi
Department Chairman

Dr. Ibrahim O.Habiballah
(Member)

Dr. Salam A. Zummo
Dean of Graduate Studies

Dr. Mohammed M. Al-Muhaini
(Member)

26/1/17

Date

Dedication

This thesis is dedicated to my beloved parents

My Brothers and Sisters

And

My Teachers

ACKNOWLEDGMENTS

Firstly, my comprehensive thanks are extended to ALLAH who is great and also most preferred in helping me reaching this educational stage in my life. My thanks are also to my great family and faithful friends and who encouraged me during all stages of my educational progress. I want also thank my advisor Dr. Ibrahim El-Amin for his great and continuous supports and help during all thesis stages, including both practical and theoretical parts. My thanks are also extended for everyone supported me through this research and for those who sincerely believed that gaining knowledge is right for everyone.

TABLE OF CONTENTS

ACKNOWLEDGMENTS V

TABLE OF CONTENTS VI

LIST OF TABLES VIII

LIST OF FIGURES IX

LIST OF ABBREVIATIONS XI

ABSTRACT (ENGLISH) XII

ABSTRACT (ARABIC) XIII
OC473206990
\H XIII

CHAPTER 1 INTRODUCTION 1
1.1 Background 1
1.2 Problem Statement 2
1.3 Thesis Motivation 3
1.4 Thesis Objectives 4
1.5 Thesis Methodology 4

CHAPTER 2 LITERATURE REVIEW 8
2.1 Overview 8
2.2 Harmonics 9
2.2.1 Total Harmonic Distortion 11
2.2.2 Types of Harmonics 13
2.2.3 Causes and Effects of Harmonics 15
2.2.4 Harmonic Reduction Techniques 15
2.3 Harmonics Distortions in Power Distribution Systems 18
2.4 The Impact of Harmonics on Power Quality 21
2.4.1 Effect of Loading on the THD 22
2.4.2 Suggested Methods to Reduce Harmonics 24
2.4.3 Harmonic Cancelation 25
2.5 Standards for Harmonics 27
2.6 Summary 29

CHAPTER 3 EFFECT OF LOAD VARYING AND SEQUENCE CHANGE ON THD VALUE 30
3.1 Simulation Results 30

3.1.1 Load Varying 30
3.1.2 Verification of Harmonic Cancelation 41
3.1.3 Sequence Change 43
3.1.4 Effect of changing in Firing Angle on THD for Control Rectifier Load. 52

CHAPTER 4 POWER QUALITY IMPROVEMENT USING SHUNT ACTIVE POWER FILTER (SAPF) 53

4.1 The Module of SAPF 53
4.2 Generation of the Reference Current Algorithm 57
4.2.1 Instantaneous Active and Reactive Power p–q Theory 57
4.3 Control Method of VSI 60
4.3.1 Hysteresis Control Method 60
4.4 DC Bus Voltage Regulation 61
4.5 Design of SAPF parameter 63
4.5.1 The DC link capacitor 63
4.5.2 The AC link reactor 63
4.6 Simulation results 64
4.6.1 Case I: Static Three Phase Diode Rectifier R Load without SAPF. 67
4.6.2 Case II: Static Three Phase Diode Rectifier R Load with SAPF. 71

CHAPTER 5 LABORATORY IMPLEMENTATION, RESULTS AND ANALYSIS ..77

5.1 Components and Devices 77
5.1.1 DC Drive 77
5.1.2 DC Motors 78
5.1.3 Active Filters 78
5.1.4 PQF Link Software and Oscilloscope 80
5.2 Experimental Setup 80
5.3 Experimental Results 81
5.3.1 Original Voltage from Utility without AF 82
5.3.2 Original Voltage from Utility with AF 83
5.3.3 Effect of Electrical Loading on THD 85
5.3.4 Effect of Varying the Firing Angle 87

CHAPTER 6 CONCLUSION AND FUTURE WORKS 89

6.1 Conclusion 89
6.2 Future Work 90

REFERENCES 92

APPENDIX A SYSTEM CONFIGURATION 101

APPENDIX B DATA OF FOUR MODULES OF LOAD 102

VITAE 106

LIST OF TABLES

Table 2.1 IEEE Standard 519-1992 Recommended Harmonic Voltage Limits for Power Producers ... 28
Table 3.1 THD Analyses for Single Unit of Arc, VFD, Diode Rectifier and Controlled Rectifier Load ... 40
Table 3.2 THD Analyses for Arc, Diode Rectifier and Controlled Rectifier Load at 25% and 50% of Transformer Capacity ... 41
Table 3.3 THD Analyses for Mixed Loads Case ... 42
Table 3.4 THD Analysis for Diode Rectifier with VFD (PWM/SVPWM) ... 42
Table 3.5 THD Analyses for Case 1, 2 and 3 of Sequence Change. ... 51
Table 3.6 THD Analyses Firing Angle Change ... 52
Table 4.1 Parameter of the System used ... 67
Table 4.2 Comparison between THD of System Parameters With SAPF and Without SAPF ... 76
Table 5.1 Characteristics of DC Drive ... 78
Table 5.2 Characterstics of DC motor ... 78
Table 5.3 Characteristics of Active Filter ... 79
Table 5.4 THD Results While Varying the Load With and Without AF ... 87
Table 5.5 THD While Varying the Thyristor Firing Angle ... 88

LIST OF FIGURES

Figure 2.1 Harmonic Distortion 10
Figure 3.1 Construction of the System 31
Figure 3.2 Subsystem of Load Block 31
Figure 3.3 System Waveform Responses for Arc Load (a) Source Current (b) Source Voltage (c) Load Current (d) Load Voltage 32
Figure 3.4 THD and Spectrum Analyses for Arc Load (a) Source Current (b) Source Voltage (c) Load Current (d) Load Voltage 33
Figure 3.5 System Waveform Responses for Diode Rectifier Load (a) Source Current (b) Source Voltage (c) Load Current (d) Load Voltage 34
Figure 3.6 THD and Spectrum Analyses for Diode Rectifier Load (a) Source Current (b) Source Voltage (c) Load Current (d) Load Voltage 35
Figure 3.7 System Waveform Responses for Controlled Rectifier Load (a) Source Current (b) Source Voltage (c) Load Current (d) Load Voltage 36
Figure 3.8 THD and Spectrum Analyses for Controlled Rectifier Load (a) Source Current (b) Source Voltage (c) Load Current (d) Load Voltage 37
Figure 3.9 System Waveform Responses for VFD Load (a) Source Current (b) Source Voltage (c) Load Current (d) Load Voltage 38
Figure 3.10 THD and Spectrum Analyses for VFD Load (a) Source Current (b) Source Voltage (c) Load Current (d) Load Voltage 39
Figure 3.11 System Analyses for Linear Load (a) Source Current (b) Source Voltage (c) Load Current (d) Load Voltage 43
Figure 3.12 THD Analyses for Linear Load (a) Source Current (b) Source Voltage (c) Load Current (d) Load Voltage 44
Figure 3.13 System Analyses for Linear and VFD Loads (a) Source Current (b) Source Voltage (c) Load Current (d) Load Voltage 45
Figure 3.14 THD Analyses for Linear and VFD Loads (a) Source Current (b) Source Voltage (c) Load Current (d) Load Voltage 46
Figure 3.15 System Analyses for Linear, VFD and Diode Rectifier Loads (a) Source Current (b) Source Voltage (c) Load Current (d) Load Voltage 47
Figure 3.16 THD Analyses for Linear, VFD and Diode Rectifier Loads (a) Source Current (b) Source Voltage (c) Load Current (d) Load Voltage 48
Figure 3.17 System Analyses for Linear, VFD, Controlled Rectifier and Diode Rectifier Loads (a) Source Current (b) Source Voltage (c) Load Current (d) Load Voltage 49
Figure 3.18 THD Analyses for Linear, VFD, Controlled Rectifier and Diode Rectifier Loads (a) Source Current (b) Source Voltage (c) Load Current (d) Load Voltage 50

Figure 4.1 Single Line Diagram of SAPF 54
Figure 4.2 Construction of Three Phase SAPF 54
Figure 4.3 Block Diagram of Instantaneous Active and Reactive Power Theory for SAPF 59
Figure 4.4 Calculation of Fundamental Active Power using Low Pass Filter 60
Figure 4.5 the Hysteresis Current Controller 61
Figure 4.6 The DC Bus Voltage Control Loop 62
Figure 4.7 Detailed Module of SAPF 64
Figure 4.8 Subsystem of Non-Linear Load 65
Figure 4.9 Subsystem of SAPF 65
Figure 4.10 Calculation of Reference Current 66
Figure 4.11 Determinations of Gate Signals 66
Figure 4.12 Source Voltage Waveform of the System in Case of Without SAPF 67
Figure 4.13 Source Current Waveform of the System in Case of Without SAPF 68
Figure 4.14 Load Voltage Waveform of the System in Case of Without SAPF 68
Figure 4.15 Load Current Waveform of the System in Case of Without SAPF 69
Figure 4.16 THD and Spectrum Analysis for Source Voltage in Case of Without APF 69
Figure 4.17 THD and Spectrum Analysis for Source Current in Case of Without SAPF 70
Figure 4.18 THD and Spectrum Analysis for Load Voltage in Case of Without SAPF 70
Figure 4.19 THD and Spectrum Analysis for Load Current in Case of Without SAPF 70
Figure 4.20 Source Voltage Waveform of the System in Case of With SAPF 71
Figure 4.21 Source Current Waveform of the System in Case of With SAPF 72
Figure 4.22 Load Voltage Waveform of the System in Case of With SAPF 72
Figure 4.23 Load Current Waveform of the System in Case of With SAPF 73
Figure 4.24 Active Power Filter Current Waveform of the System in Case of With SAPF 73
Figure 4.25 DC Voltage Waveform of the System 74
Figure 4.26 Reference Current Waveform of The System in Case of With SAPF 74
Figure 4.27 THD and Spectrum Analysis of Source Voltage in Case of With SAPF 75
Figure 4.28 THD and Spectrum Analysis of Source Current in Case of With SAPF 75
Figure 4.29 THD and Spectrum Analysis of Load Voltage in Case of With SAPF 75
Figure 4.30 THD and Spectrum Analysis of Load Current In Case of With SAPF 76
Figure 5.1 Experimental Setup Connections 80
Figure 5.2 Experimental Equipment used 81
Figure 5.3 Original Voltage Obtained Form Utility before Connecting AF 82
Figure 5.4 Harmonic Spectrums Before Connecting the AF. 83
Figure 5.5 Original Voltage Obtained from Utility after Connecting AF 84
Figure 5.6 Harmonic Spectrum Values After Connecting AF. 84
Figure 5.7 Result of 1.5A Load without AF 85
Figure 5.8 Results of 1.5A Load With AF. 86

LIST OF ABBREVIATIONS

CFL	:	Compact Fluorescent Lamp
DFT	:	Discrete Fourier Transform
FFT	:	Fast Fourier Transform
HCC	:	Hystersis Current control
IEC	:	International Electrotechnical Commission
IEEE	:	Institute of Electrical and Electronics Engineers
LV	:	Low Voltage
MV	:	Medium Voltage
RMS	:	Root Mean Square
PCC	:	Point of Common Coupling
PDS	:	Power Distribution system
PWM	:	Pulse Width Modulation
SAPF	:	Shunt Active Power Filter
SMPS	:	Switch-Mode Power Supply
SVPWM	:	Space Vector Pulse Width Modulation
TDD	:	Total Demand Distortion
THD	:	Total Harmonic Distortion
VFD	:	Variable Frequency Drive
VSI	:	Voltage Source Inverter

ABSTRACT

Full Name	:	[Bandar Suliman Alsharif]
Thesis Title	:	[The Influence of Loading and Voltage Supply Conditions LV Feeder on Harmonic Emission]
Major Field	:	[Electrical Engineering]
Date of Degree	:	[May 2016]

Power Distribution Systems have a great and critical importance in our life due to their applicability in daily life. One essential concern is how to ensure the best achievable performance for these systems in order to provide the users with the acceptable level of service quality. These systems suffer from common phenomena known as harmonic distortion, which in turns badly affects system efficiency. It also causes faults, reduction in the system service life, increases in system loss, reduction in the power factor and effectiveness of the electric consumption use, and increase in the economic loss.

The aim of this thesis is to investigate the effect of electrical loading for different types of loads on the total harmonic distortion along a low voltage feeder. The module of the power distribution system was simulated using the MATLAB/SIMULINK program. An Active Filter was implemented in order to reduce the harmonic effect. Different cases and conditions were considered and investigated. Laboratory experiments were also performed in order to estimate the real performance. They also showed that increasing the non-linear loads change the level of THD but the new level depends on load module type. The effectiveness of the proposed active filter module in reducing the harmonics was also confirmed on one type of load.

ملخص الرسالة

الاسم الكامل : بندر سليمان الشريف

عنوان الرسالة : تقيم أثر الأحمال الكهربائية على التوافقيات في مغذيات الفولتية المنخفضة

التخصص : هندسة كهربائية

تاريخ الدرجة العلمية : مايو 2016

أنظمة التوزيع الكهربائي لها تأثير مهم في حياتنا بسبب تطبيقاتها اليومية. ومن الامور المهمة في الانظمة الكهربائية الحصول على أفضل مستوى من الاداء لهذه الأنظمة في سبيل تقديم خدمة ذات جودة للمستخدمين. بيد أن هذه الأنظمة قد تكون عرضة لمجموعة من الظواهر ذات التأثيرات السيئة على أدائها مثل التوافقيات والتي تؤدي الى فشل المنظومة أو تقليل العمر التشغيلي لها، أو زيادة الضياعات الكهربائية، أو تقليل معامل القدرة، وبالتالي زيادة الخسائر المالية.

إن الهدف من هذه الرسالة هو بحث أثر الأحمال الكهربائية لأنواع مختلفه من الأحمال على التوافقيات في مغذيات الفولتية المنخفضة. تم تمثيل نموذج التوزيع الكهربائي باستخدام برنامج MATLAB/SIMULINK. كما تم تطبيق مرشح نشط لتقليل تأثير التوافقيات. وتم دراسة وبحث مجموعة مختلفة من الحالات. كذلك تم الاستعانة بالتجارب العملية في المختبر لتقيم الأداء العملي للنظام. أظهرت الدراسة أن تاثر زيادة الأحمال غير الخطية سوف يؤثر على مستوى تشوه الموجه الكهربائية، ولكن المستوى الجديد سوف يعتمد على طبيعة الحمل ونوعه إما زيادة أو نقصاناً. وفي النهاية تم التأكد من فعالية المرشح النشط في تقليل هذه التوافقيات على نوع من الأحمال.

درجة الماجستير في العلوم

جامعة الملك فهد للبترول والمعادن

الظهران المملكة العربية السعودية

مايو 2016

CHAPTER 1
INTRODUCTION

1.1 Background

Ideally, a power distribution system must offer perfect sinusoidal waveform voltage for customers. In practice, this is difficult to achieve where there is always a difference among the actual and measured waveforms of both the current and voltage. This waveform distortion may result from faults, nonlinear load, switching and other factors. Nonlinear loads generate harmonics [1].

In practice, the increasing deployment of nonlinear loads negatively affects both the stability and reliability of power systems. Such loads draw nonlinear currents from power systems, where these currents distort the voltage waveform and have effects on the whole system [2]-[3]. Harmonics are defined as sinusoids that have frequencies equal to the fundamental power system frequency multiplied by an integer [4]. The harmonics propagate through distribution and transmission system. The increase in nonlinear loads results in high level of harmonics. The harmonics have a negative impact on quality of both voltage and current [1].

The distortion in the voltage waveform has a major effect on the equipment connected to the systems. Harmonics also cause a reduction in the efficiency of these systems and their equipment. This in turn causes faults, reduction in the system service life, increase in the system loss, reduction in the power factor and effectiveness of the electric consumption use and increase in the economic loss [2]-[5]. Therefore, efficient harmonic detection, measurement and cancellation methods must be proposed [4].

The main two solutions for the problem of these harmonics are decreasing the load's harmonic excitation, and adjusting the impedances of the network to shift, eliminate or damp the resonance. Particularly, there is no sufficient solution for the generation of harmonics by the aggregate load on feeders. These harmonics still have enough magnitude to produce resonance excitation. This problem increases mainly with the presence of highline impedances, as in distribution systems with low voltage and with adding shunt capacitors for the compensation of reactive power. Both the line inductance and shunt capacitors result in an increase in the harmonic voltages across specific range of frequencies. This problem is influenced by the variable loads nature [6]-[7].

1.2 Problem Statement

In practice, the continuing use of nonlinear loads in power distribution systems generates harmonic voltage distortion that causes harmonic pollution. This in turn causes various problems in these systems. These problems range from errors during the execution of protection equipment to physical damage in the loads and components of these systems. Therefore, these harmonics must be eliminated or at least minimized.

Generally, standard emission limits are defined for electrical equipment to ensure having low voltage distortion levels. These limits are defined based on conducting either measurements or simulations with considering harmonics in this equipment. Although conducting simulations using specific software programs is cheaper and easier than performing measurements and experiments, the design processes and parameters differ among networks. This in turn increases the need to perform numerous simulations. Another problem is that there is a need to find unknown parameters or ignore others.

1.3 Thesis Motivation

The main motivation of this work is the growing need for more investigation and analysis concerning the harmonic propagation and its impact on the design of distribution systems. This increases due to the continuous deployment and growth of nonlinear loads. Another motivation is the use of various electrical appliances in networks with low voltage. This affects both the level and amount of the produced harmonic pollution. Harmonic existence causes various problems in networks, such as damages in appliances and devices, capacitors destruction and insupportable voltage distortion levels.

There is a wide need to focus on issues concerning the levels of harmonic distortion in networks, because the increase in these levels results in various problems in network operations, as the decrease in the network electrical voltage quality and poor quality of power because of the harmonic distortions that decrease the lifetime of network elements. From the literature, it was observed that harmonic distortions have critical effects on the efficiency and performance of power distribution systems. Therefore, this research estimates and investigates the effect of electrical loading, and change of different connected load sequence on the harmonic distortion in a power distribution system and the efficiency of using an active filter to reduce such harmonic distortions.

1.4 Thesis Objectives

The main aim of this research is to investigate and estimate the electrical loading, change of sequence of connected loads, harmonic cancelation, and firing angle change of controlled rectifier effect on the harmonic emissions along the low voltage feeders. The following objectives must be met to achieve this aim:

- ✓ Implement a system module in power quality laboratory and simulation program.
- ✓ Perform various laboratory and simulation tests on the module for various operating modes to achieve a detailed understanding concerning the effect of loading for different type of load on harmonic emissions in the network
- ✓ Verify the outcomes from simulation part by using the laboratory equipment (DC drive, DC motor, mechanical load, measurement devices and active filter).
- ✓ Study how the harmonic emissions are affected along the Low Voltage feeders.
- ✓ Implement active filter that would lead to the minimization of the harmonic emissions effects on the low voltage networks for both laboratory and simulation part.

1.5 Thesis Methodology

This section presents the research methodology that was followed in simulating the Power Distribution System (PDS) in MATLAB/SIMULINK environment. Four main tasks are introduced and investigated.

Task one:

- Building MATLAB module for PDS.
- Building Arc, controlled rectifier, Variable Frequency Drive (VFD) and diode rectifier load MATLAB module.

Task two:

- Investigate the effect of electrical loading on THD for different load types.
- Investigate harmonic cancelation using the previous load modules during running different type of loads in the same time.
- Study the effect of sequence change of different connected loads on THD.
- Investigate the effect of firing angle change of controlled rectifier connected to a DC motor load on THD

Task three:

- Investigate the effectiveness of Active Filter in reducing the THD for a Diode rectifier load.

Task four:

- Build the laboratory prototype of DC drive and study the effect of loading and firing angle change on THD values.

Task five:

- Highlighting the main findings and recommendations.

1.6 Thesis Breakdown

To achieve the above objectives, the presented thesis is organized in six chapters in additions to the list of references and appendixes. The chapters are organized as follows:

- **Chapter One** is titled "Introduction." It demonstrates the main purposes, statement of problem, and contains some background information as well as introduces summary of each chapter.
- **Chapter Two** is titled "Literature Review." It includes a review concerning relevant published works. The review includes summaries of conducted methodologies, performed stages, obtained results, and limitations.
- **Chapter Three** is titled **"**Effect of Load Varying and Sequence Change on THD Value.**"** It presents the implemented system module with all the conducted simulations are explored in details
- **Chapter Four** is titled **"**Power Quality Improvement using Shunt Active Power Filter.**"** This chapter presents the implementation of SAPF for Diode rectifier connected load with a DC motor.
- **Chapter Five** is titled **"**Laboratory Implementation, Results and Analysis**".** In this chapter, the obtained results during laboratory experiments are illustrated, discussed and evaluated**.**
- **Chapter Six** is titled "Conclusion and Future Works." In this chapter, a summary about the work and the results are presented. The chapter also introduces recommendations that might be used in the studying and improvement of the

system and several of the upcoming enhancements that can be done in order to develop this thesis.

CHAPTER 2
LITERATURE REVIEW

This chapter offers a general overview concerning power distribution systems and the effect of nonlinear loads on their efficiency. Furthermore, it demonstrates some of the related works that focused on analyzing the impact of harmonics on these systems and their power quality, and shows some of the suggested solutions in this field. In addition, it reviews the most commonly applied standards for harmonics in power distribution systems.

2.1 Overview

Research works in the field of power distribution systems in the last two decades presented the importance of enhancing the power quality for both energy providers and electrical loads developers. The design of electrical loads must be based on their effects on the power quality. In practice, the optimization of voltage waveform through power distribution systems depends on defining the power system parameters, and both the location and performance of polluting loads based on designing loads with enhanced behavior [8].

The presence of nonlinear loads in power distribution systems is the main source of harmonic production. The recent improvements in power electronic technologies have resulted in an increase in the networks' scale. This in turn resulted in more harmonic pollution problems, mainly in networks that have low voltage distribution. The effect of harmonics on these networks can be divided into the following types; the impact on power equipment and the impact on electrical equipment [9, 10].

In power equipment, harmonics affect their parallel capacitors and cause damages in power cables. The source of harmonic resonance is considered a fixed current. The resonance conditions represent the combination between distributed capacitance and system components, such as transformer inductance. These conditions are mainly generated when motors and transformers of power systems are not fixed loading. [9, 10]

Harmonics can affect various electrical equipment and appliances, such as televisions, lamps, computers and converters. The effect is based on the harmonics in the voltage waveforms of the power supply. Therefore, suitable harmonic voltage limits must be offered. Harmonics result in power loss in both users' equipment and power distribution systems. In power systems, harmonics decreases the equipment and network efficiency and results in changing the distortion power among that equipment and the network. Therefore, these effects must be considered an investigated in any power distribution system [9, 10].

2.1.1 Harmonics

Recently, the increased use of nonlinear loads resulted in a rapid development in injected harmonic voltages and currents into power systems. Harmonics exist in numerous power systems due to the saturation of loads, as cables, switching mode power supplies and transformers [11].A harmonic is a sinusoidal current or voltage wave, where its frequency is a multiple of the fundamental frequency that is 50 or 60 Hz in a standard power system. It can be expressed as illustrated below, where h is an integer [12, 13].

The waveform of harmonic distortions in turn changes the sinusoid shape. It is mainly a combination of harmonics, regardless of the fundamental wave complexity level [11]. Harmonics can be expressed also as superimposed frequency periodic components on the fundamental frequency waveform. In practice, harmonics in power systems are mainly odd integer multiples of the fundamental power frequency. Thus, the odd orders are considered as the most common harmonics. On the other hand, signal components, which are not integer multiples of the fundamental frequency can be simply faced. These components in turn are known as “inter-harmonics”, which are mainly encountered during coping with non-periodic signals [14]. An example of harmonic distortion is shown in the Figure 2.1.

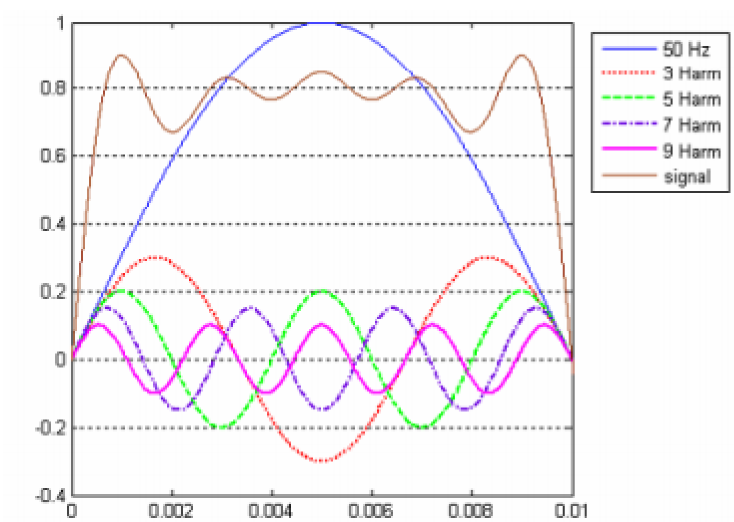

Figure 2.1 Harmonic Distortion

2.2.1 Total Harmonic Distortion

Modern PDS have a large number of power electronic convertors and other non-linear loads. Actually, the application and the development for IEEE-519 standards and guidelines increased the requests for designs of current and voltage waveform interfacing among the electric source and rectifier loads. All periodic waveforms can be represented via sinusoidal waveform summation at different multiples from the fundamental frequency of this waveform, as illustrated in the following equations

$$f(t) = \frac{a_0}{2} + \sum_{n=0}^{\infty} a_n \cos\left(n\pi \frac{t}{L}\right) + b_n \sin\left(n\pi \frac{t}{L}\right) \tag{2.2}$$

Where;

$$a_n = \frac{1}{L}\int_{-L}^{L} f(t) \cos\left(n\pi \frac{t}{L}\right) dt \tag{2.3}$$

$$b_n = \frac{1}{L}\int_{-L}^{L} f(t) \sin\left(n\pi \frac{t}{L}\right) dt \tag{2.4}$$

$f(t)$ Denotes the concerned function in time domain

n denotes the index of the harmonic

L referred to one cycle length measured in seconds.

Fourier transform for current or voltage waveforms can be calculated by major procedures. The first one is performed using the spectrum analyzer and the harmonics are then measured directly during online mode. The information corresponding to the phase angle cannot be provided by this method. The second method is performed by sampling the waveforms in time domain and then storing it in discrete form. Harmonic components are then computed digitally via microprocessor during off line mode. The waveform relative magnitudes would be reduced to suitable levels that are compatible with the used testing components. The harmonic phase and magnitude can be calculated using Discrete Fourier Transform (DFT) as shown in the following equation

$$F_n = \frac{1}{N}\sum_{k=0}^{N-1} f_k\, e^{-j2\pi kn/N} \tag{2.5}$$

Where;

F_n is defined as the fourier coefficient corresponds to the n^{th} harmonic.

f_k defined as the data point corresponds to the k^{th} sample.

N denotes the total samples number for each cycle.

n denotes the harmonic index.

k denotes the index of the data point.

Several indices are commonly employed for the purposes of analyzing the harmonics of the PDS. The most widely used is the Total Harmonic Distortion (THD). This index has two different available definitions in the literature; the first one is concerned with measuring the waveform harmonic content within fundamental component. The second one is concerned with measuring the waveform harmonic content in relation to the corresponding RMS value. The following two equations illustrate how the two types of THD can be calculated;

$$\mathrm{THD_F} = \sqrt{\frac{\sum_{n=2}^{\infty} I_n{}^2}{I_1{}^2}} \tag{2.6}$$

$$\mathrm{THD_R} = \sqrt{\frac{\sum_{n=2}^{\infty} I_n{}^2}{\sum_{n=1}^{\infty} I_n{}^2}} \tag{2.7}$$

I_n denotes the harmonics amplitudes or their RMS values.

Actually, THD_F results in more accurate measurement for the harmonics contents compared to THD_R. THD_R results large error when it is used with waveforms that contain high harmonics. Measurements in terms of the fundamental component are usually employed.

2.2.2 Types of Harmonics

There are two types of harmonics; namely odd and even harmonics. The dominant type in load current and supply voltage is the odd harmonics distortion. Its impact is mainly a 10 % decrease or increase of the signal amplitude. Such impact is the same for the positive and negative halves of the sine wave. When only odd harmonics exist in the voltage, the positive and negative voltage wave cycles are the same. Conversely, even harmonics distortion is usually small and results from large converters, transformer stimulating. It happens only when there is the presence of a DC component. Such distortion causes a difference among the positive and negative half cycles of the sine wave [14].

The two main deployed indices used to measure harmonic distortion in power systems are the Total Harmonic Distortion (THD) and Total Demand Distortion (TDD) [12, 14]. The THD represents the efficient value of the whole added voltage or current together in comparison with the fundamental current or voltage value. It can be computed using the following formula [15]:

$$THD_U = \frac{1}{U_I}\sqrt{\sum_{h=2}^{\infty} U_h^2} = \sqrt{\left(\frac{U_{rms}}{U_{Irms}}\right)^2 - 1} \tag{2.8}$$

Where:

THD_U	denotes the current or voltage THD
U_{Irms}	denotes the RMS fundamental current or voltage

In practice, the definition of THD may offer a misleading value for the level of harmonic distortion, since the fundamental voltage and current of a distribution system do not have a static magnitude all the time. This is mainly true for fundamental currents of a distribution system that are close to zero at specific periods of the day. This in turn causes a large value of current THD. Thus, the TDD is deployed, where it differs from the THD in that the calculation of TDD compares among the measured harmonics and the maximum demand current. In practice, the difference among the THD and TDD is essential since it keeps users from being wrongly penalized for harmonics in the periods of low loads. The TDD can be computed using the following formula [12]:

$$TDD_U = \frac{1}{U_{nom}}\sqrt{\sum_{h=2}^{\infty} \frac{1}{\sqrt{2}} U_h^2} \tag{2.9}$$

2.2.3 Causes and Effects of Harmonics

Generally, harmonics result from the presence of nonlinear loads. The main reason behind the low power quality is electronic device proliferation. The application of a sinusoidal voltage to a nonlinear electrical load does not represent a sinusoidal current. As well, there is no proportion among the current and applied voltage. The main reason for the non-sinusoidal current is the change in the device impedance over a voltage cycle. Such loads in turn can distort the supply voltage waveform [14].

Harmonic voltage distortion can appear in the supply voltage of a utility system from the injection of harmonic current into the utility supply system from customer loads. Such distortion can overheat the rotating equipment and raise the winding temperature of the transformer, where this in turn decreases both the life span and efficiency. Harmonics have critical impacts on protective device operation. As well, the presence of such distortion in a utility system causes problems in the equipment of customers [14]. Other effects of harmonics are tripping circuit breakers, failure of computers, generating false readings, and flickering electronic displays and lighting [16]. When the distortion level in a supply voltage reaches 10 %, a critical reduction occurs in the equipment service life [17]. The equipment service life reduction was estimated at 5 %, 18 % and 32.5 % for transformers, three-phase machines and single-phase machines, respectively [18]

2.2.4 Harmonic Reduction Techniques

In practice, there are various techniques that can be deployed to reduce harmonics. To ensure improving the power quality, filters must be used, on connecting them at the sensitive load terminals. Among various types of filters, the deployment of active filters can offer efficient harmonic reduction via the injected voltage, using series compensation and enhanced power quality [13]. The most common harmonic solutions are the drive and rectifier and solutions for commercial facilities. The drive and rectifier solutions have cheap current harmonics, available percent of impedance at various values, reduction in current and voltage harmonics with the use of source reactance, and less drop in voltage. Conversely, solutions for commercial facilities reduce both the phase and neutral currents [11]. The most common used techniques for harmonic reduction are the passive filters and active power filters.

Passive Filters

Passive filters are composed of various components, such as inductors, capacitors, and resistors. Such filters are simply used for a specific transfer function, where they get low impedance to nonlinear load current harmonics. Such harmonics flow to the lower impedance of those filters where they are finally trapped. The main benefit of passive filters is that they require less power supply as well as generating little noise in comparison with active gain elements [19]. The main types of passive filters are the notch and high pass filters. The first type is connected with the load in shunt to offer a substitute route to the harmonic current, while the second type is deployed to remove several harmonics from the system. Among high pass filters, the 2^{nd} order harmonic filters are the most deployed in the elimination of harmonic contents that are bigger than the cut-off frequency [20]

Active Power Filters

In active filters, op amps are deployed with capacitors and resistors. The main benefits of using active filters are their high input impedance, small output impedance and simple design when compared with passive filters. No inductors are included in active filters, which in turn assist in reducing harmonics [11]. The most efficient types of active filters are the Active Power Filters (APFs), which are power electronics that depend on devices injecting equal and opposite to the produced harmonic current by the nonlinear loads. Such filters are mainly deployed in three-phase systems due to their enhanced transient performances and their multiple compensation utilities [21] - [23]. As well, single-phase filters are widely proposed in the recent literature [24].

Active power filters have been deployed to reduce harmonics since 1970s. These filters inject the needed compensation current in the system, where this leads to minimizing the characteristic harmonics amplitudes in the supply current [25]. One of the most efficient active power filters is the shunt one, which is connected in parallel with loads. Such filters can be deployed with non-sinusoidal supply voltages, in which the voltages at the filter Point of Common Coupling (PCC) are harmonics-polluted and result from the presence of harmonic loads in the environment [26]-[30]. In practice, shunt active power filters are the best solution for reducing harmonics. The ratings of such filters are dependent on the RMS compensating current and terminal voltage of the filter [31] - [32]. In addition, these filters compensate for the harmonic currents resulting from the nonlinear load.

In recent years, various methods and investigations have been presented to study, analyze, mitigate and solve the problem of harmonics in power distribution systems. Some of those studies are reviewed in the following subsections.

2.3 Harmonics Distortions in Power Distribution Systems

In practice, harmonics that are present in distribution systems have major impacts on reducing the system efficiency, equipment functions and system lifetime, and raise both the system and economic loss. This increases the need for further research concerning those effects. Authors focused on studying the effect of harmonics on the energy of a power distribution system and how it could be saved based on analyzing the harmonic production mechanism in the system and investigating its impact on the power of a transformer, electric motor and power lines [5]. Results demonstrated that the energy consumption for the equipment is directly related to the rate of harmonic distortion. Thus, mitigating these harmonics can enhance the quality of power and offer several financial benefits.

Authors in [33] assessed the effect of harmonic distortion, which resulted from several nonlinear residential loads, on power distribution systems. A classic distribution system was simulated using experimentally designed harmonic spectrums for various home appliances. This was performed using the Transient Analyzer Program (ETAP). Results revealed the presence of high level of harmonic distortion, specifically at the system Point of Common Coupling (PCC) that becomes aggravated when considering a higher distribution transformer loading level.

Authors in [34] investigated the propagation of harmonic voltage and current in power systems and realized their effects on both the end user equipment and utility system components. As well, they proposed effective techniques via the application of phase shifting transformers. This was based on the concepts of combination and cancellation and the analysis of harmonic waveforms. They also presented alternatives for the mitigation of harmonic effects on the components of the systems with the use of harmonic filters. Results revealed that the use of phase shift and filter transformer reduced both the voltage and current distortion in the system while improving the transformer k-factor.

Authors studied the impact of various loads, resistive, inductive and capacitive, on the power distribution system based on computing the harmonic distortion in both input and output [35]. The work depends on using combinations between loads and various inductance values and fixed capacitance and resistance values, then recording the input and output voltages for these combinations with the use of the Gold wave program. The harmonic distortions were computed in the system input and output based on designing a computer signal processing algorithm in a voltage measurement stage in the system that has a current transformer. The computed voltages were then used in a controller, which was connected with a microcontroller to decide the power stabilization. An isolator circuit was used to stabilize voltage drop. The results demonstrated that the use of microcontroller in the system has major effects in decreasing the distortion in the system output.

Bhattacharyya and his colleagues [36] studied the pollution of harmonic current in a specific low voltage system. They demonstrated that the main source of this pollution was the daily used electrical equipment. This pollution in turn causes an increase in the voltage distortions in this system. The work in this research depended on investigating and detecting the harmonic current emissions in various devices to be compared using laboratory computations and available limits. This in turn offered general ideas concerning the emission levels of harmonic current in various installations of the presented system.

The authors investigated the effect of the continuous increase in harmonics of nonlinear loads on the level of feeder voltage distortion [37]. This was performed since many utilities do not control the level of harmonics in feeders. Furthermore, the available harmonic distortion levels are unidentified where this affects the capability of predicting harmonic distortions in feeders. The authors presented an analysis concerning the increased feeder level distortion depending on various clients who generate harmonic currents similar to standard threshold limits. Various tests were conducted to determine the relation among generated harmonic current by a client and the related harmonic impedance. With the use of a test feeder and the function of harmonic impedance, the current injection technique was used with clients to assess the aggregate clients' impacts with high harmonics of nonlinear loads. The results demonstrated utility companies must consider the generated harmonic distortion amount from the increased design of nonlinear devices. In addition, the voltage distortion amount is based on the impedance of systems.

Kaushik, and his colleagues investigated the produced voltage distortions by nonlinear loads taking into account the specifications of harmonics; and both the characteristic and non-characteristic harmonics [38]. Harmonic distortions have been computed in a power system using the Mi Power program. The work depends on establishing precise harmonic modules for these nonlinear loads. Furthermore, passive filters were implemented in two buses to reduce the impressed harmonic voltages on certain system parts. Results demonstrated that these filters effectively decreased the generated harmonics.

2.4 The Impact of Harmonics on Power Quality

In practice, harmonic distortions are the main reason behind the problems of power quality. These distortions result from nonlinear loads that have currents with non-sinusoidal harmonics, which in turn causes line voltage distortion. Particularly, the use of these loads increases daily by users, where this increases the creation of disturbances in equipment. These distortions also cause degradation in the power factor. Therefore, the precise estimation of power loss has an essential role in deciding the commercial and technical losses share in the whole loss. Various methods have been presented in previous works to approximate the power loss and effect of harmonics in distribution systems.

Iagar, A. and his colleagues studied the impact of various home appliance nonlinear devices on the power quality of distribution systems with a focus on investigating the impacts of the operating mode on the emissions of harmonics from these devices [39]. This was performed with the use of a three phase-power quality analyzer. Results demonstrated that nonlinear devices have major effects on reducing the power quality. In addition, these distortions depend on the operation mode of the system.

The authors studied the impact of harmonic distortion on both losses and power quality of distribution systems based on simulating a distribution feeder; 20 kV/400V [40]. The work was based on deciding the quantity of produced harmonics via nonlinear loads in three types of loads in feeders; office, commercial and residential. The nonlinear loads had been modeled with the use of their Norton equivalent. The Norton model and the modeling of the three types of loads depend on the bottom-up method. The impact of each nonlinear load on the feeder power quality was then studied. Results demonstrated that harmonic distortions raise the power losses by approximately 20% from the level without nonlinear loads.

The authors studied the impact of nonlinear loads on quality of power of the power distribution system in New Zealand [41]. The authors proposed that energy consumption can be reduced by removing large useless loads and deploying smaller effective loads. Nonlinear loads cause harmonics in power systems with around 5 % THD in New Zealand. But this percent can increase due to the replacement of large linear loads with small multiple nonlinear ones. The authors investigated the impacts of the increasing use of nonlinear loads on the power quality of the weak distribution system in New Zealand. Results demonstrated the major effect of those loads in reducing the quality of power. The work can be utilized in further investigations with laboratory measurements.

2.4.1 Effect of Loading on the THD

In the past, the majority of electrical equipment was based on using balance linear load, which is a component in power system distribution where the voltage and current are perfectly sinusoidal. On the other hand, the quick increase in the electronics device technology, such as Thyristors and diodes transformed such loads into nonlinear ones. Some of these loads are the inverters, switching mode power supplies and changeable frequency drives. Such nonlinear loads when connected to power system distributions, in turn produce voltage and current harmonics [11].

Resultant harmonics from nonlinear loads increase transmission losses, decrease the equipment efficiency, overheat conductors and transformers, cause malfunctions in the system, and threaten its stability and reliability. Nonlinear loads draw nonlinear current from the power system, and current flows through the system and distorts the voltage wave, which influences the whole system [2]-[3]. As well, they have either magnetic or electrical circuit nonlinear characteristics [42]. The relation among the current and voltage of a nonlinear load is expressed as follows:

$$I = K_1 + K_2V + K_3V^2 + K_4V^3 + \cdots \tag{2.10}$$

Where

k is a set of constant values different among nonlinear loads.

The effect of loads, which are combinations of capacitive, inductive and resistive, on the THD of IGBT-dependent voltage stabilization was investigated in [11]. Authors computed the harmonic distortion in both the system input and output voltages. They considered eight load combinations with fixed resistance (36 Ω), fixed capacitance (2.5 μF) and variable inductance in the range from 1.232 H to 269.1 mH. The Gold wave was used to record the input voltage, while the output one was recorded using digital signal processing program. Results revealed that the decrease in the impedance values changed in the inductance value from H to mH and increased the input and output THD value. As well, the leakage of the capacitive or inductive components caused some difference in the THD input and output values. It was also observed that the output harmonic distortion was less than that of the input.

Khandakji [43] investigated the impact of Voltage Source Inverter (VSI) -fed three phase induction motor loading on the line current THD. The author developed the line current THD curve versus the line current fundamental harmonic for various inverters. Results revealed that high order harmonics were generated in the line current due to the presence of under-loaded Variable Speed Drives (VSDs). This in turn increased the current THD to 100 % at no-load mode and reduced the power system quality. The author suggested the use of filters with modifiable parameters to reduce harmonics and the dependence of the line current THD on the driven motor and to improve both the power system quality and efficiency.

2.4.2 Suggested Methods to Reduce Harmonics

The authors suggested that harmonics can be eliminated from power distribution systems based on using AC filter equipment that has a high pass filter near the harmonics source to absorb its generated current [5]. Other solutions are enhancing and modifying the design of the interference source to avoid large interference, and preventing capacitors from amplifying the generated harmonics based on modifying their series reactor or its by-pass into a filter. Furthermore, limiting the input capacity and using equipment, as active filters to filter harmonics can also help in reducing the generated harmonics in power distribution systems.

The main suggested solutions to cancel harmonics in these systems are the use of active or passive harmonic filters in order to restrain the frequencies of the harmonics [44]. The active type depends on measuring the system harmonic currents and then producing opposite harmonics to remove them, while the passive type depends on filtering certain frequencies. Other solutions are using rectifiers that have high pulses, using AC line reactors with the input AC power lines to smooth the current flow, and using “Pulse Width Modulated” (PWM) rectifier to reduce the generated current distortion in the input.

2.4.3 Harmonic Cancelation

In practice, when a set of various nonlinear loads that operate together are connected to the same low voltage network, the resultant harmonics emission is lower than the summation of emitted harmonics by individual loads. This is called the harmonic cancellation effect. Such effect is a result of differences in electrical characteristics of a load, which is marked as the differences in the phase angles related to the same generated harmonics by various loads [45].

The Compact Fluorescent Lamps (CFLs) nonlinear load was investigated previously in several studies [46]-[47]. It was found that as individual CFLs generated by several manufacturers with various rated powers can feature changes in their electrical components, the harmonic cancelation can happen in a group of CLFs. Previous studies presented efficient levels of harmonic cancellation of nonlinear loads, such as power electronics [48]. However, the investigation of CFLs presented that a small cancellation level can happen [46].

Authors in [45] measured the harmonic cancellation levels in various CFLs groups based on applying an equivalent circuit modeling approach. A set of independent measurements was used to verify the approach accuracy. Results revealed that the harmonic cancellation level of the aggregate CFL load is relatively insensitive to the real composition of individual CFLs.

Another type of nonlinear loads is the Switch-Mode Power Supply (SMPS), which is widely used in recent power supply systems. Such loads cause nonlinear currents with systems, where this in turn is the source of harmonics. The emission of harmonics from individual SMPS loads differs depending on the difference among their circuits and operation conditions. Such variations allow the cancellation of harmonics in the same order because of the phase angle dispersion [49]. Authors in [49] introduced standard parameter values for various types of SMPS and investigated their impact on harmonic cancellation with the use of the Monte Carlo method. Results revealed that the harmonic cancellation among SMPS with high power is larger than that among SMPS with low power. Conversely, considering mixed-type aggregation among both types that connected to a network with low voltage, the effects of harmonic cancellation are stronger for the mixed-type aggregation than individual loads.

Authors in [50] investigated the harmonic cancellation amount when single-phase loads have different harmonic characteristics. The focus of the research was on the Scott transformer load. It is broadly deployed in electric railway systems with the presence of two unbalanced single-phase loads since it can decrease unbalanced currents. The conducted analysis demonstrated that such load was able to decrease the harmonic current for single-phase loads with different harmonic characteristics. The reduction in harmonic current happens by the harmonic cancellation of the single-phase loads included in the transformer windings. In addition, it was found that the cancellation degree is based on both the harmonic order and the load balance factor.

Authors in [51] presented a gainful harmonic cancellation approach to be used for Silicon Carbide MOSFET dependent single phase inverter with high frequency. Such method was able to eliminate harmonics with even-order at PWM stage in the control part contrasting the traditional even-order harmonic cancelation method used in power stage. In addition, this method is a cost effective one due to the switching of one leg at high frequency. As well, a regular sampling technique that depends on actual calculation was deployed confirm the proposed method viability on a 500W single-phase voltage source inverter. On the other hand, this method was compared with a classic inverter modulation one in terms of harmonic distortions and switching losses. Results revealed that such method was able to cancel even-order harmonics and offer more efficient THD figure in comparison with the other method, mainly at sampling frequencies.

2.5 Standards for Harmonics

The most commonly used standards for harmonics in power distribution systems are illustrated below.

- **IEEE 519-1992 Standard**

In practice, the IEEE 519 is considered as the main standard for harmonics as stated by the IEEE. Thus, various efforts and changes are being conducted on this standard [44]. The IEEE 519-1992 standard mainly determines the limits on the allowed harmonics amount at connection points in the grid [52]. These limits in turn ensure delivery of clean power for customers and saving electrical equipment from several problems, such as overheating, life loss due to high harmonic currents and voltage stress due to high harmonic voltages. In addition, these limits depend on the maximum loads of customer and the location on the power distribution system. There is a reviewed version which is IEEE STD 519^{TM} 2014 [53]. In this standard, the limits of voltage distortion are illustrated in table 2.1 [54]:

Table 2.1 IEEE Standard 519-1992 Recommended Harmonic Voltage Limits for Power Producers

Harmonic voltage distortion in % at PCC			
	2.3-68.9 kV	69-138 kV	>138 kV
Maximum for individual harmonic	3.0	1.5	1.0
Total harmonic distortion	5.0	2.5	1.5

- **IEC 61000-3-2 and IEC 61000-3-4 Standards**

Both the IEC 61000-3-2 and 3-4 standards specify the limits of harmonic current, which are injected to a supply system, below 16A and above 16A, respectively. Such standards determine the harmonic components limits of the input current generated by tested equipment [55].

Both standards assist in determining the required information to allow evaluating equipment based on the disturbance or harmonics and determining the capability of this equipment for connection, taking into account the harmonic distortion [6]

- **IEEE 1159-1995 Standard**

This standard addresses the main methods that can be used to measure the power quality. It also demonstrates the most common devices used for power quality measurement while demonstrating their significance for workers in various fields of power distribution, communication and processing. Furthermore, it covers the main techniques used to control the quality of power of various power systems, defines the terminology of power quality, demonstrates the effect of low power quality on equipment, and illustrates the electromagnetic phenomena measurement [7].

2.6 Summary

In summary, harmonics that are generated from nonlinear loads in power distribution systems have major effects on these systems. Some of these effects are decreasing the system operation efficiency, and decreasing the efficiency of the systems' equipment. Furthermore, harmonics can cause errors and faults in these systems, reduce their service life, decrease the power quality and power factor, decrease the electric on consumption use efficiency and cause economic loss. Various suggestions have been put forth to cancel or at least minimize these harmonics. It was demonstrated that the type of load model, conductors and transformers of the feeder have major effects on the generation of voltage distortion, thus they must be decided carefully.

Previous works focused on the impact of nonlinear loads in these systems and how they generate harmonics with suggesting some solutions. The current work focuses on studying the impact of loading, change of sequence of connected loads, and harmonic cancelation all along a low voltage feeder, on the emissions of harmonics.

CHAPTER 3

EFFECT OF LOAD VARYING AND SEQUENCE CHANGE ON THD VALUE

In this chapter the effect of change in load on the percentage existence of harmonic in the system and change in loads sequence is studied. As well as harmonic cancelation and firing angle changing effect on THD of load current and voltage is verified

3.1 Simulation Results

The simulation is divided into four main groups. The first one is for load varying (The data for the used loads are shown in Appendix B which are Arc load, diode rectifier, controlled rectifier and VFD load), where the load value is change to 25% and 50% of distributed transformer capacity. The second group is for change in sequence of the connected loads on the system. The third and fourth are harmonic cancelation and firing angle changing effect, respectively.

3.1.1 Load Varying

Figure 3.1 and Figure 3.2 show a system configuration of load varying consisting of 3 phase source voltage, medium voltage load, 2 feeders, step down transformer using MATLAB/SIMULINK. The data for the used system is shown in Appendix A.

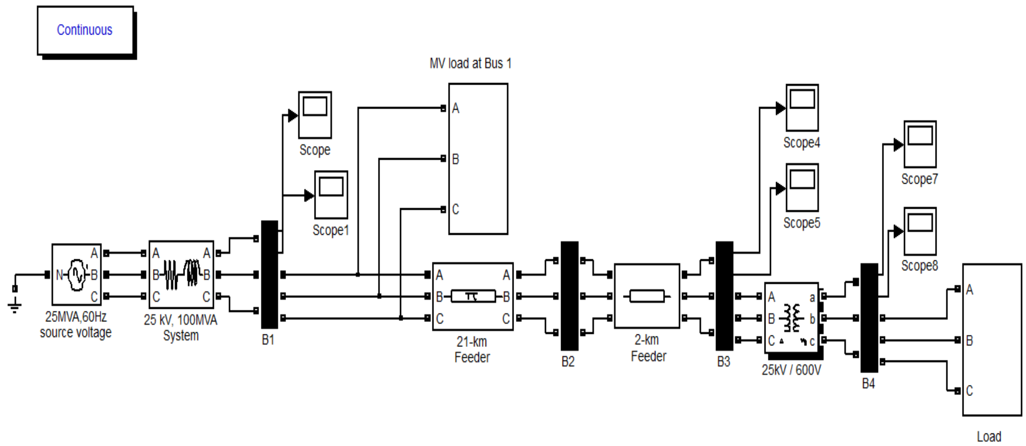

Figure 3.1 Construction of the System

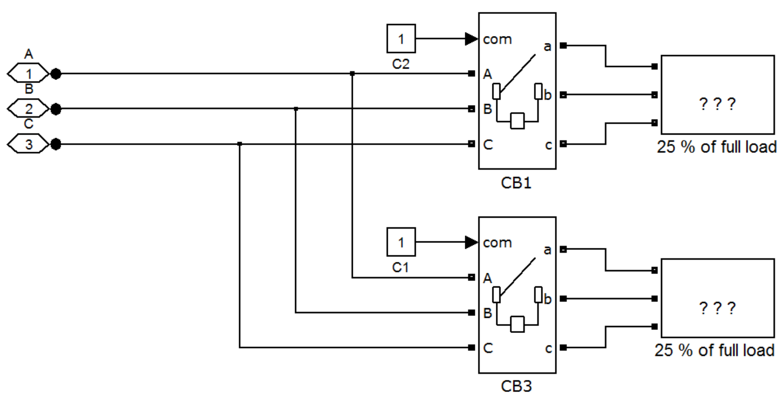

Figure 3.2 Subsystem of Load Block

Firstly, the system is loaded by Arc (Figure 3.3 and Figure 3.4), diode rectifier (Figure 3.5 and Figure 3.6), controlled rectifier (Figure 3.7 and Figure 3.8) and VFD load (Figure 3.9 and Figure 3.10). First figure of each load shows the waveform response and the second figure shows THD and spectrum of harmonic order. Moreover, the figures show all of voltage source, current source, voltage load and current load results. All the results are summarized in table 3.1 for each single unit of load type.

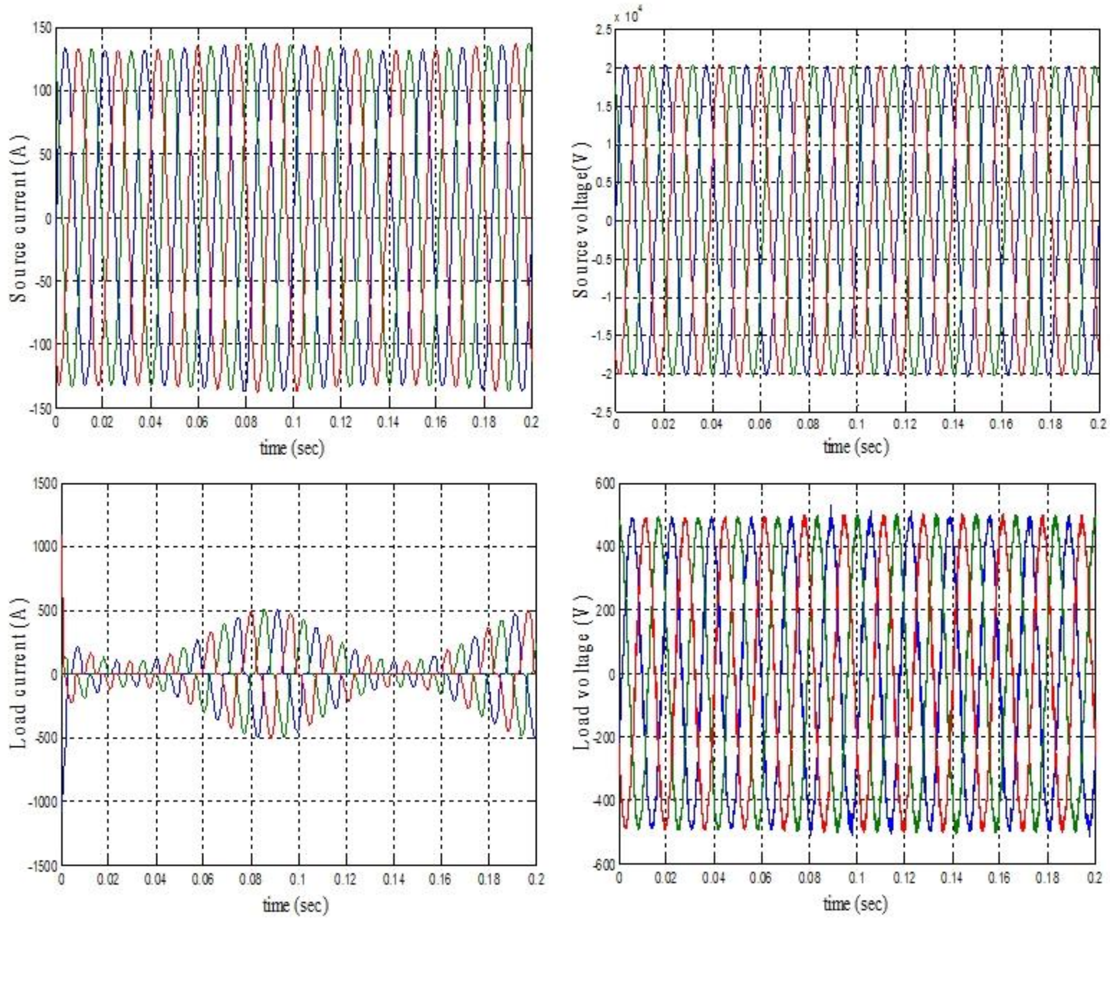

Figure 3.3 System Waveform Responses for Arc Load (a) Source Current (b) Source Voltage (c) Load Current (d) Load Voltage

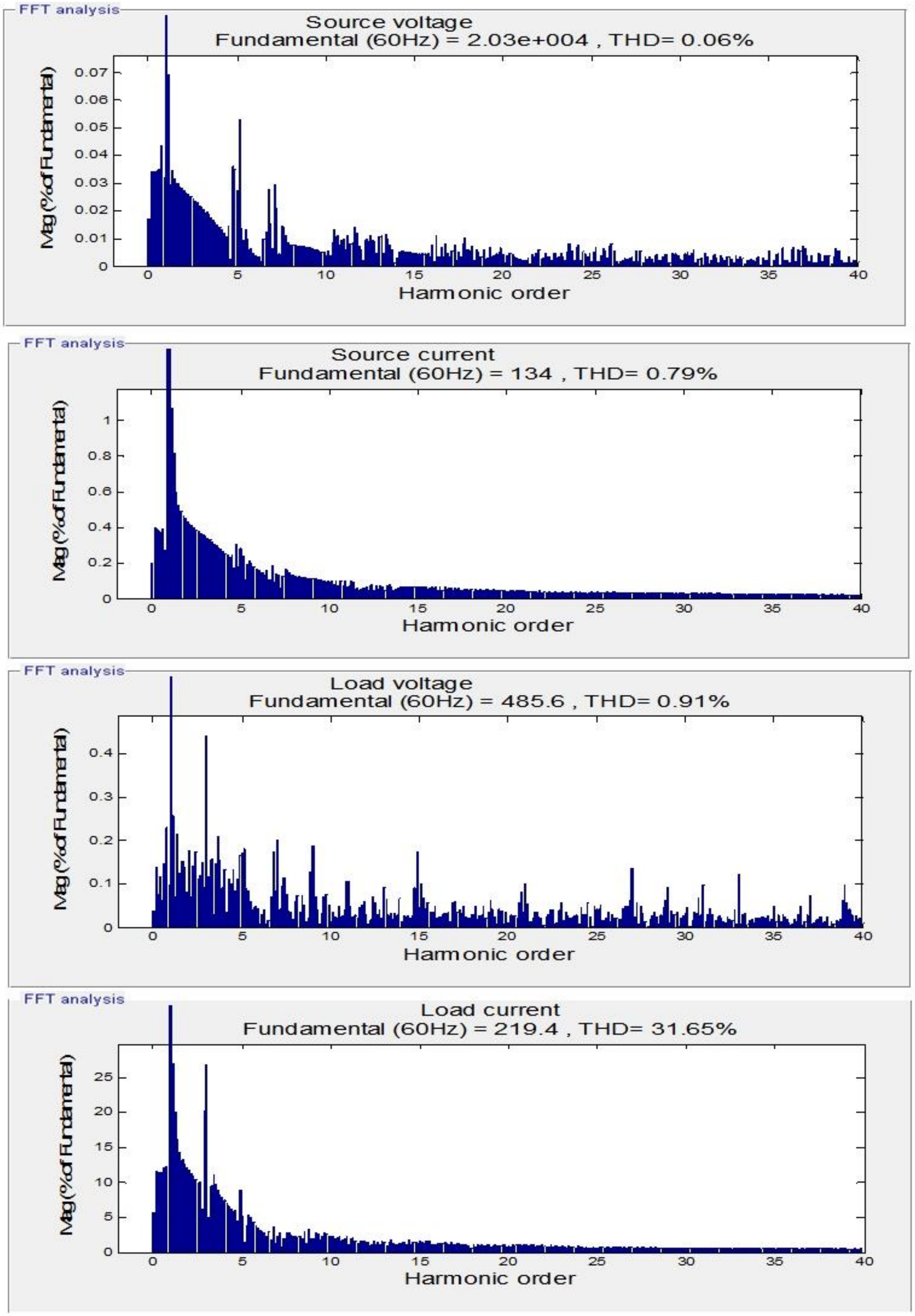

Figure 3.4 THD and Spectrum Analyses for Arc Load (a) Source Current (b) Source Voltage (c) Load Current (d) Load Voltage

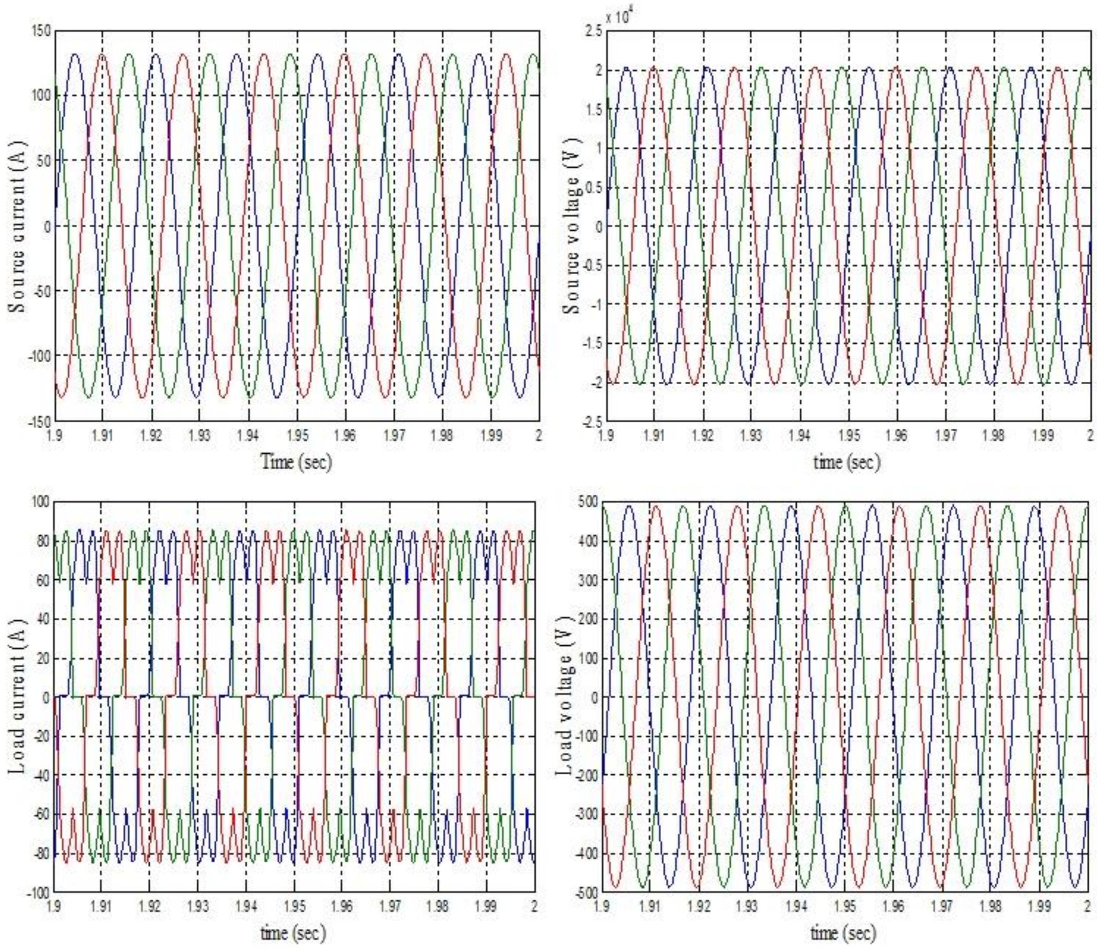

Figure 3.5 System Waveform Responses for Diode Rectifier Load (a) Source Current (b) Source Voltage (c) Load Current (d) Load Voltage

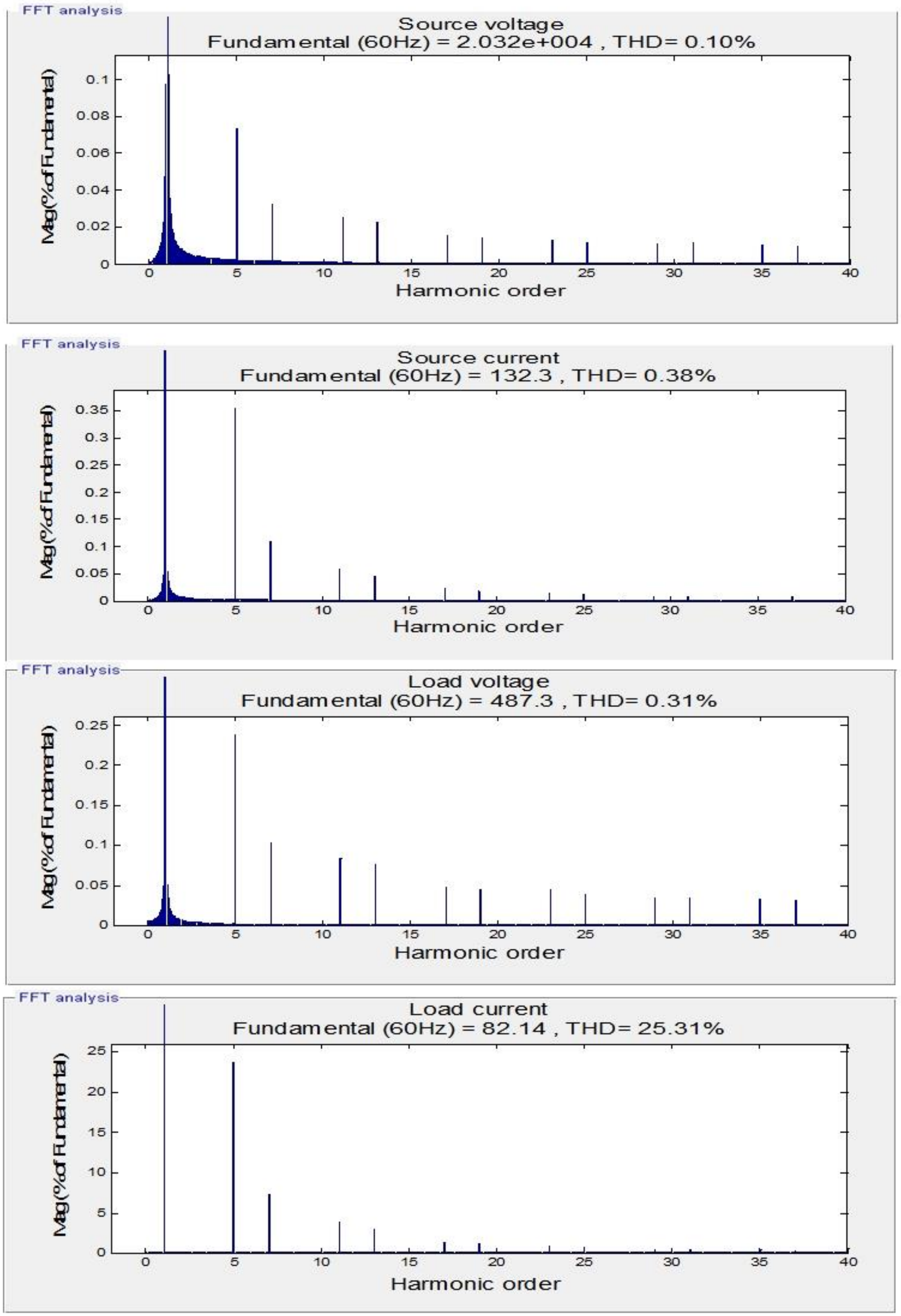

Figure 3.6 THD and Spectrum Analyses for Diode Rectifier Load (a) Source Current (b) Source Voltage (c) Load Current (d) Load Voltage

:

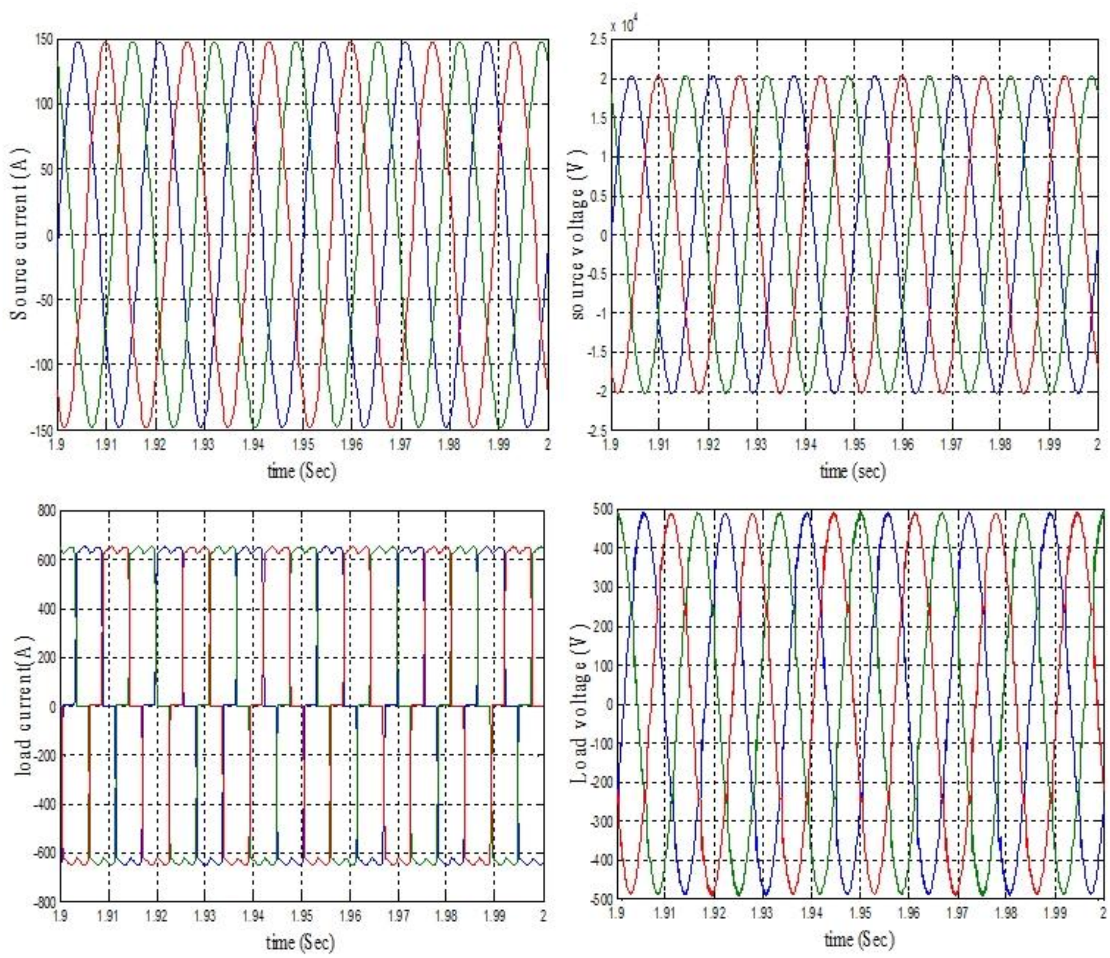

Figure 3.7 System Waveform Responses for Controlled Rectifier Load (a) Source Current (b) Source Voltage (c) Load Current (d) Load Voltage

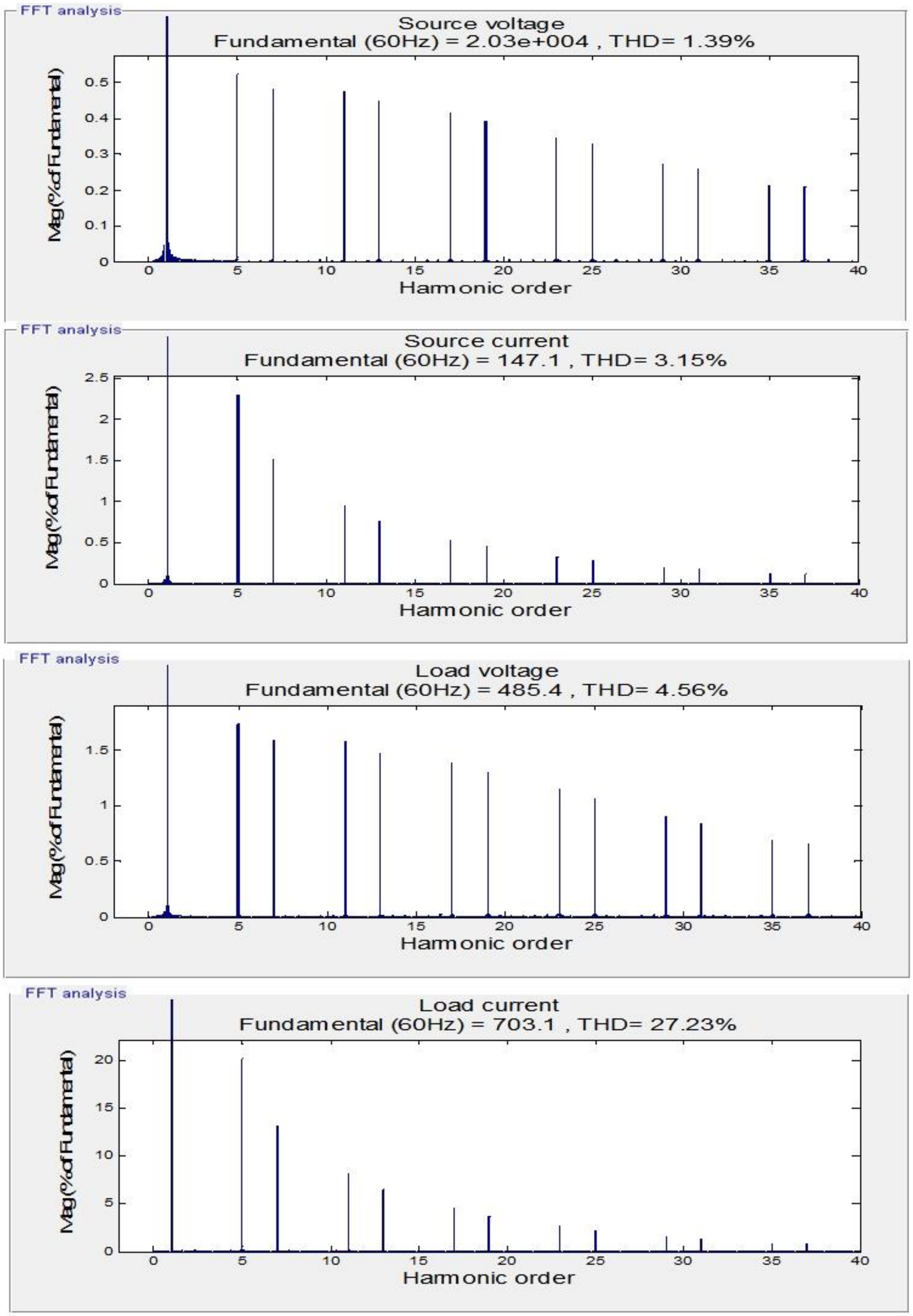

Figure 3.8 THD and Spectrum Analyses for Controlled Rectifier Load (a) Source Current (b) Source Voltage (c) Load Current (d) Load Voltage

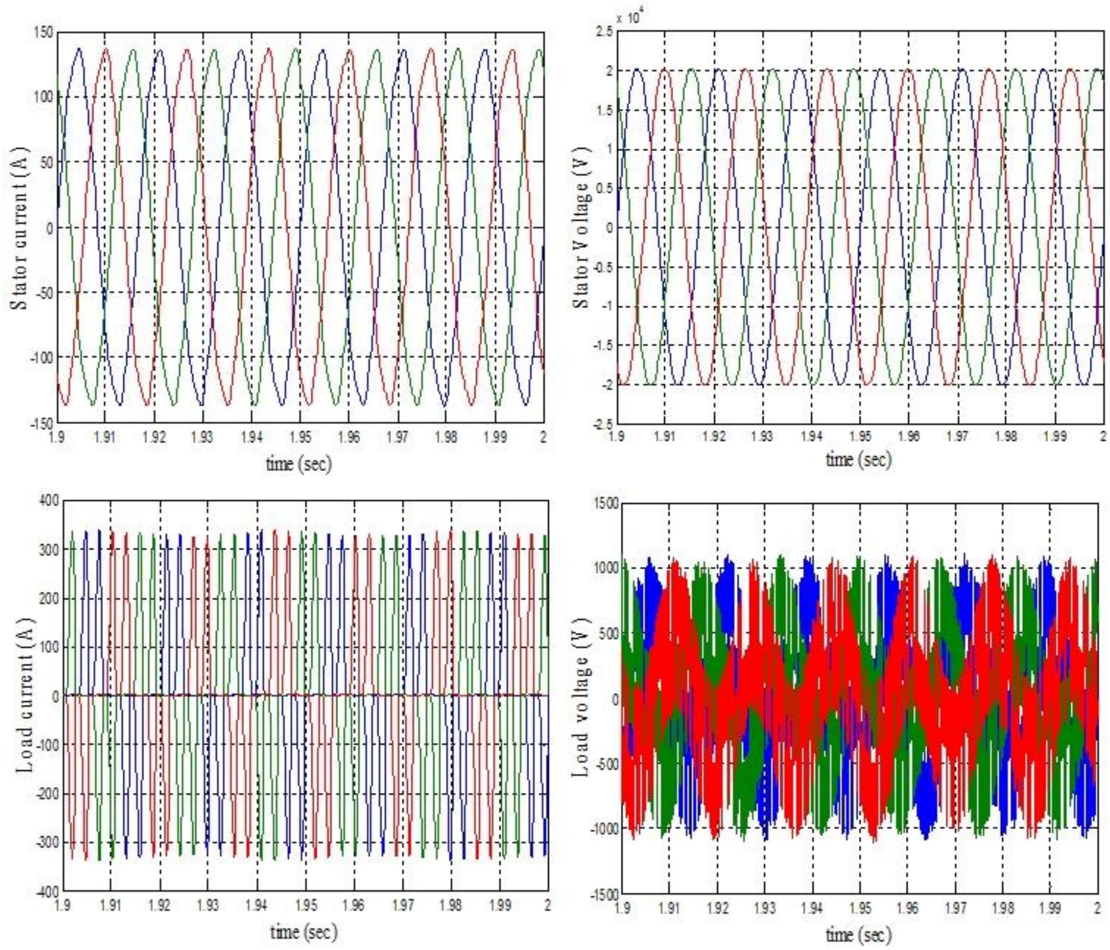

Figure 3.9 System Waveform Responses for VFD Load (a) Source Current (b) Source Voltage (c) Load Current (d) Load Voltage

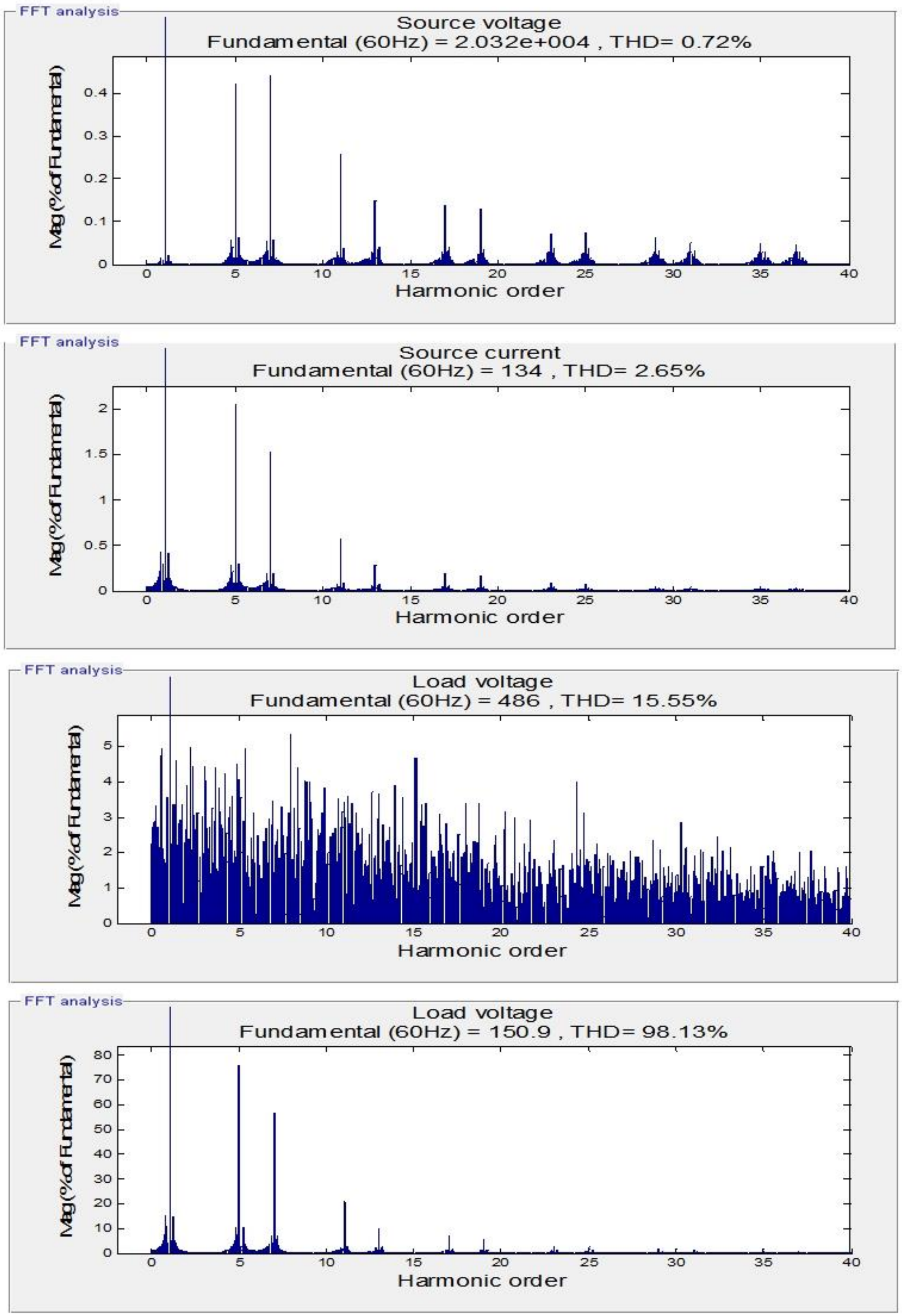

Figure 3.10 THD and Spectrum Analyses for VFD Load (a) Source Current (b) Source Voltage (c) Load Current (d) Load Voltage

Table 3.1 THD Analyses for Single Unit of Arc, VFD, Diode Rectifier and Controlled Rectifier Load

	ARC	VFD	Diode rectifier	Controlled rectifier
I_{Laod} THD %	31.65	98.13	27.23	25.31
N	Pu	Pu	Pu	pu
3	0.26	0	0	0
5	0.08	0.75	0.23	0.2
7	0.05	0.67	0.07	0.13
9	0.04	0	0	0
11	0.03	0.2	0.04	0.07
13	0.02	0.09	0.03	0.06
15	0.01	0	0	0
17	0	0.05	0.01	0.04
19	0	0.04	0.01	0.03
21	0	0	0	0

It is clear that the most effected load was VFD (98.13%) and the ARC (31.65%) comes after followed by uncontrolled (27.23%) and controlled rectifier (25.31%). Also, for VFD, controlled and uncontrolled rectifier the triple harmonic orders (third, ninth, fifteenth …) do not appear since they are three phase system.

Then the load is increased to 25 % of transformer capacity (6 MVA) and after that to 50% for the four types of load (the data of the used loads is shown in Appendix B). Table 3.2 shows the THD results using FFT MATLAB tools 25 % and 50 % loading .It is clearly seen that by increasing the loading for diode rectifier and controlled rectifier the THD in load current is decreased so it can be consider as harmonic cancelation. In contrast for Arc load the THD for load current is increased with loading increased. From these results, it is clear that the harmonic behavior during the loading depends on the module type of load.

Table 3.2 THD Analyses for Arc, Diode Rectifier and Controlled Rectifier Load at 25% and 50% of Transformer Capacity

	25% loading			50% loading		
	ARC	Diode rectifier	Controlled rectifier	ARC	Diode rectifier	Controlled rectifier
THD in load voltage	5.67	6.77	9.39	11.22	11.60	15.12
THD in load current	37.47	21.03	24.06	39.68	18.07	20.94

3.1.2 Verification of Harmonic Cancelation

In this section the harmonic cancelation is verified by connecting different loads in the same Bus and the individual THD and total THD is obtained and tabulated in Table 3.3. This table reveals that there a cancelation occurs when two or more different loads connected together. For instance, the THD values in case of run each alone of Arc and VFD loads are 31.6% and 98.13% respectively. When these two loads connected together the THD will be 46.12%. From Arc point view there is increase in THD but from VFD point view there is decrease from THD value. Since this is subjective, the next section will study and analyze the loading sequence effect on THD for different cases. Also, before writing about the loading sequence, the changing the module itself effects on THD for same type of load will be study. The gate pulse signal generation control strategy has been changed from PWM to SVPWM and sees what its impacts are in table 3.4.

Table 3.3 THD Analyses for Mixed Loads Case

Harmonic order	Arc	VFD	Controlled rectifier	Diode rectifier	Arc/ Controlled rectifier	Controlled rectifier /Diode rectifier	Diode rectifier/ VFD	Arc/ VFD	Arc/VFD/ Controlled rectifier
I_{Load}THD %	31.6	98.13	25.31	27.23	27	24.81	69.65	46.12	40.48
N									
3	0.26	0	0	0	0.77	0	0	0.2	0.16
5	0.08	0.75	0.2	0.23	0.17	0.18	0.55	0.31	0.29
7	0.05	0.67	0.13	0.07	0.1	0.13	0.37	0.24	0.18
9	0.04	0	0	0	0.01	0	0	0	0
11	0.03	0.2	0.07	0.04	0.05	0.07	0.16	0.1	0.08
13	0.02	0.09	0.06	0.03	0.04	0.05	0.05	0.05	0.03
15	0.01	0	0	0	0	0	0	0	0
17	0	0.05	0.04	0.01	0.01	0.04	0.06	0.04	0.04
19	0	0.04	0.03	0.01	0.01	0.03	0.03	0.03	0.02
21	0	0	0	0	0	0	0	0	0

Table 3.4 THD Analysis for Diode Rectifier with VFD (PWM/SVPWM)

Harmonic order	Diode rectifier	VFD (PWM)	VFD (SVPWM)	Diode rectifier/ VFD (PWM)	Diode rectifier/ VFD (SVPWM)
I_{Load}THD %	27.23	98.13	103.03	69.65	69.57

It can be seen in table 3.4 that changing the module from the same load will not affect too much. The THD has been changed from 69.65% to 69.57%.

3.1.3 Sequence Change

In this section, the sequence of loading is changed according to Table 3.4 and the THD of system voltage and current is measured. Figure 3.11 to Figure 3.18 show the performance of the system for case one of sequence change. The system is loaded with a linear load, then VFD load, after that diode rectifier load, and finally with controlled rectifier. In each time of loading the THD of system voltages and current is measured and tabulated in Table 3.4.

Case 1: Linear, VFD, Diode Rectifier and Controlled Rectifier Load.

Step 1: Linear Load

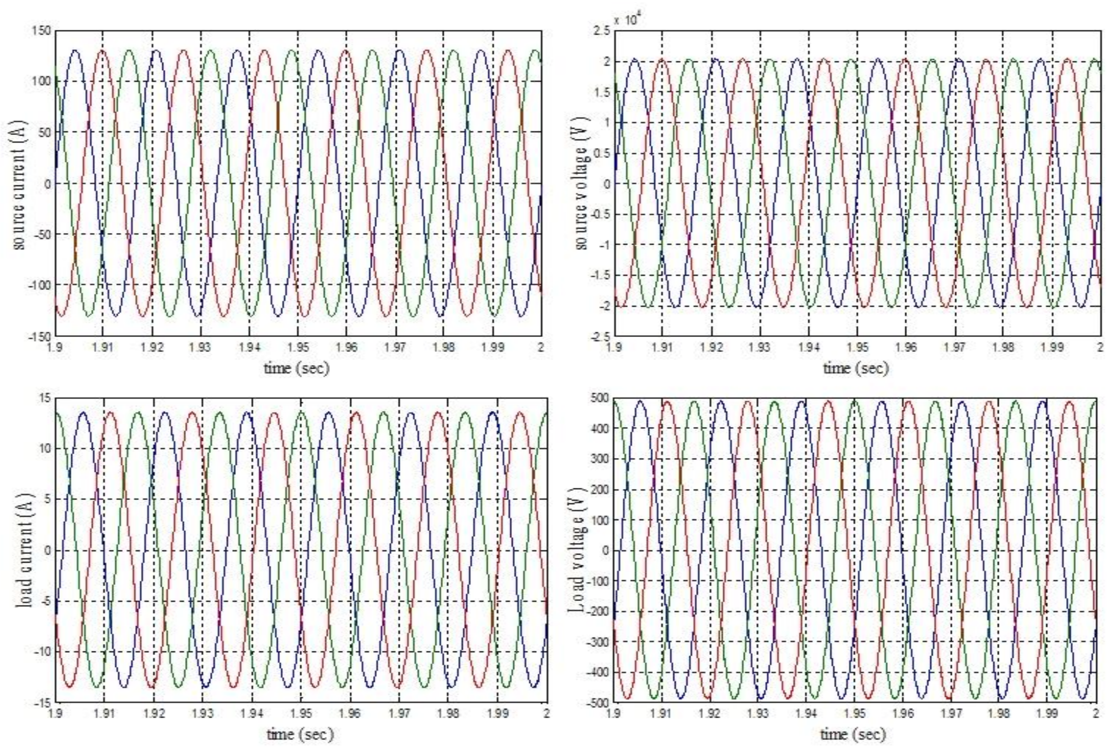

Figure 3.11 System Analyses for Linear Load (a) Source Current (b) Source Voltage (c) Load Current (d) Load Voltage

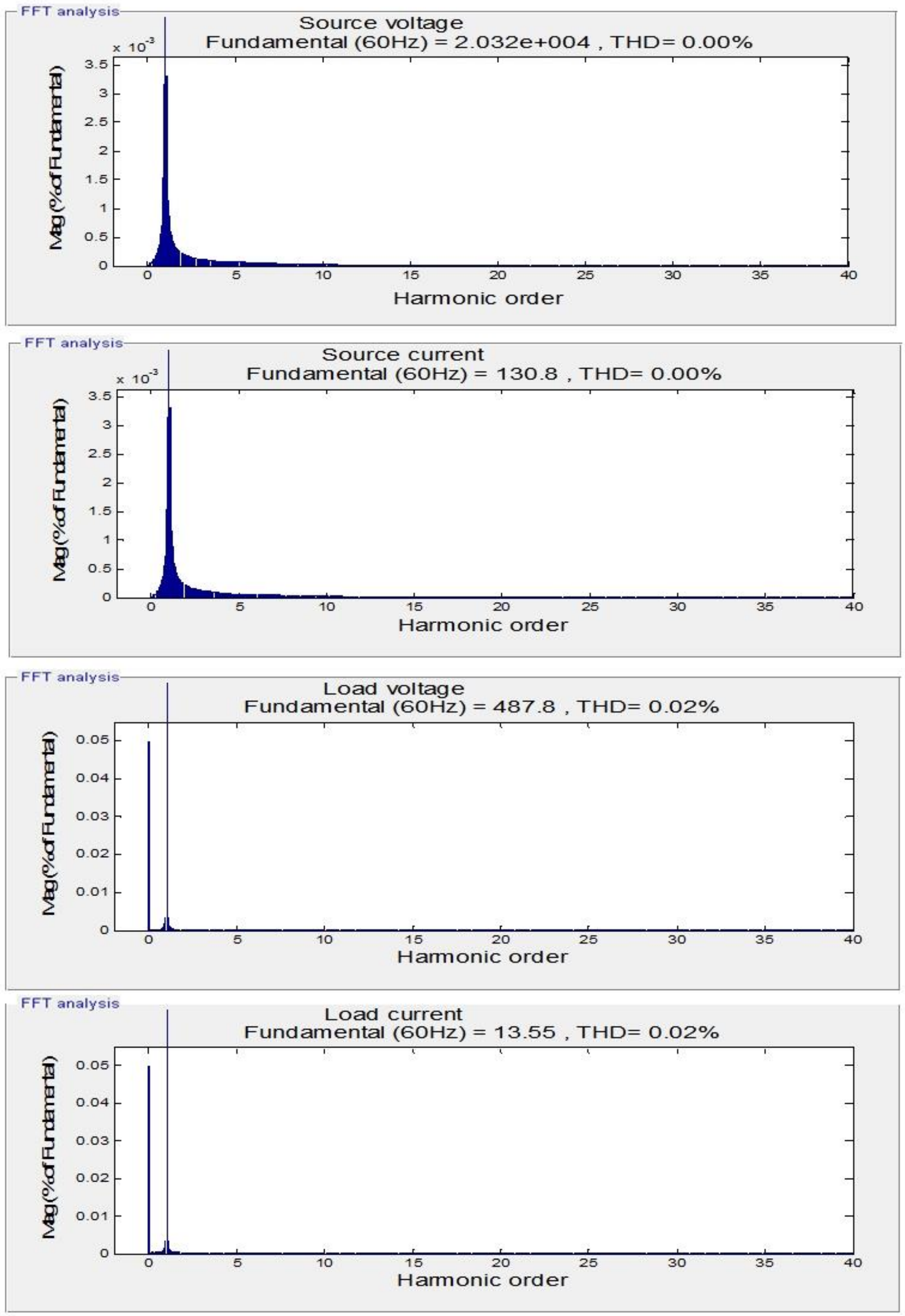

Figure 3.12 THD Analyses for Linear Load (a) Source Current (b) Source Voltage (c) Load Current (d) Load Voltage

Step 2: Linear and VFD Load

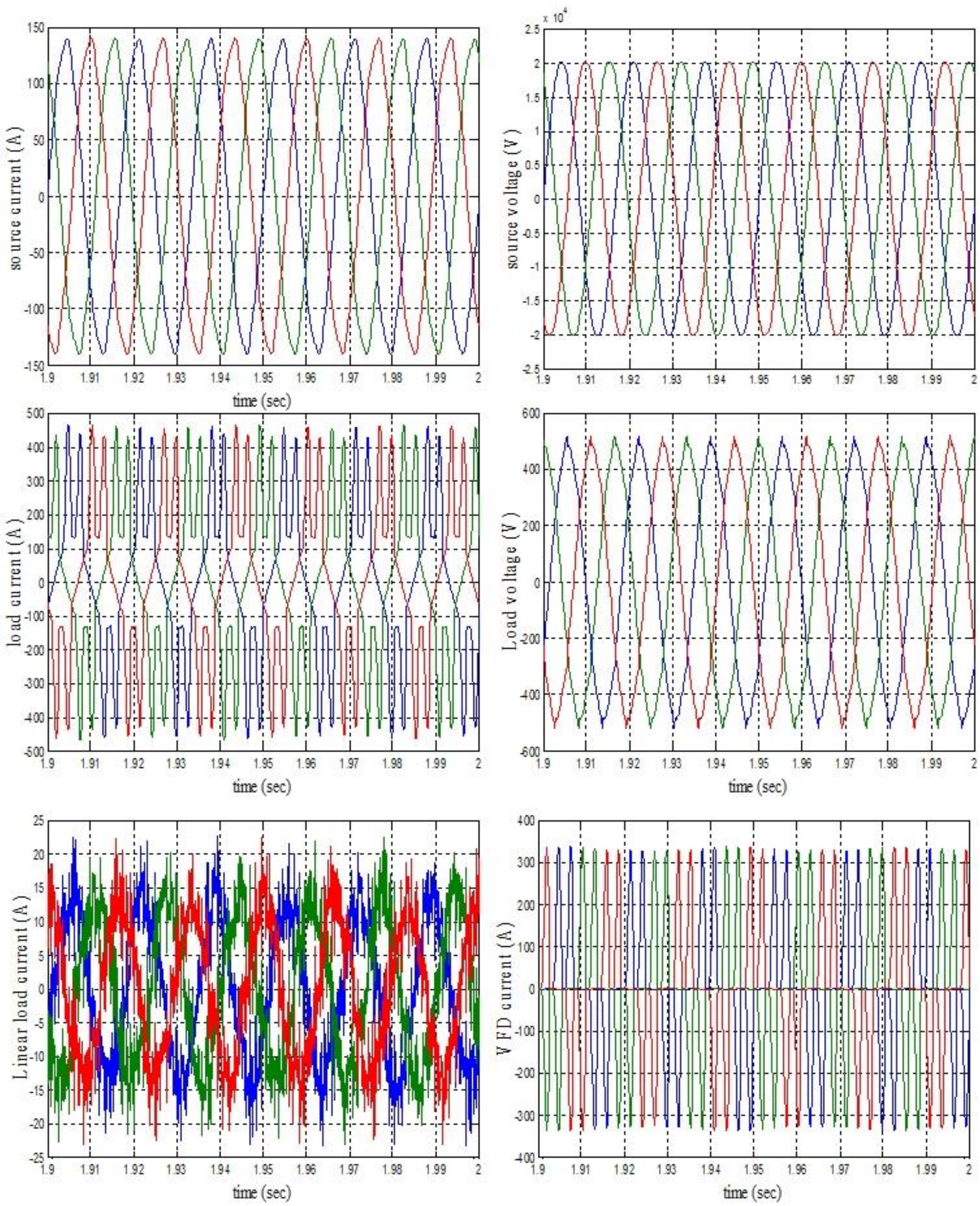

Figure 3.13 System Analyses for Linear and VFD Loads (a) Source Current (b) Source Voltage (c) Load Current (d) Load Voltage

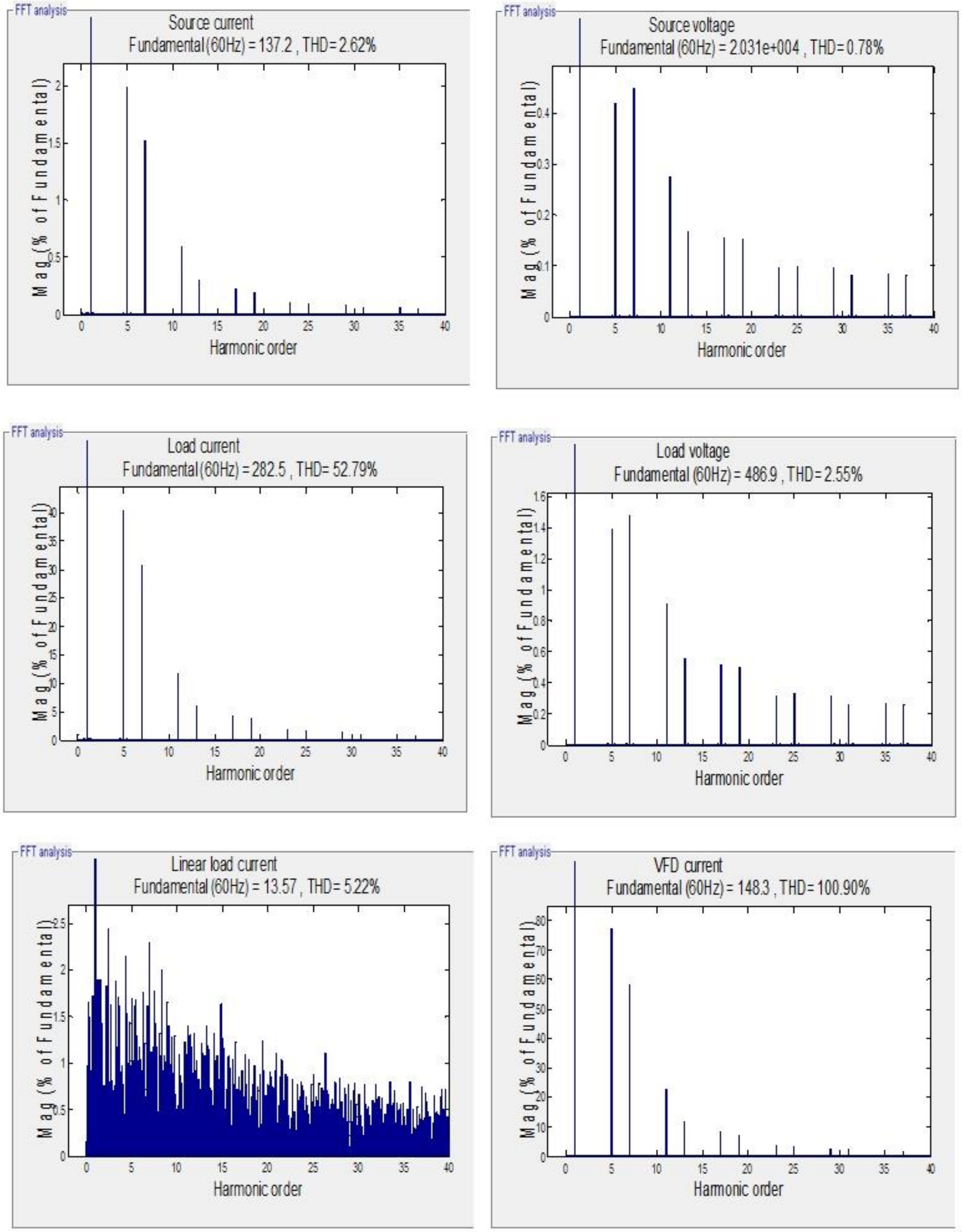

Figure 3.14 THD Analyses for Linear and VFD Loads (a) Source Current (b) Source Voltage (c) Load Current (d) Load Voltage

Step 3: Linear, VFD and Diode Rectifier Loads

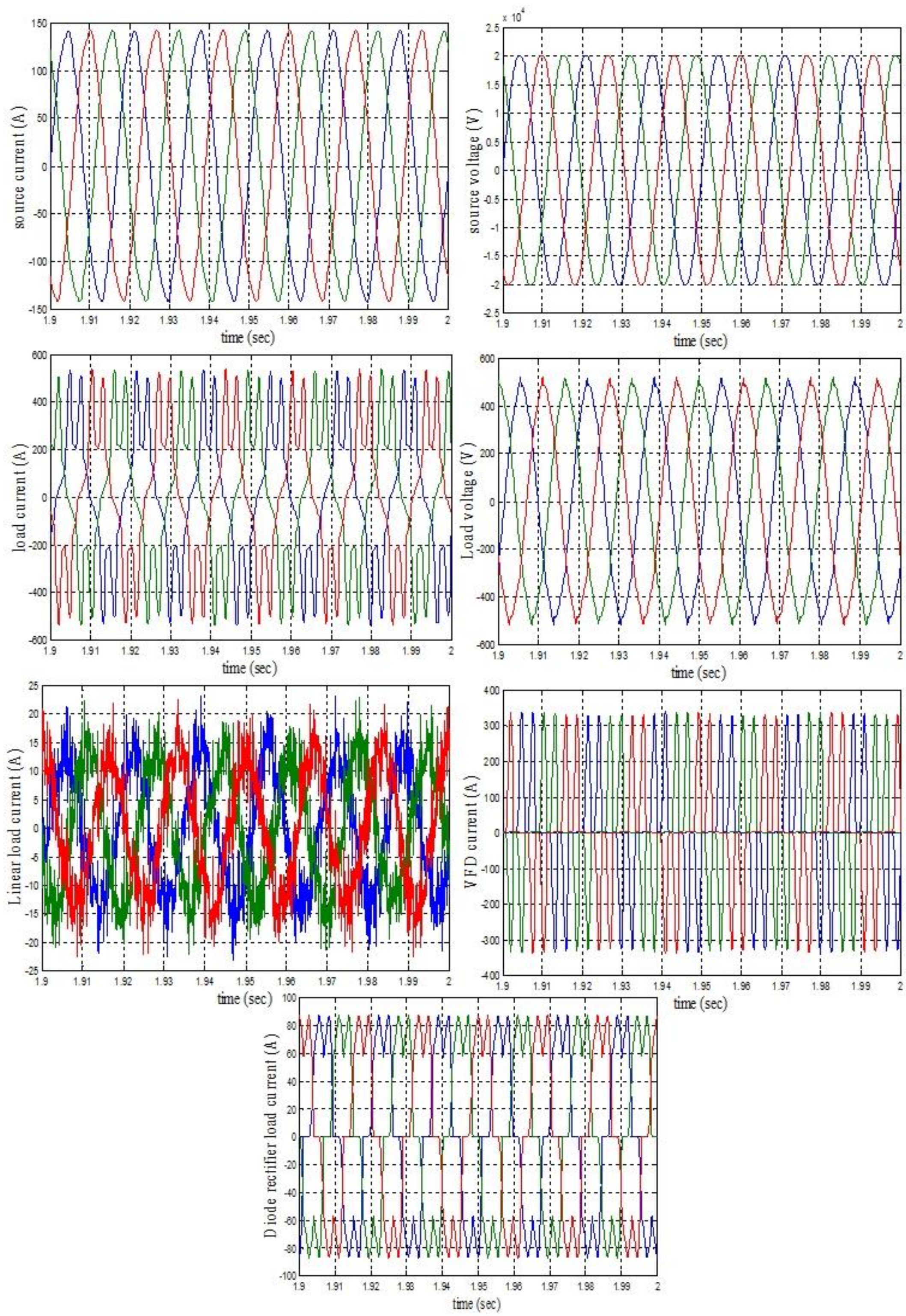

Figure 3.15 System Analyses for Linear, VFD and Diode Rectifier Loads (a) Source Current (b) Source Voltage (c) Load Current (d) Load Voltage

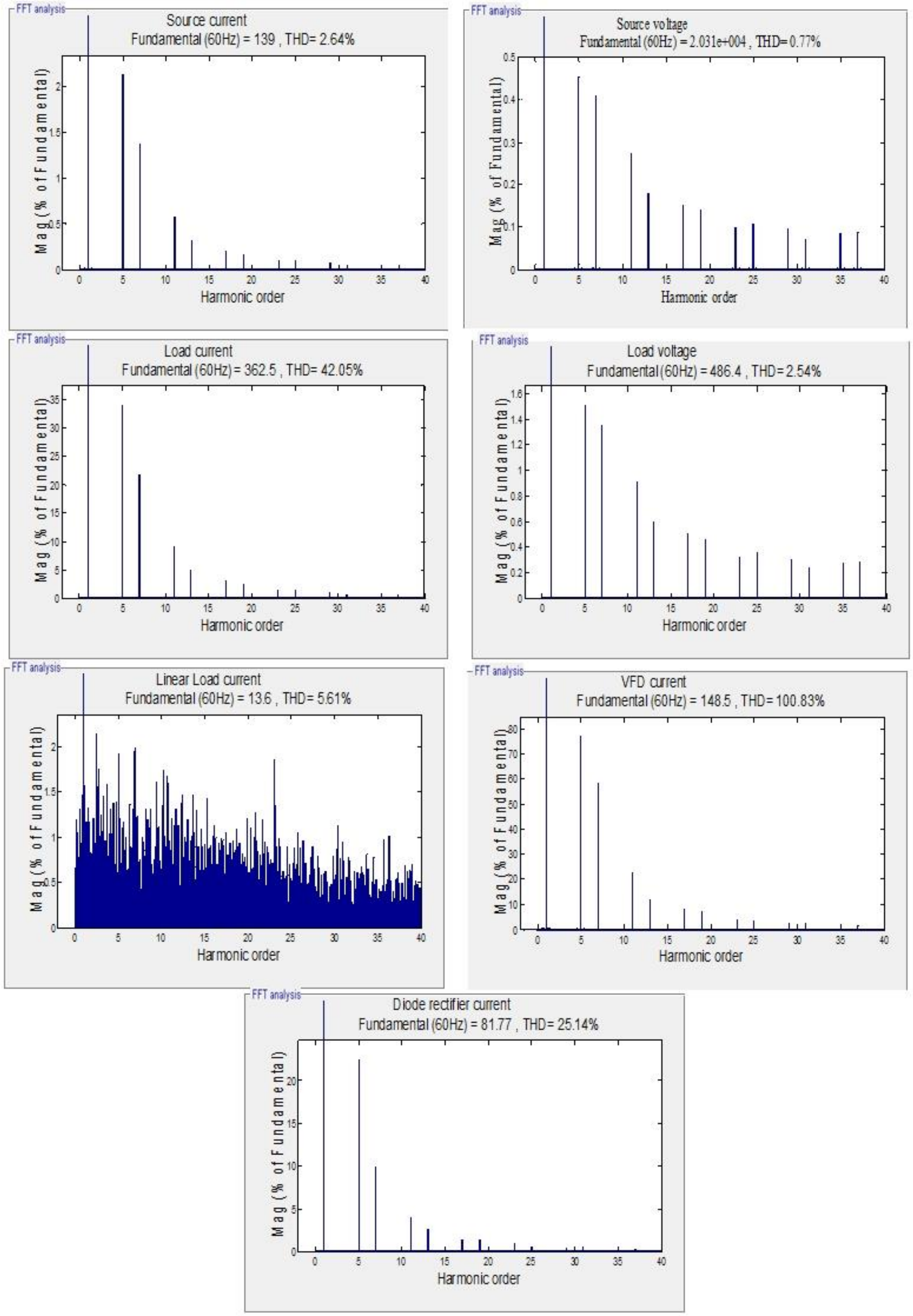

Figure 3.16 THD Analyses for Linear, VFD and Diode Rectifier Loads (a) Source Current (b) Source Voltage (c) Load Current (d) Load Voltage

Step 4: Linear, VFD, Diode Rectifier and Controlled Rectifier Loads

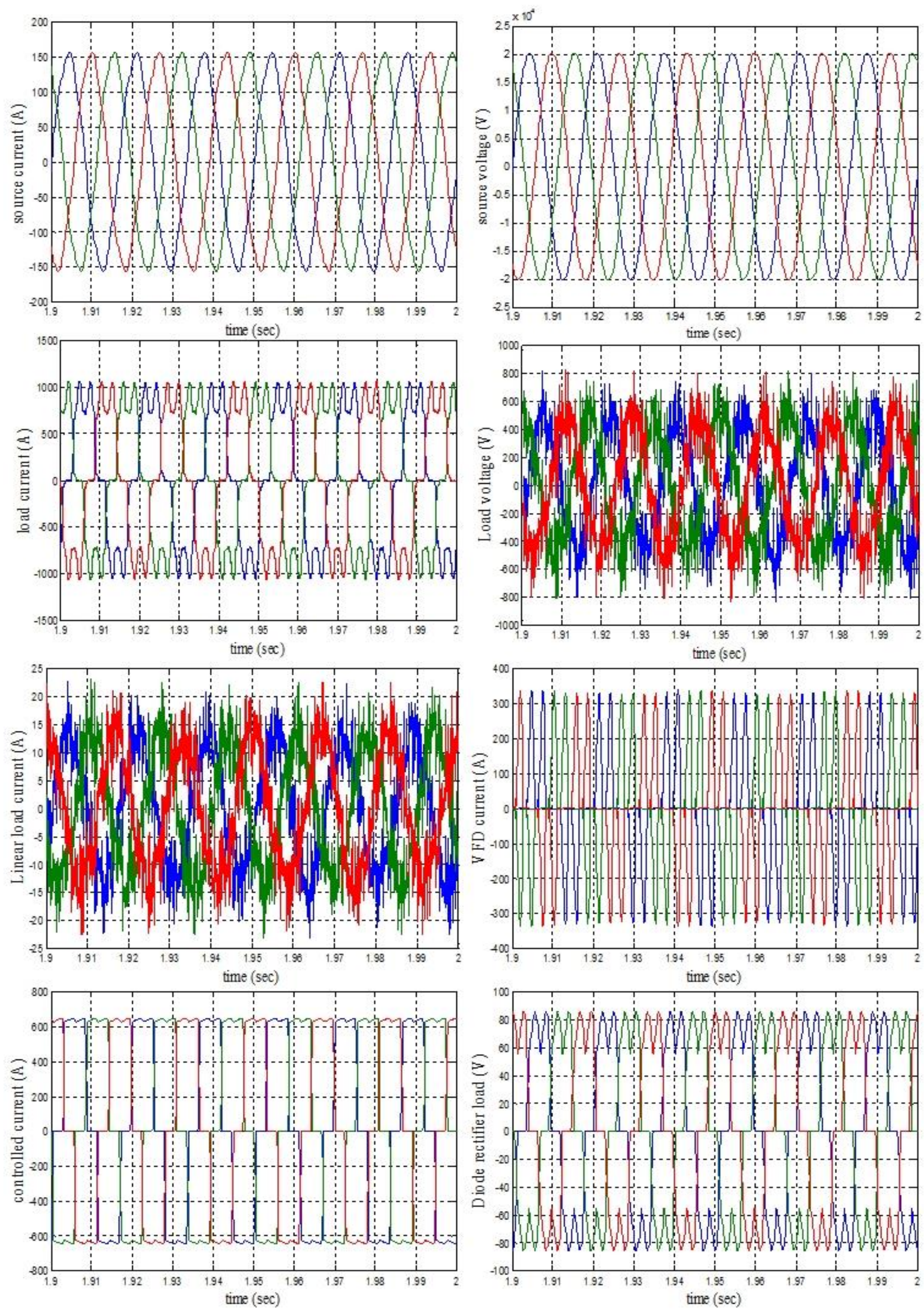

Figure 3.17 System Analyses for Linear, VFD, Controlled Rectifier and Diode Rectifier Loads (a) Source Current (b) Source Voltage (c) Load Current (d) Load Voltage

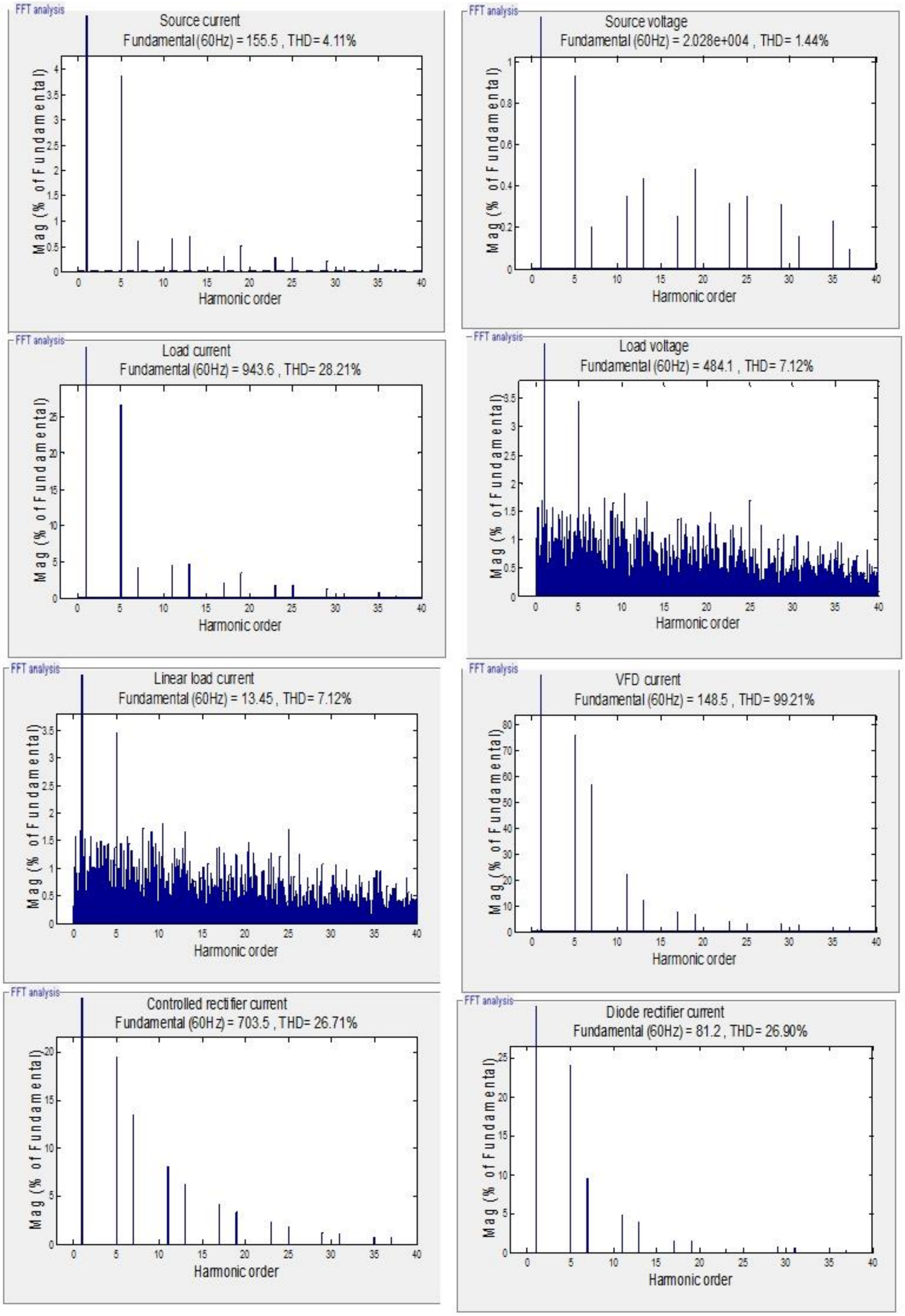

Figure 3.18 THD Analyses for Linear, VFD, Controlled Rectifier and Diode Rectifier Loads (a) Source Current (b) Source Voltage (c) Load Current (d) Load Voltage

The sequence of load is changed according to Table 3.5 and the value of THD is obtained. This table shows that the THD value of linear, VFD, diode rectifier (+Diode r.) and controlled rectifier (+Cntrlld r.) loads by adding them in different sequence. It is noticed that the sequence of connecting loads doesn't effect on the final total THD of voltages and currents in source and load sides which are similar for all of three cases.

Table 3.5 THD Analyses for Case 1, 2 and 3 of Sequence Change.

Case		Step1	Step2	Step3	Step4
		Linear	+VFD	+ Diode r.	+Cntrlld r.
1	THD of Source voltage %	0.00	0.78	0.77	1.44
	THD of Source current %	0.00	2.62	2.64	4.11
	THD of load voltage %	0.02	2.55	2.54	7.12
	THD of Load current %	0.02	52.79	42.05	28.21
	THD of linear load current %	0.00	5.22	5.61	7.12
	THD of VFD load current %	--	100.9	100.83	99.22
	THD of Diode rectifier load current %	--	--	25.14	26.90
	THD of controlled rectifier load current %	--	--	--	26.71
2		Linear	+ Diode r.	+ Cntrlld r.	+VFD
	THD of Source voltage	0.00	0.09	1.28	1.44
	THD of Source current	0.00	0.38	3.09	4.11
	THD of load voltage	0.02	1.15	5.42	7.12
	THD of Load current	0.02	21.86	23.97	28.21
	THD of linear load current %	0.00	1.15	5.42	7.12
	THD of VFD load current	--	--	--	99.22
	THD of Diode rectifier load current %	--	25.31	26.61	26.90
	THD of controlled rectifier load current %	--	--	26.83	26.71
3		+Linear	+Cntrlld r.	+ Diode r.	+VFD
	THD of Source voltage	0.00	1.26	1.28	1.44
	THD of Source current	0.00	3.02	3.09	4.11
	THD of load voltage	0.02	4.22	5.42	7.12
	THD of Load current	0.02	22.45	23.97	28.21
	THD of linear load current	0.00	5.92	5.42	7.12
	THD of VFD load current	--	--	--	99.22
	THD of Diode rectifier load current %	--	--	26.61	26.90
	THD of controlled rectifier load current %	--	26.85	26.83	26.71

3.1.4 Effect of changing in Firing Angle on THD for Control Rectifier Load.

The effect of firing angle of a Thyristor on THD value of current and voltage load is checked. The firing angle is changed from 0 to 90 degree for the control rectifier load shown in Appendix B. The corresponding THD value of load current and load voltage is measured and tabulated in Table 3.6.

From this table the THD of load current increased with firing angle continue increasing till 70° degree then it fall at 80° degree the increased at 90° degree this abnormal condition so it is prefered to operate between 0 ° - 50 ° degree.

Table 3.6 THD Analyses Firing Angle Change

Firing angle	THD in load current	THD in load voltage
0°	27.23	4.56
10°	29.04	6.61
20°	28.6	5.79
30°	29.66	6.96
40°	30.08	5.75
50°	30.38	6.99
60°	34.25	5.86
70°	34.41	6.68
80°	30.4	6.1
90°	170.08	0.17

CHAPTER 4

POWER QUALITY IMPROVEMENT USING SHUNT ACTIVE POWER FILTER (SAPF)

This chapter presents the modeling of SAPF, generation of reference current algorithms, control strategies and parameter design for SAPF. Eventually, simulation results are presented to validate the module using MATLAB/SIMULINK.

4.1 The Module of SAPF

The SAPF can be modeled as controlled current source, which injects the current in the power system to decrease the harmonic which generated by the non-linear load [56]–[58]. The source provides only the fundamental sinusoidal current to the load by calculating the nonlinear or compensation current and injecting it into the system using SAPF. In Figure 4.1 an SAPF is connected at point of common coupling, where i_s represents the source current, i_l is the distorted load current and i_f is and compensation shunt active power filter current.

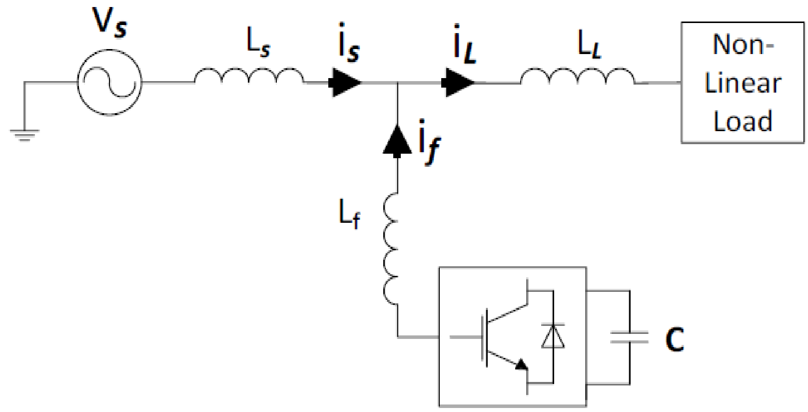

Figure 4.1 Single Line Diagram of SAPF

The construction of SAPF module contains a three phase IGBT based switching devices, its function is provide the harmonic compensation current i_f through the input inductor l_f as shown in Figure 4.2. The non-linear load consisted of a three-phase diode bridge rectifier with R load on its dc side.

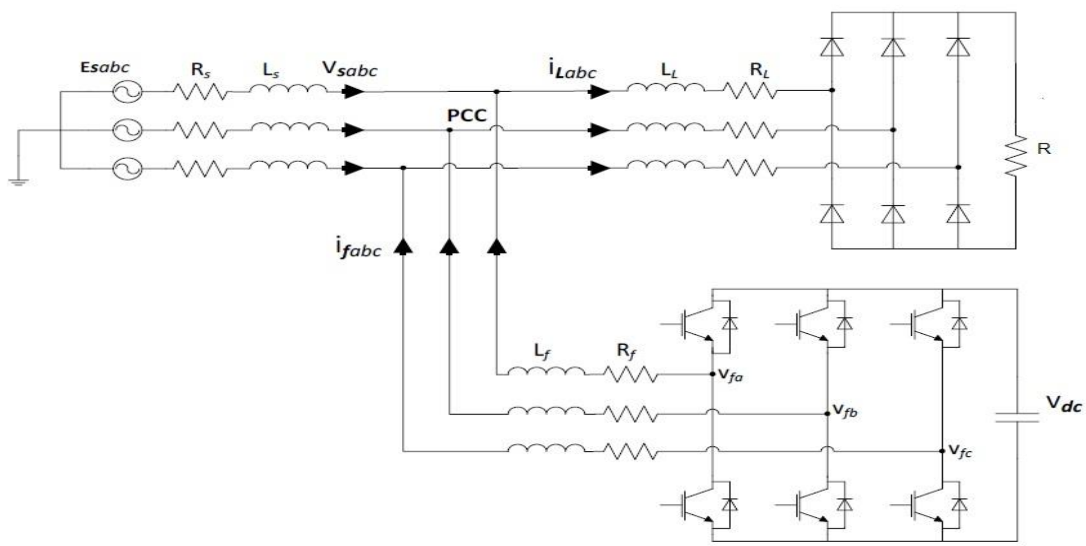

Figure 4.2 Construction of Three Phase SAPF

Where:

E_{sabc} is the three phase source voltage.

i_{labc} is the three phase load current.

i_{fabc} is the three phase filter current.

R_s and L_s are the source resistor and reactor.

R_l and L_l are the load side resistor and reactor.

R_f and L_f are the filter resistor and the reactor.

V_{dc} is the DC side capacitor voltage.

R is the resistive load.

Assume the three-phase source voltage source E_{sabc} is a balanced source such that:

$$E_{sa}(t) = E_{sm}\sin(\omega t) \tag{4.1}$$

$$E_{sb}(t) = E_{sm}\sin\left(\omega t - \frac{2\pi}{3}\right) \tag{4.2}$$

$$E_{sc}(t) = E_{sm}\sin\left(\omega t + \frac{2\pi}{3}\right) \tag{4.3}$$

Where

E_{sm} is the maximum source voltage.

ω is the angular frequency (rad/sec).

The voltage source is assumed to be a balanced. The following assumptions are considered:

$$\begin{gathered} E_{sa} + E_{sb} + E_{sc} = 0 \\ i_{sa} + i_{sb} + i_{sc} = 0 \\ i_{la} + i_{lb} + i_{lc} = 0 \\ i_{fa} + i_{fb} + i_{fc} = 0 \end{gathered} \tag{4.4}$$

A low pass *RL* filter is used to connect the SAPF with the PCC such that:

$$v_{sk} = v_{fk} - v_{lfk} - v_{rfk} \tag{4.5}$$

$$v_{sk} = v_{fk} - L_f \frac{di_{fk}}{dt} - R_f i_{fk} \tag{4.6}$$

Where

k = a, b, c is the three phase system.

By applying Kirchhoff law, the nonlinear current supplied by the inverter can be obtained as:

$$L_f \frac{di_{fa}}{dt} = -R_f i_{fa} + v_{fa} - v_{sa} \tag{4.7}$$

$$L_f \frac{di_{fb}}{dt} = -R_f i_{fb} + v_{fb} - v_{sb} \tag{4.8}$$

$$L_f \frac{di_{fc}}{dt} = -R_f i_{fc} + v_{fc} - v_{sc} \tag{4.9}$$

Where

i_{fa} , i_{fb} and i_{fc} are the three phase compensation current injected by the inverter.

The DC side capacitor equation can be written as:

$$C_{DC} \frac{dV_{DC}}{dt} = S_a i_{fa} + S_b i_{fb} + S_c i_{fc} \tag{4.10}$$

Where

C_{DC} is the capacitance of the DC side capacitor.

The above equations can be written in a stationary α-β reference frame as [59]:

$$L_f \frac{di_{f\alpha}}{dt} = -R_f i_{f\alpha} + v_{f\alpha} - v_{s\alpha} \tag{4.11}$$

$$L_f \frac{di_{f\beta}}{dt} = -R_f i_{f\beta} + v_{f\beta} - v_{s\beta} \tag{4.12}$$

$$C_{dc} \frac{dV_{dc}}{dt} = S_\alpha i_{f\alpha} + S_\beta i_{f\beta} \tag{4.13}$$

4.2 Generation of the Reference Current Algorithm

Active power filters are designed to inject the nonlinear part of the load current in such a way that the source should provide the purely sinusoidal current to the load. The calculation of nonlinear load current is significant, because the performance of the active filter is highly dependent on it. With the aid of reference current generation algorithms the nonlinear current (compensation current) is calculated. There are two main categories of current extraction algorithms, known as frequency domain current extraction algorithms [60]–[63] and time domain current extraction algorithms. In the frequency domain to extract the compensation current, DFT and wavelet transform is used [64]–[67]. The disadvantages of the frequency domain method are filtering and inverse transformation, degraded performance during transients, larger delays in transformation, large amounts of processing delays, and memory usage restricts their applicability in real time applications. In contrast, the time domain methods are faster, accurate and require less processing delays and memory [68]. In this chapter, instantaneous active and reactive power theory has been utilized to obtain the compensation current for SAPF.

4.2.1 Instantaneous Active and Reactive Power p–q Theory

The instantaneous active and reactive power theory (p-q) used in SAPF design is proposed by Akagi [69]. The p-q theory computes the instantaneous powers defined in the time domain [70]–[72]. To transform the distorted currents and voltage signals from three phase frame abc into stationary frame α-β, a Clark Transformation (CT) is used [69]. Figure 4.2 shows the basic block diagram of instantaneous active and reactive power methodology. Firstly, the voltage and the current signals are converted to a stationary reference frame using CT, then the fundamental power is extracted using low pass filter, and finally the compensation current is converted back from stationary axis into three phase *abc*.

The instantaneous active and reactive power methodology is given as following:

The converted three phase voltage and current signals in stationary α-β reference frame is given by:

$$\begin{bmatrix} v_\alpha \\ v_\beta \\ v_o \end{bmatrix} = \sqrt{\frac{2}{3}} \begin{bmatrix} 1 & -\frac{1}{2} & -\frac{1}{2} \\ 0 & \frac{\sqrt{3}}{2} & -\frac{\sqrt{3}}{2} \\ \frac{1}{\sqrt{2}} & \frac{1}{\sqrt{2}} & \frac{1}{\sqrt{2}} \end{bmatrix} \begin{bmatrix} v_a \\ v_b \\ v_c \end{bmatrix} \tag{4.14}$$

$$\begin{bmatrix} i_\alpha \\ i_\beta \\ i_o \end{bmatrix} = \sqrt{\frac{2}{3}} \begin{bmatrix} 1 & -\frac{1}{2} & -\frac{1}{2} \\ 0 & \frac{\sqrt{3}}{2} & -\frac{\sqrt{3}}{2} \\ \frac{1}{\sqrt{2}} & \frac{1}{\sqrt{2}} & \frac{1}{\sqrt{2}} \end{bmatrix} \begin{bmatrix} i_a \\ i_b \\ i_c \end{bmatrix} \tag{4.15}$$

The instantaneous active and reactive power $p(t)$ and $q(t)$ in three phase system abc and stationary frame α-β is given as:

$$p(t) = v_a i_{la} + v_b i_b + v_c i_{lc} \tag{4.16}$$

$$p(t) = v_\alpha i_{l\alpha} + v_\beta i_{l\beta} \tag{4.17}$$

$$q(t) = -\frac{1}{\sqrt{3}}\left(v_\alpha i_{l\beta} + v_\beta i_{l\alpha}\right) \tag{4.18}$$

Equations (4.17-4.18) can be written in matrix form as

$$\begin{bmatrix} p \\ q \end{bmatrix} = \begin{bmatrix} v_\alpha & v_\beta \\ -v_\beta & v_\alpha \end{bmatrix} \begin{bmatrix} i_{l\alpha} \\ i_{l\beta} \end{bmatrix} \tag{4.19}$$

Equation (4.19) contains AC and DC power components. To obtain the purely sinusoidal source current, the compensation current is calculated from AC power. The cut-off frequency of the low pass filter and the fundamental component frequency should be the same.

The compensation current using the filtered power can be calculated as:

$$\begin{bmatrix} {i_\alpha}^* \\ {i_\beta}^* \end{bmatrix} = \frac{1}{{v_\alpha}^2+{v_\beta}^2}\begin{bmatrix} v_\alpha & -v_\beta \\ v_\beta & v_\alpha \end{bmatrix}\begin{bmatrix} \tilde{p} \\ \tilde{q} \end{bmatrix} \tag{4.20}$$

Where

$\tilde{p}$ is the fundamental active power obtained after passing through the low pass filter as shown in Figure 4.3. Using inverse Clark transformation to obtain the three phase compensation current from α-β reference frame as:

$$\begin{bmatrix} {i_a}^* \\ {i_b}^* \\ {i_c}^* \end{bmatrix} = \sqrt{\frac{2}{3}}\begin{bmatrix} 1 & 0 \\ -\frac{1}{2} & \frac{\sqrt{3}}{2} \\ -\frac{1}{2} & -\frac{\sqrt{3}}{2} \end{bmatrix}\begin{bmatrix} {i_\alpha}^* \\ {i_\beta}^* \end{bmatrix} \tag{4.21}$$

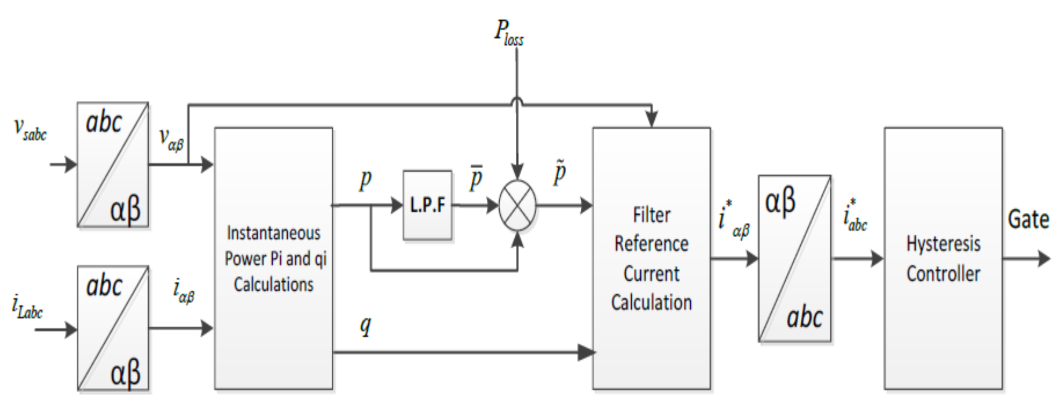

Figure 4.3 Block Diagram of Instantaneous Active and Reactive Power Theory for SAPF

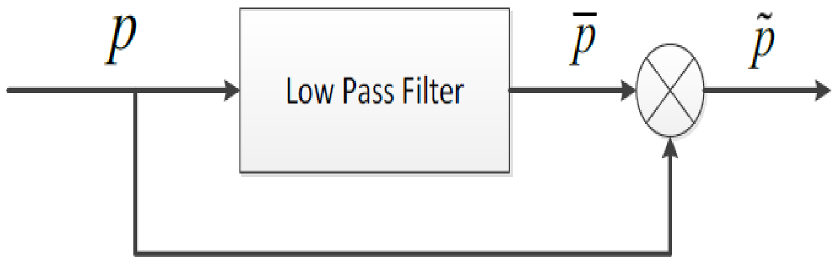

Figure 4.4 Calculation of Fundamental Active Power using Low Pass Filter

4.3 Control Method of VSI

The current control strategies play a vital role in generating the switching signals for fast and accurate response of inverters such as SAPF. The current controller is used to generate the switching patterns for SAPF.

4.3.1 Hysteresis Control Method

To generate the switching pattern of the VSI, the hysteresis current control method is used. The advantages of Hysteresis current control method are simple structure for implementation, fast and robust response, and computationally light as it does not required any separate controller or a modulator. This makes it the most commonly used control method [73]–[78]. Figure 4.4 shows the generation of gate signals using a Hysteresis current controller by comparing the actual current with the reference current. Then if the error between the actual current and the reference current value is larger than the predefined hysteresis band (Upper or lower band) a switching pulse is generated immediately to open or close a specific inverter gate [79].

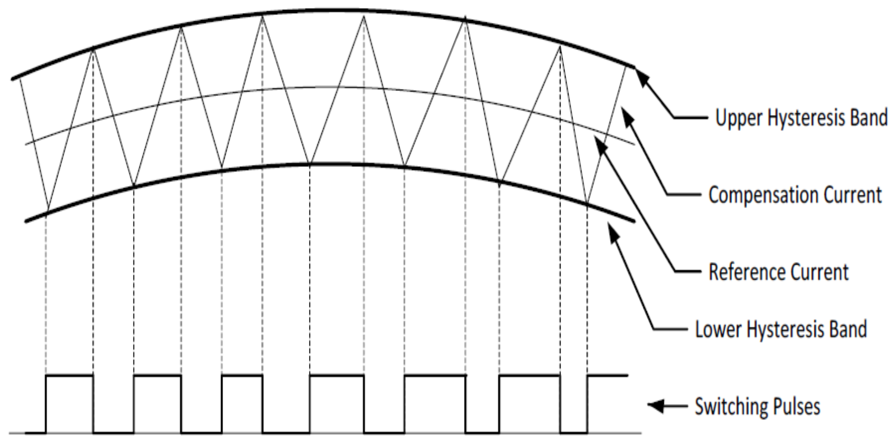

Figure 4.5 the Hysteresis Current Controller

The switching pulses for SAPF three phases are generated as follows:

1- If ${I_{ca}}^{*} - I_{ca} > HB$, the switching gate g_1 is OFF while g_4 is ON.

2- If, ${I_{ca}}^{*} + I_{ca} > HB$ the switching gate g_1 is ON while g_4 is OFF.

Where

HB is the hysteresis band

${I_{ca}}^{*}$ is the compensation current

I_{ca} is the reference current for the phase a of SAPF.

The switching pulses for the remaining phases b and c can be generated in a similar way.

4.4 DC Bus Voltage Regulation

The DC-bus capacitor C_{dc} is utilized as a source by the VSI-based SAPF to supply the reactive power and compensation current at high switching frequency. To provide the required compensation current under steady state conditions, the DC link capacitor should be charge and discharge during the source voltage period. The primary factors that determine the value of the DC link capacitor are the peak harmonic and reactive loads.

The voltage across the DC link capacitor is kept high enough as compared to the peak source voltage in order to inject the required non-linear compensation current at PCC [80].

Figure 4.5 reveals the block diagram of the DC bus voltage control through PI controller [81]. The error between the reference voltage and the measured DC bus voltage can be calculated as:

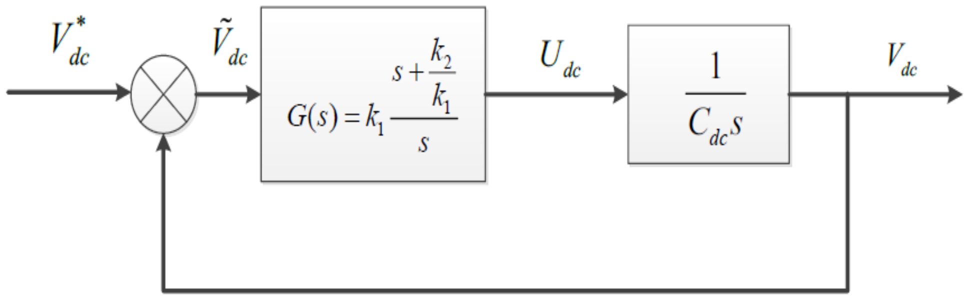

Figure 4.6 The DC Bus Voltage Control Loop

$$\widetilde{v_{dc}} = v_{dc}{}^* - v_{dc} \tag{4.22}$$

The error signal $\widetilde{v_{dc}}$ is passed through a PI controller to regulate the voltage across the DC link, as:

$$u_{dc} = k_1 \widetilde{v_{dc}} + k_2 \int \widetilde{v_{dc}}\, dt \tag{4.23}$$

The transfer function of the PI controller is given as:

$$G(s) = \frac{U_{dc}(s)}{\widetilde{V_{dc}}(s)} = k_1 \frac{s + \frac{k_2}{k_1}}{s} \tag{4.24}$$

The closed loop transfer function is given by:

$$\frac{V_{dc}(s)}{V_{dc}{}^*(s)} = 2\xi\omega_n \frac{s + \frac{\omega_n}{2\xi}}{s^2 + 2\xi\omega_n s + \omega_n{}^2} \tag{4.25}$$

The gain of the PI controller is:

$$k_1 = 2\xi\omega_n C_{dc} \tag{4.26}$$

$$k_2 = \omega_n{}^2 C_{dc} \tag{4.27}$$

4.5 Design of SAPF parameter

The performance of SAPF depends on the selection of SAPF parameters such as the DC link capacitor and the AC link reactor values.

4.5.1 The DC link capacitor

To design the DC bus voltage across the DC link capacitor the following relation is used [82]:

$$V_c = \frac{(V_s - Li_L)i_L}{CV_c} \tag{4.28}$$

The energy stored across the capacitor can be calculated as:

$$\Delta W = \frac{1}{2}C\left(V_c{}^2 - V_o{}^2\right) \approx C\Delta V_c V_o \tag{4.29}$$

The maximum allowable voltage variation across the capacitor is

$$\Delta V_c = \varepsilon V_o$$

$$C \approx \frac{\Delta W}{\Delta V_c V_o} = \frac{\Delta W}{\varepsilon V_o{}^2} \tag{4.30}$$

4.5.2 The AC link reactor

The interfacing inductor value can be calculated as follows [83]:

$$L_{min} = \frac{\Delta V_{min}}{\omega I_{max}} \tag{4.31}$$

Where,

ω is the source voltage angular frequency

I_{max} is the maximum current to be provided by the SAPF

ΔV_{min} is the difference between the source voltage and the fundamental inverter voltage.

4.6 Simulation results

This section presents the simulation results of the SAPF to suppress the harmonics generated by non-linear loads. The simulation of the SAPF is carried out using MATLAB/SIMULINK software. Figure 4.7 to Figure 4.9 show the detailed module which consists of 3-phase source supply, Non-linear load and SAPF.

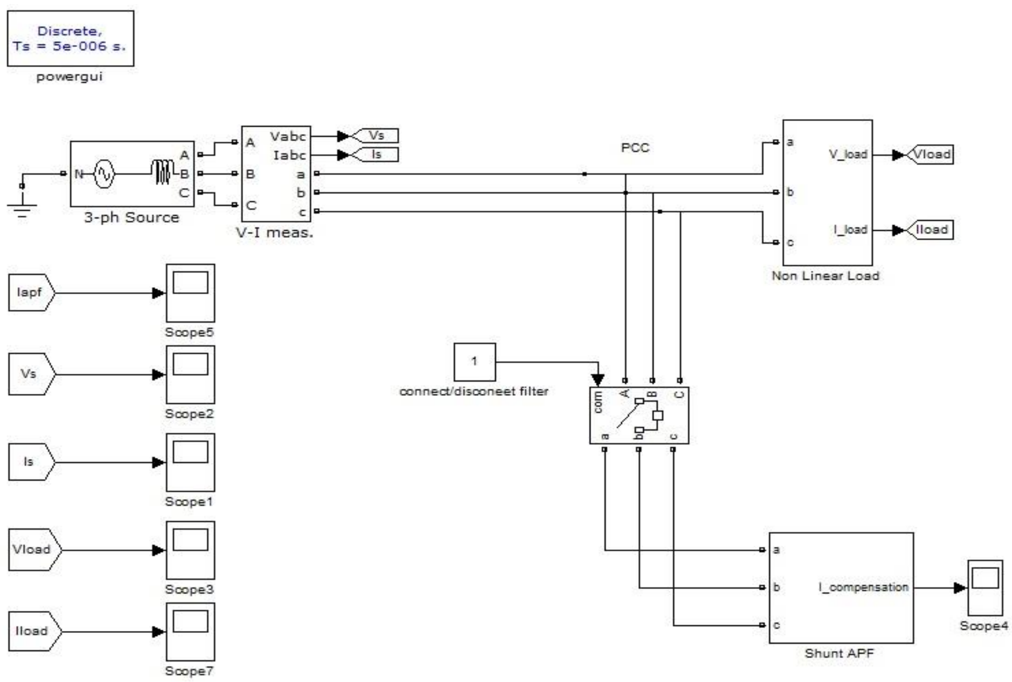

Figure 4.7 Detailed Module of SAPF

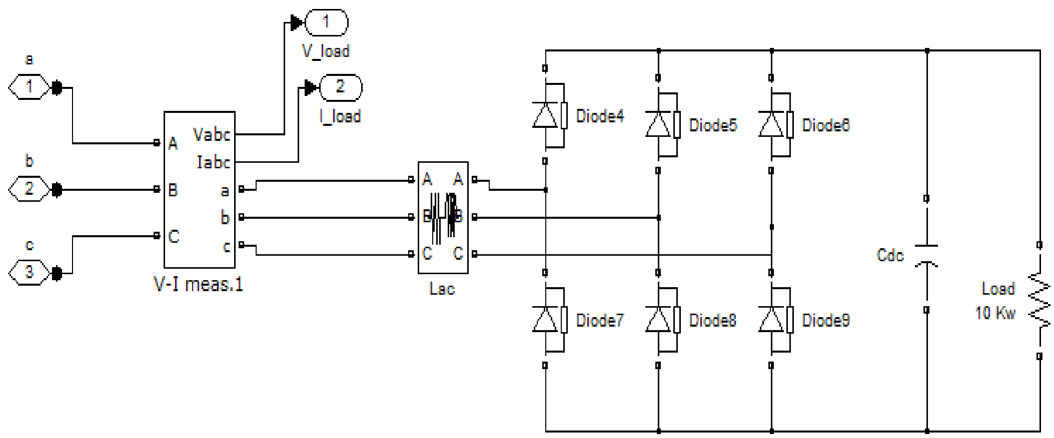

Figure 4.8 Subsystem of Non-Linear Load

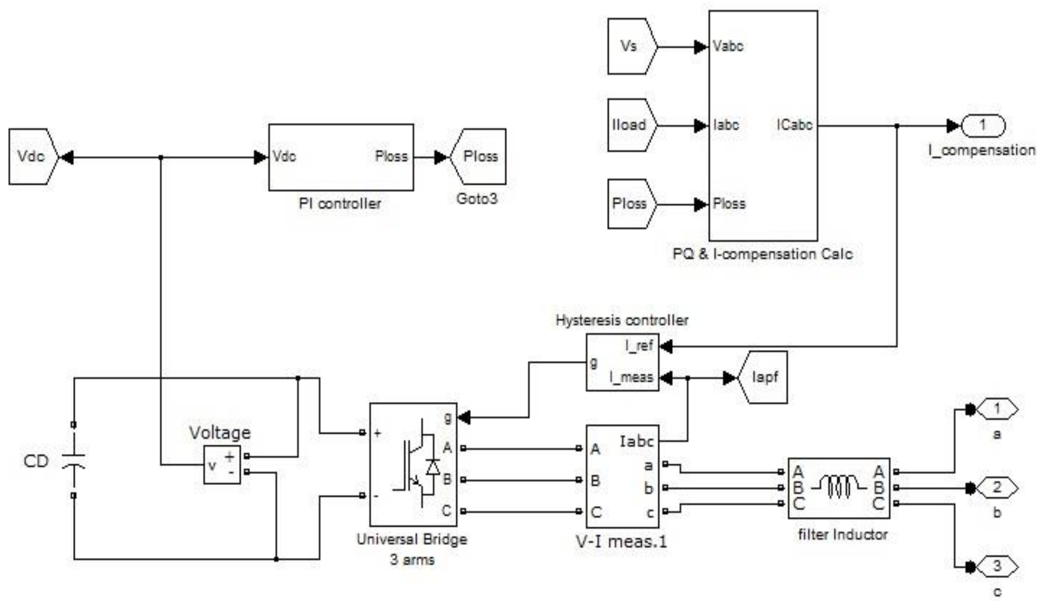

Figure 4.9 Subsystem of SAPF

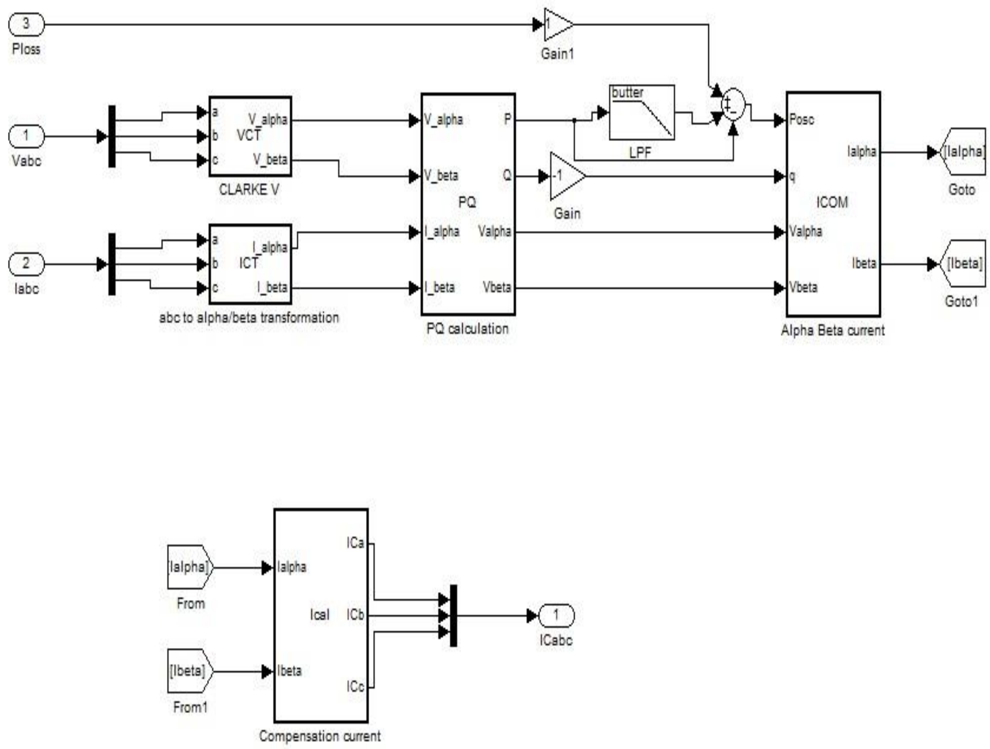

Figure 4.10 Calculation of Reference Current

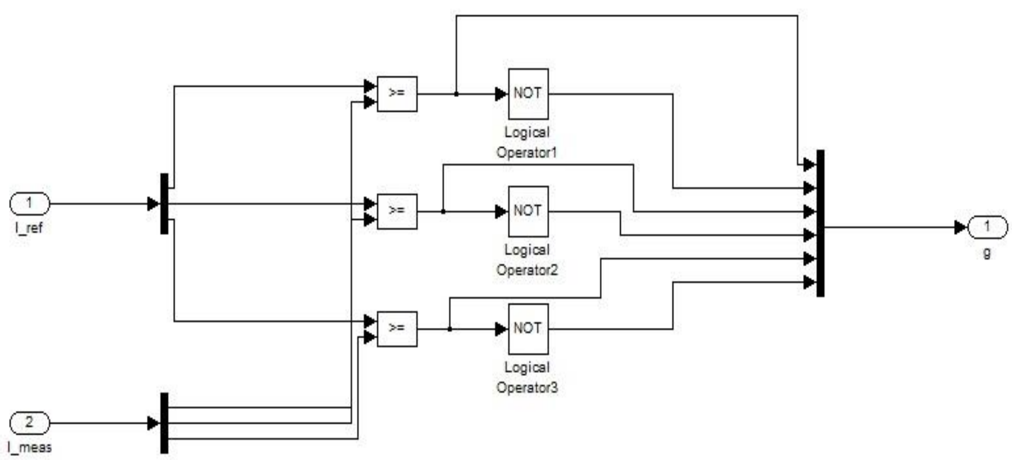

Figure 4.11 Determinations of Gate Signals

The system parameters used for the simulation are presented in Table 4.1[84].

Table 4.1 Parameter of the System used

Supply voltage V_s	480
Supply frequency f_s	60
DC Link Capacitance and Voltage (C_D, V_{dc})	1500µf , 750 VDC
Load Impedance L_{ac}	1.5mH
Filter Inductance	2.5mH
p - q Controller (K_1, K_2)	0.1 , 1
C_{dc}	1500 µf
Load rating	20 KW

4.6.1 Case I: Static Three Phase Diode Rectifier R Load without SAPF.

In this case, a static R load is connected on the DC side of the rectifier. The rectifier injects the harmonics in the system. The simulation results present a detailed analysis of the system including three phase source voltage, three phase source current, load current, dc link voltage and THDs of source and load current.

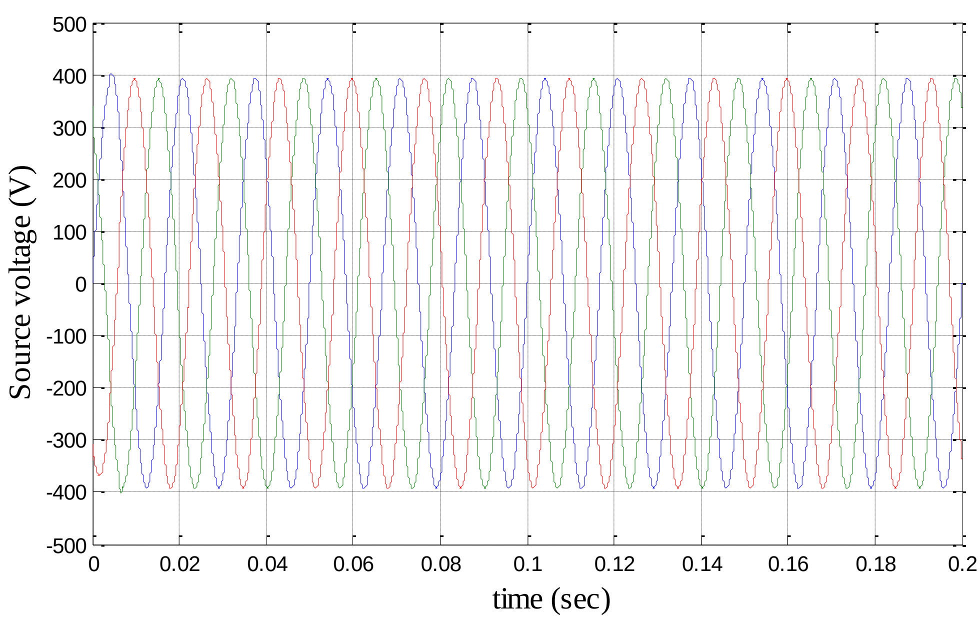

Figure 4.12 Source Voltage Waveform of the System in Case of Without SAPF

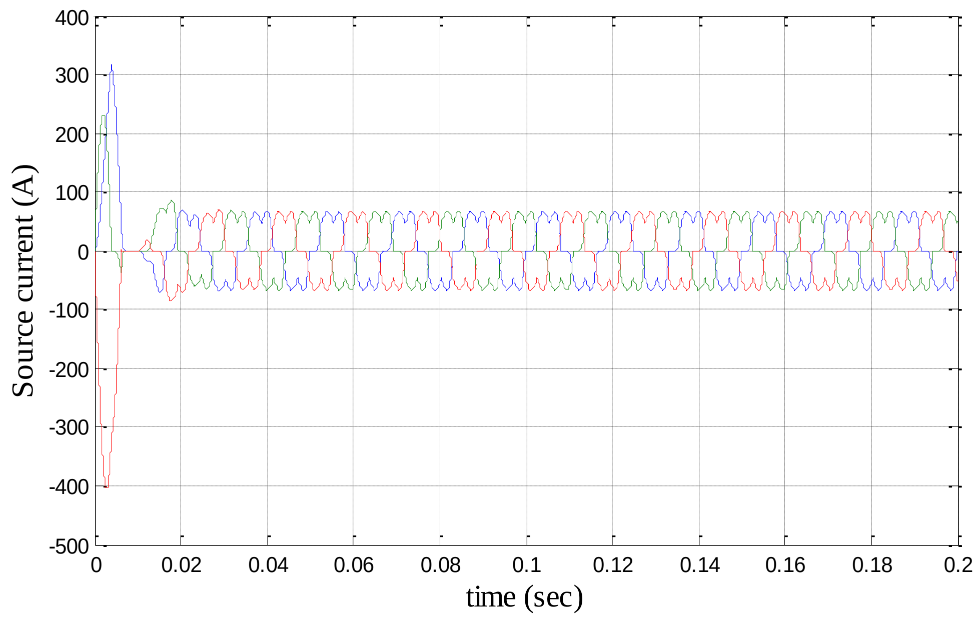

Figure 4.13 Source Current Waveform of the System in Case of Without SAPF

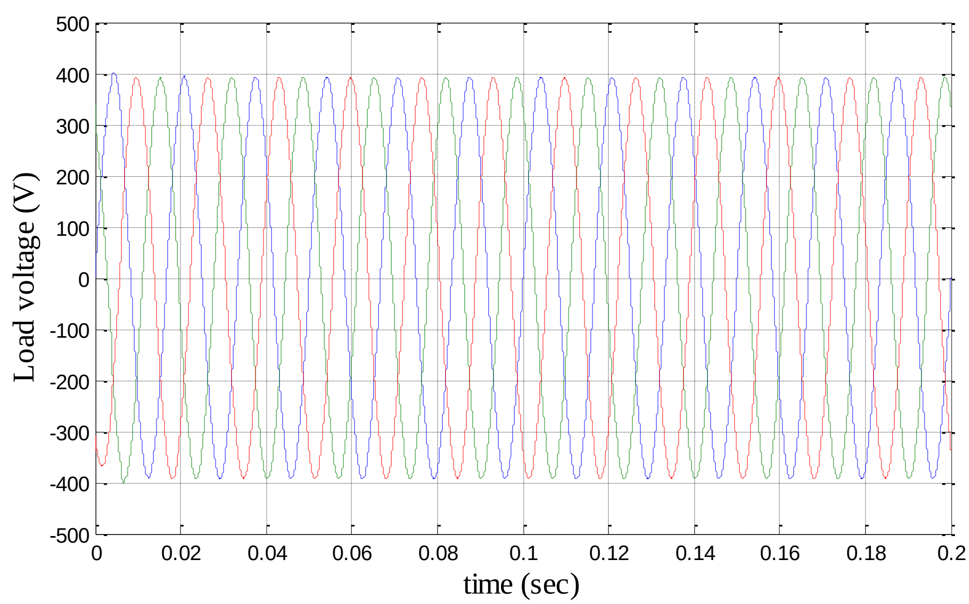

Figure 4.14 Load Voltage Waveform of the System in Case of Without SAPF

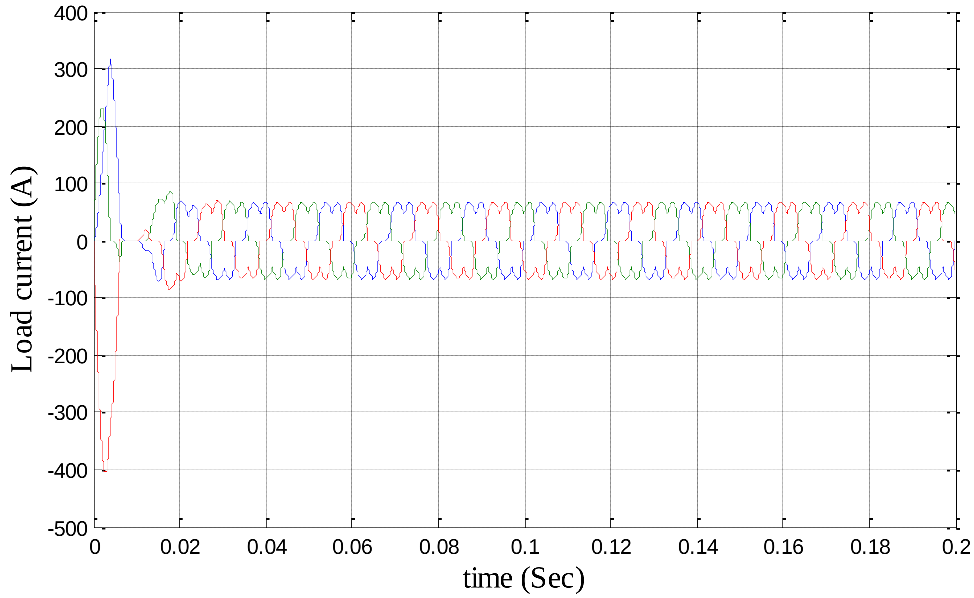

Figure 4.15 Load Current Waveform of the System in Case of Without SAPF

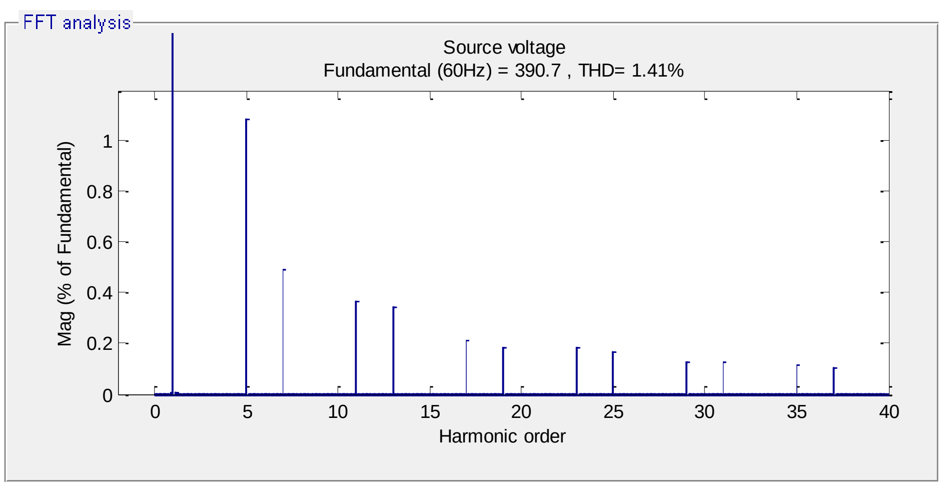

Figure 4.16 THD and Spectrum Analysis for Source Voltage in Case of Without APF

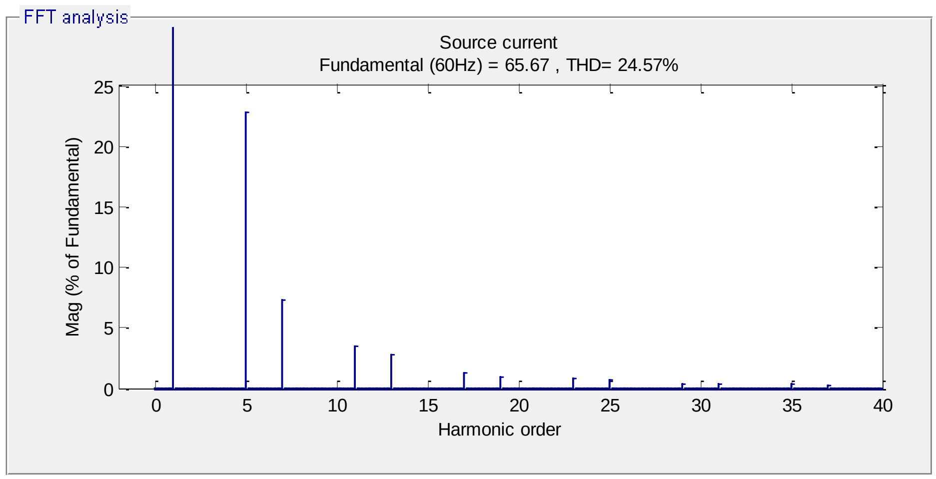

Figure 4.17 THD and Spectrum Analysis for Source Current in Case of Without SAPF

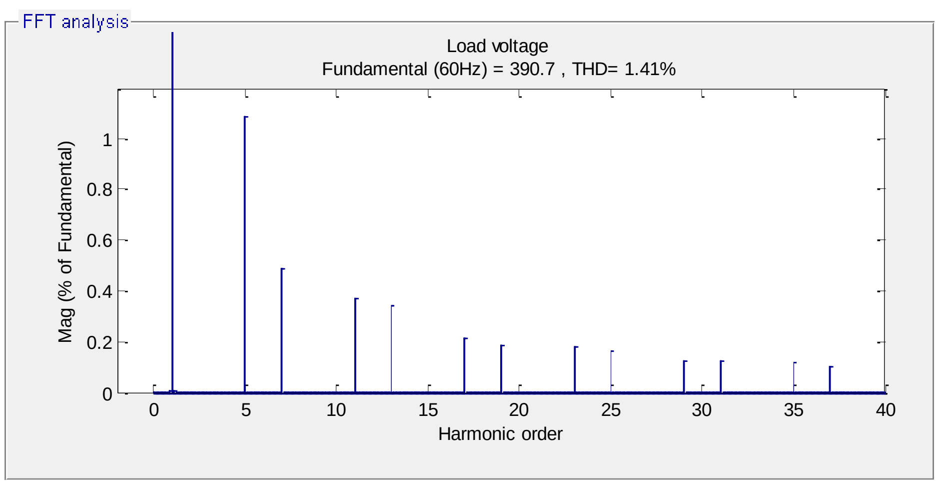

Figure 4.18 THD and Spectrum Analysis for Load Voltage in Case of Without SAPF

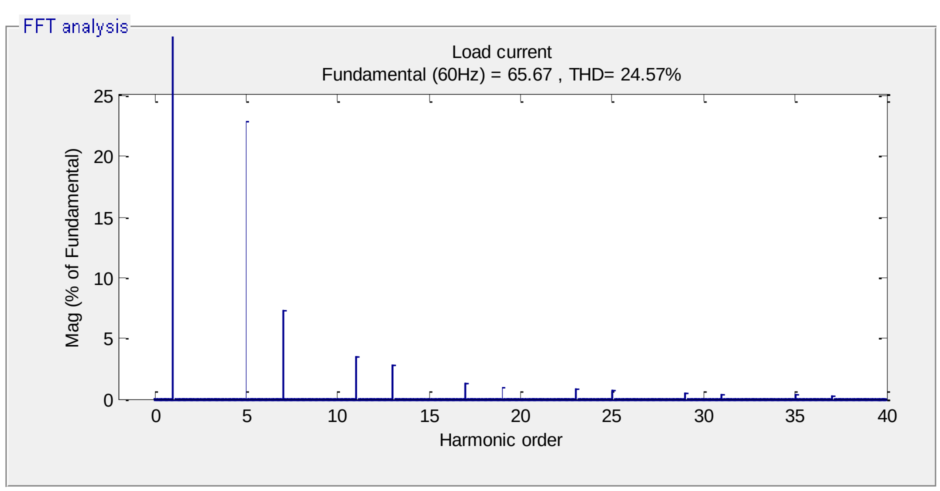

Figure 4.19 THD and Spectrum Analysis for Load Current in Case of Without SAPF

4.6.2 Case II: Static Three Phase Diode Rectifier R Load with SAPF.

The simulation results present a detailed analysis of the system including three phase source voltage, three phase source current, load and active filter current, DC link voltage and THDs of source and load current.

Figure 4.20 to Figure 4.30 present the system response for instantaneous power $p-q$ controller for 0.2 sec window. The SAPF starts its operation at 0.04 sec and injects the nonlinear current required by the load.

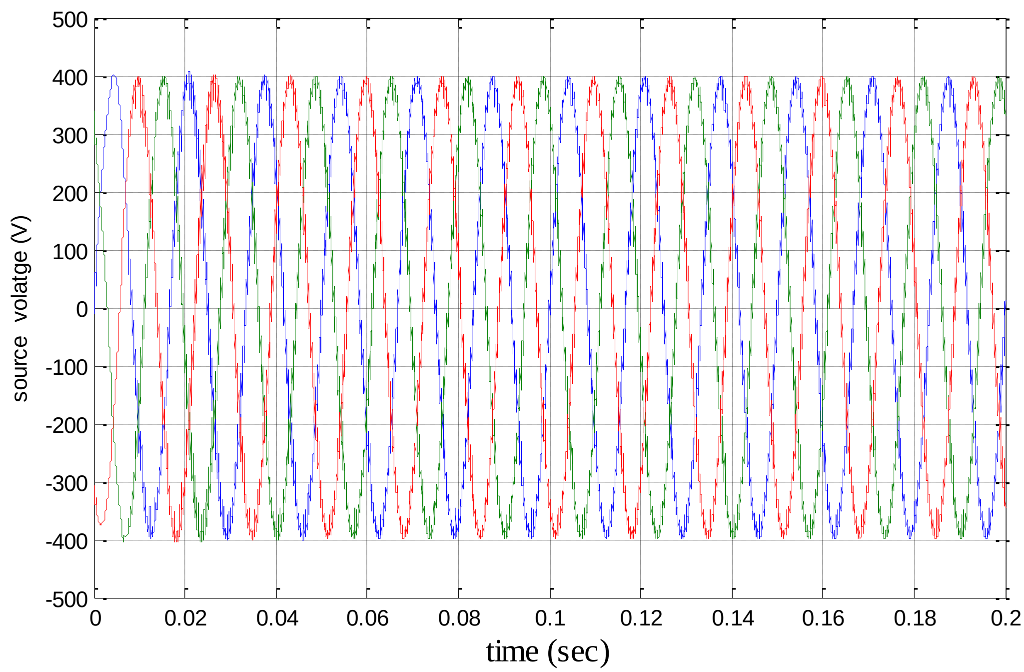

Figure 4.20 Source Voltage Waveform of the System in Case of With SAPF

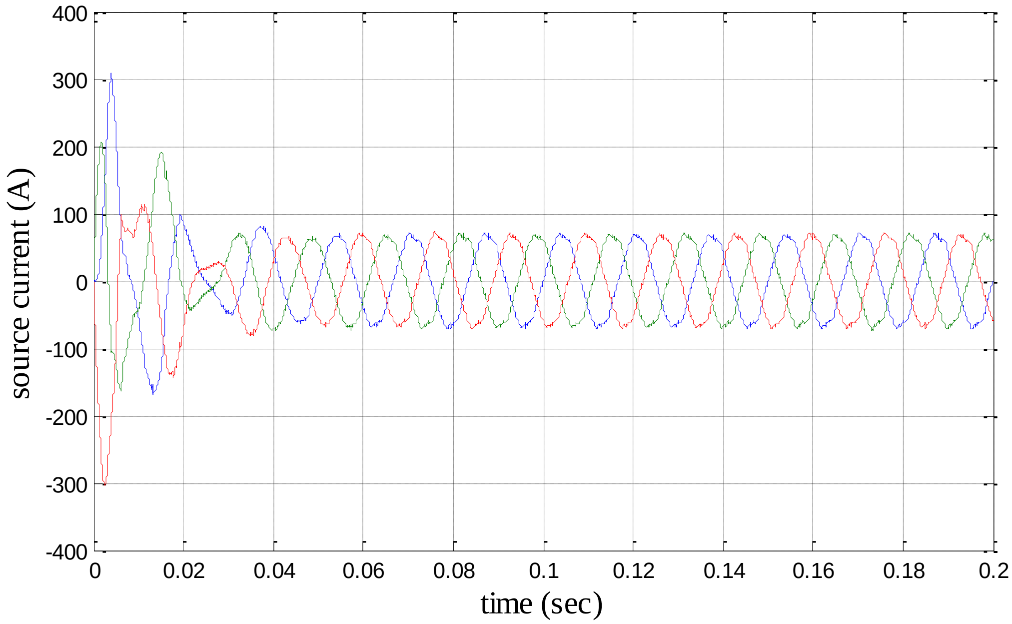

Figure 4.21 Source Current Waveform of the System in Case of With SAPF

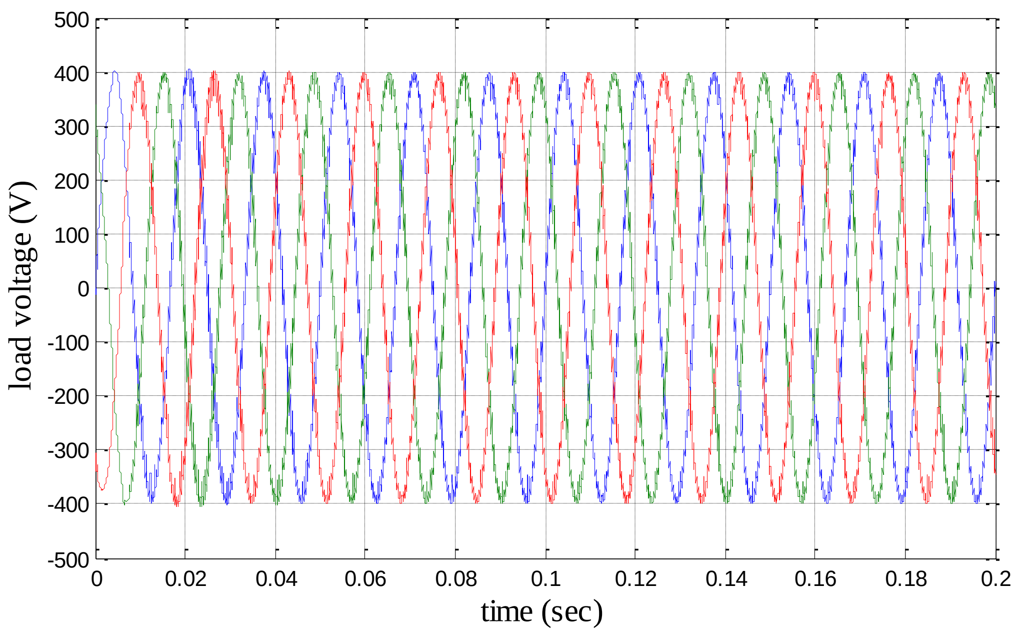

Figure 4.22 Load Voltage Waveform of the System in Case of With SAPF

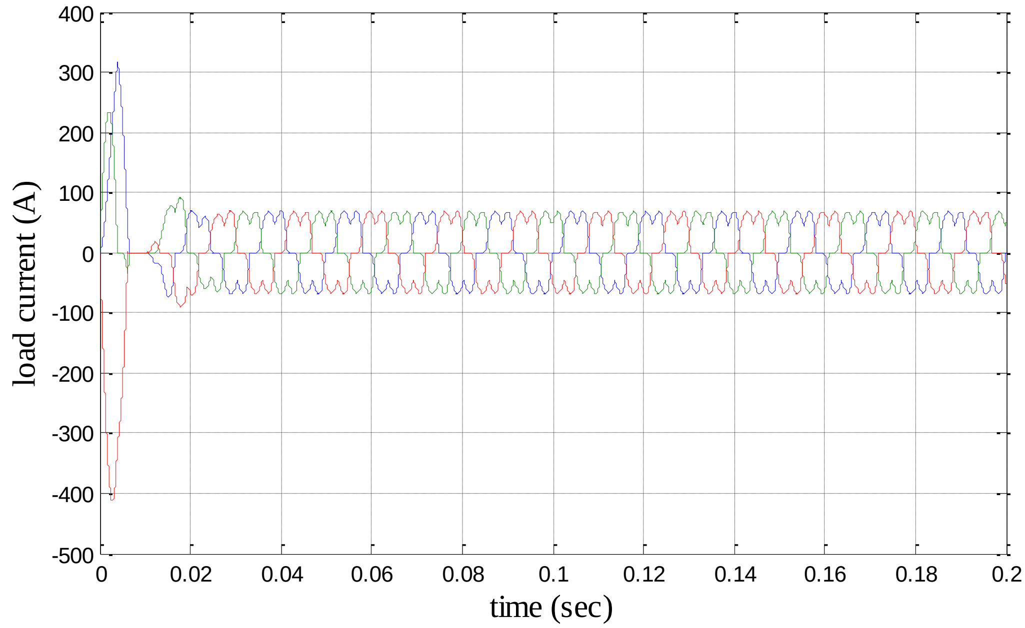

Figure 4.23 Load Current Waveform of the System in Case of With SAPF

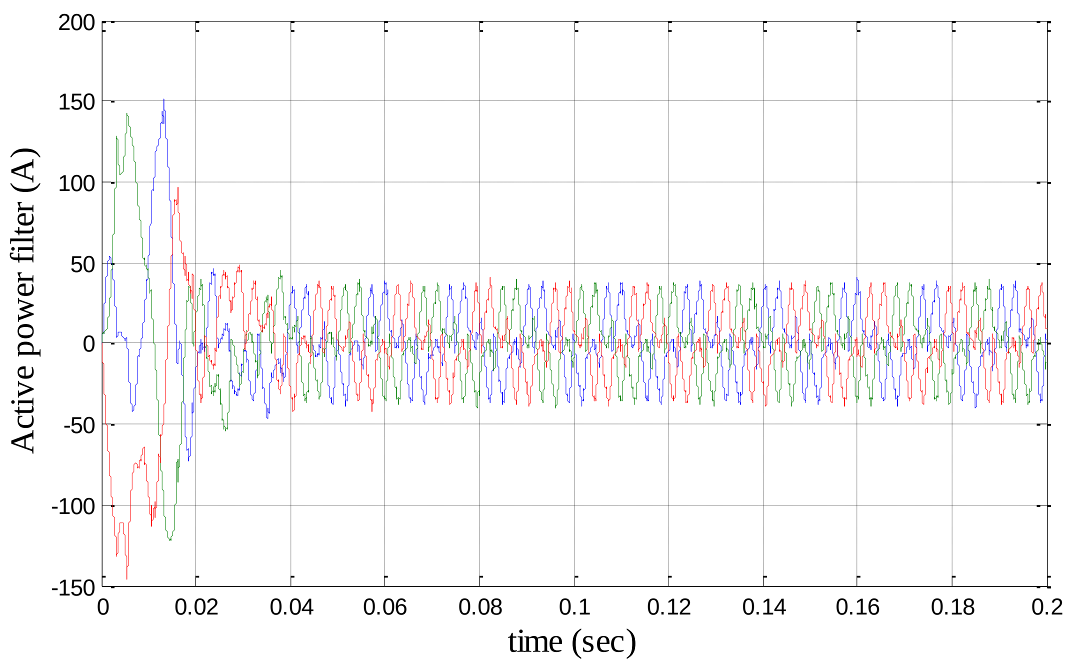

Figure 4.24 Active Power Filter Current Waveform of the System in Case of With SAPF

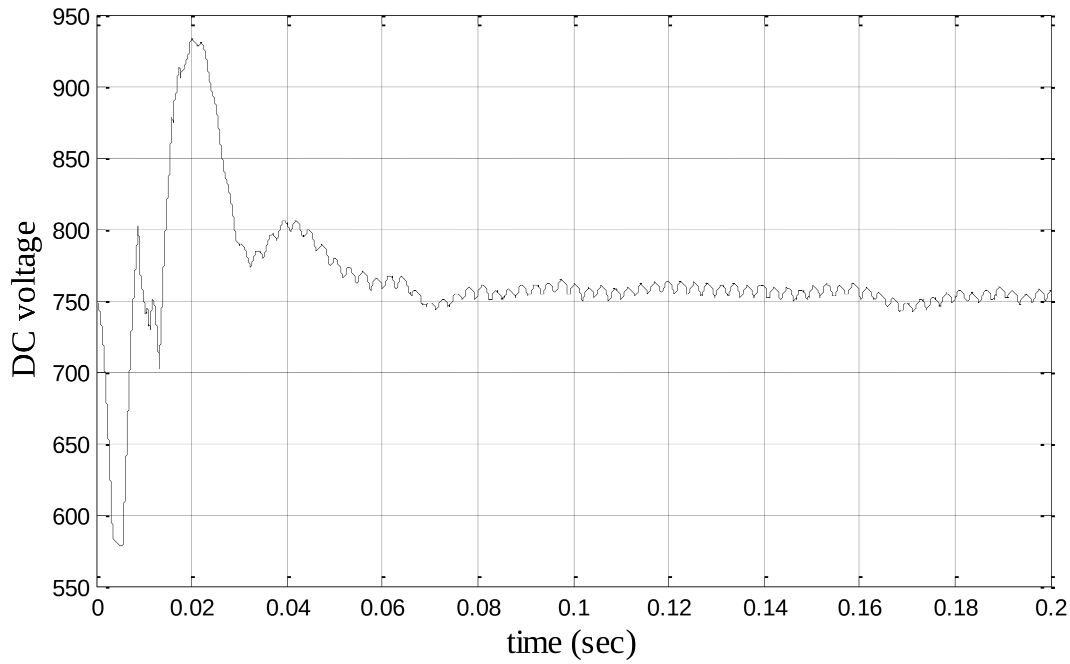

Figure 4.25 DC Voltage Waveform of the System

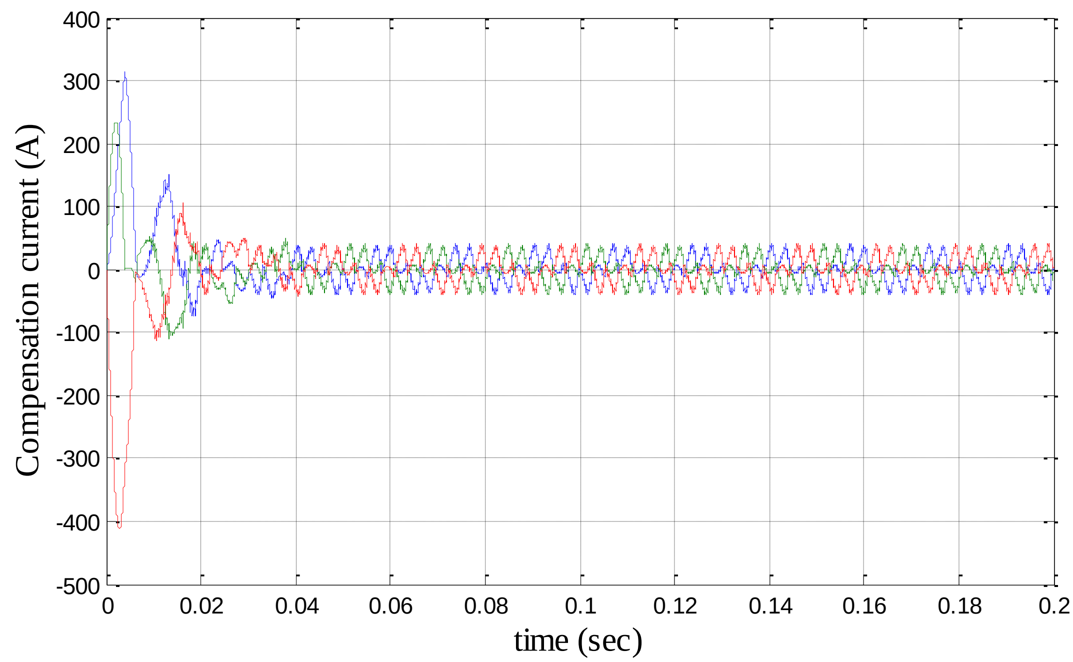

Figure 4.26 Reference Current Waveform of The System in Case of With SAPF

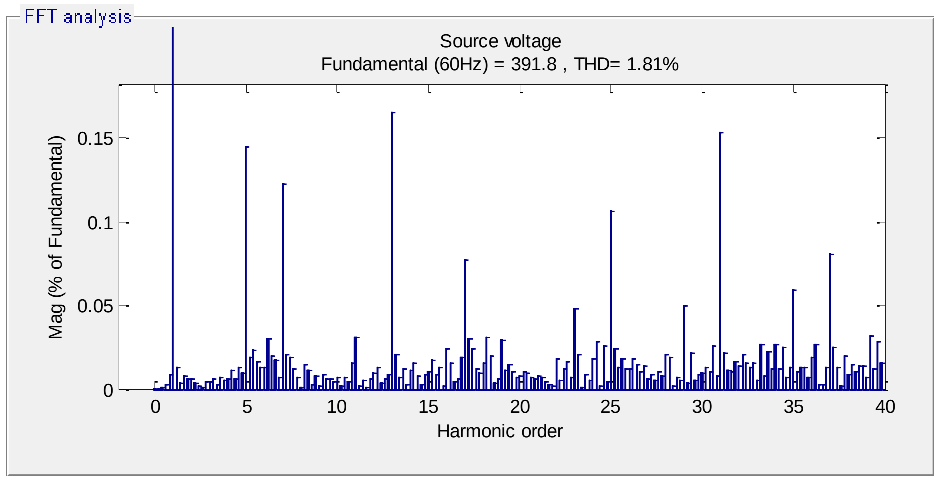

Figure 4.27 THD and Spectrum Analysis of Source Voltage in Case of With SAPF

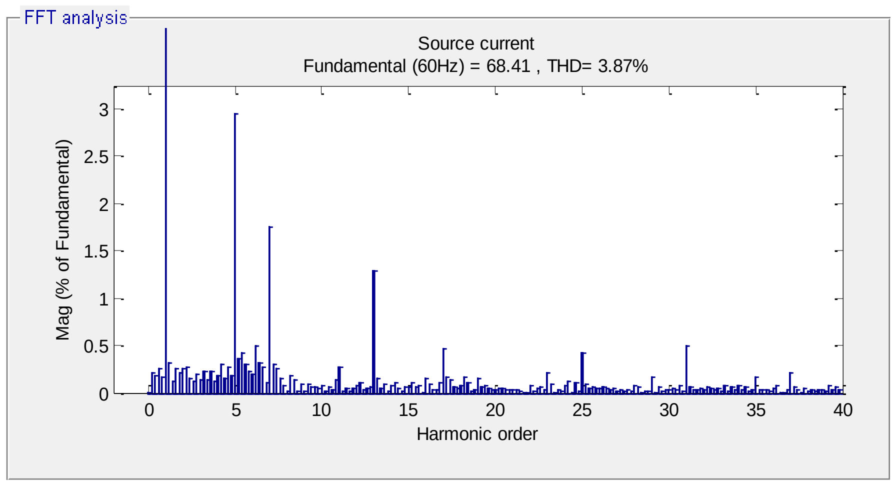

Figure 4.28 THD and Spectrum Analysis of Source Current in Case of With SAPF

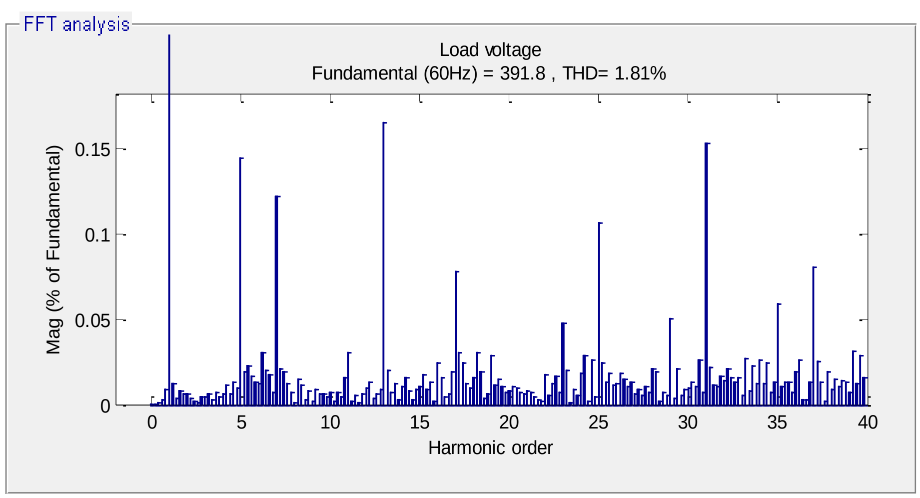

Figure 4.29 THD and Spectrum Analysis of Load Voltage in Case of With SAPF

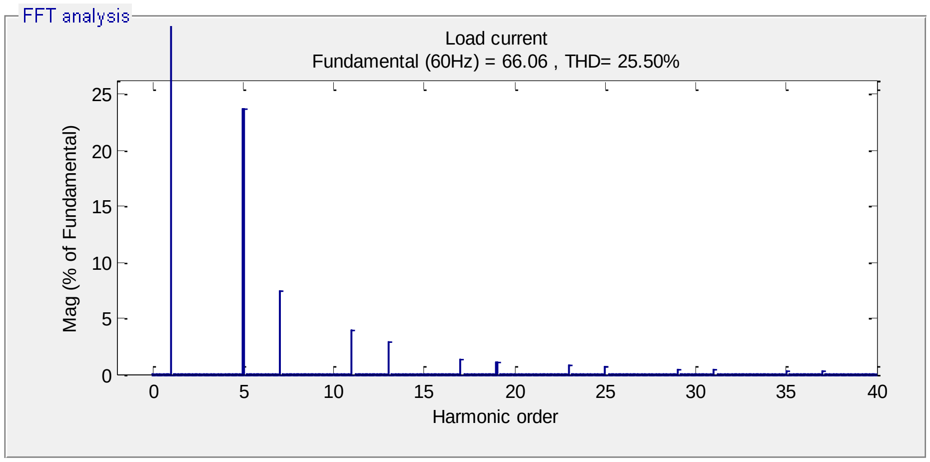

Figure 4.30 THD and Spectrum Analysis of Load Current In Case of With SAPF

Table 4.2 shows a comparison between the two cases for THD analysis of source current. It is clearly seen that the THD of source current after adding SAPF is less than before SAPF.

Table 4.2 Comparison between THD of System Parameters With SAPF and Without SAPF

	Without SAPF	With SAPF
THD for Source current	24.57	3.87

CHAPTER 5

LABORATORY IMPLEMENTATION, RESULTS AND ANALYSIS

In this chapter, Power Distribution System (PDS) system will be experimentally set up and established in the laboratory in order to estimate the real performance. The developed experimental PDS has been established by connecting several components and devices to each other. The main devices used are; distribution panel loads, DC drive, DC motor, mechanical load and active filter, in addition to set of measurement devices will be listed in the following sections. This chapter illustrates the experimental setup preparation in details, THD measurement procedure, and the use of active filter for reducing the harmonics in addition to analyzing the obtained results.

5.1 Components and Devices

This section briefly introduces and describes the components that have been employed in setting up the PDS in order to measure the THD under different conditions and cases.

5.1.1 DC Drive

This drive characterizes with process interface and common user with field-bus. It is also supported by familiar software tools used for sizing, maintenance, and commissioning, in addition to familiar spare parts. This type of drive module is DCS800. It can be used for different applications in the industrial field. All demanding requirements of various applications are met by this drive, such as: rolling mill, mine hoist, testing, in addition to the applications of non-motoric types, such as; electrolysis, battery charger, magnetic, etcetera. Application software maybe also included within DCS800. Table 5.1 summarizes the characteristics of the DC drive used during the laboratory experiments [85].

Table 5.0.1 Characteristics of DC Drive

ABB Drive(DCS 800)			
U_f	3-400 V	U_z	415 V
I_f	20 A	I_z	25 A
F_f	50/60 Hz	I_p	6 A

5.1.2 DC Motors

Table 5.2 illustrates the characteristics of the DC motor used throughout the experimental set up.

Table 5.0.2 Characterstics of DC motor

DC motor	
220/135 V	4.8/5.6/5.4
0.75 kW	2040/1700 U/min
U_{err}=200 V	I_{err}=0.24 A

5.1.3 Active Filters

Power quality is associated with distortion, frequency and amplitude in the supply system. The frequency and amplitude of the supply can be controlled and managed by the utility, while the waveform distortion is usually caused by the loads or the user. A sinusoidal current is usually drawn by the linear loads and it follows the supplied voltage wave-shape. On the other hand, the drawn current by non-linear loads does not follow the supplied voltage wave-shape; this will in turn distort the signal.

Via Power Quality Filters (PQF), the network can be cleaned effectively from the harmonics, in addition to providing load balancing and smooth compensation for the reactive power. PQFS are appropriate to be connected to electrical networks without and with neutral. Its compact design makes it suitable for installation in almost any location, especially when space is limited. The modularity of PQFS consists of a single master in addition to up to three units of slave type. The specification of the used ABB filter is summarized in Table 5.3 [86].

Table 5.0.3 Characteristics of Active Filter

LV Active Filter (PQFS)			
U_e	208-415 V	Ui	415 V
/n	30 A	Prot. Degree	IP30
Cat.:		**-5/40 ^{o} C**	

5.1.4 PQF Link Software and Oscilloscope

This software provides direct control, monitoring and programming capability from a PC via an RS-232 serial port. All PQF-link features can be directly accessed via clicking on the shortcut menu icons. Different features are obtainable depending on the user's login level. "Mixed domain oscilloscope MDO4000B series (Tektronix)" is another measurement tool used during the evaluation [87].

5.2 Experimental Setup

All previously mentioned devices and tools were used to construct the experimental setup so that the results of the THD could be recorded and compared to the simulation results. Figure 5.1 and Figure 5.2 illustrates the experimental set up after connecting these devices together and the equipment that used respectively.

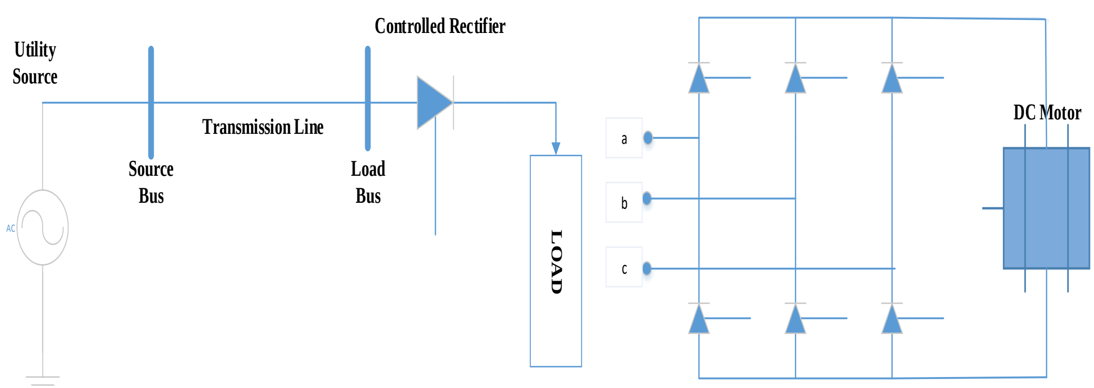

Figure 5.1 Experimental Setup Connections

Figure 5.2 Experimental Equipment used

5.3 Experimental Results

Several cases are considered in order to estimate the performance of the PDS in terms of the THD.

5.3.1 Original Voltage from Utility without AF

The evaluation of the THD will be performed considering only one bus connected to the PDS. The estimation will be done with and without connecting the active filter. Figure 5.3 illustrates the original voltage obtained from utility before connecting the AF with the PDS.

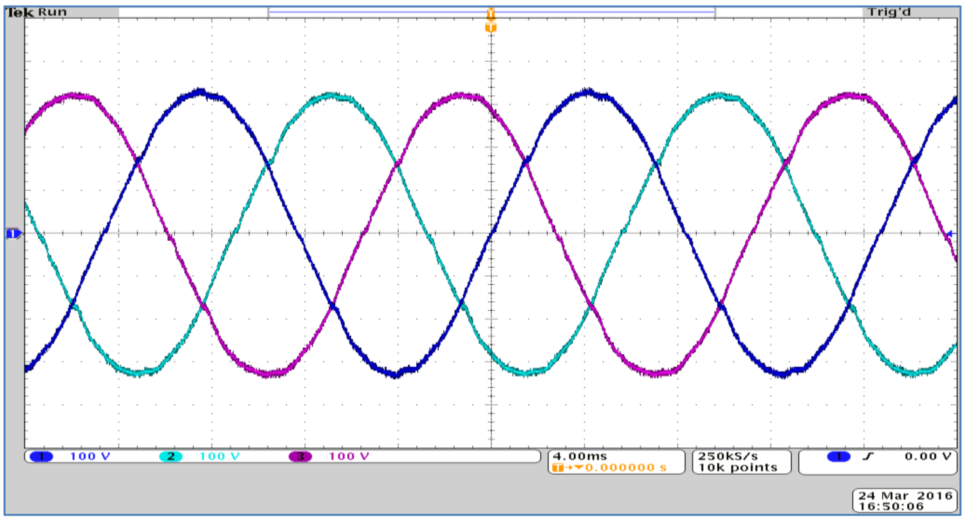

Figure 5.3 Original Voltage Obtained Form Utility before Connecting AF

The spectrum was measured under these conditions and the obtained results are as shown in Figure 5.4.

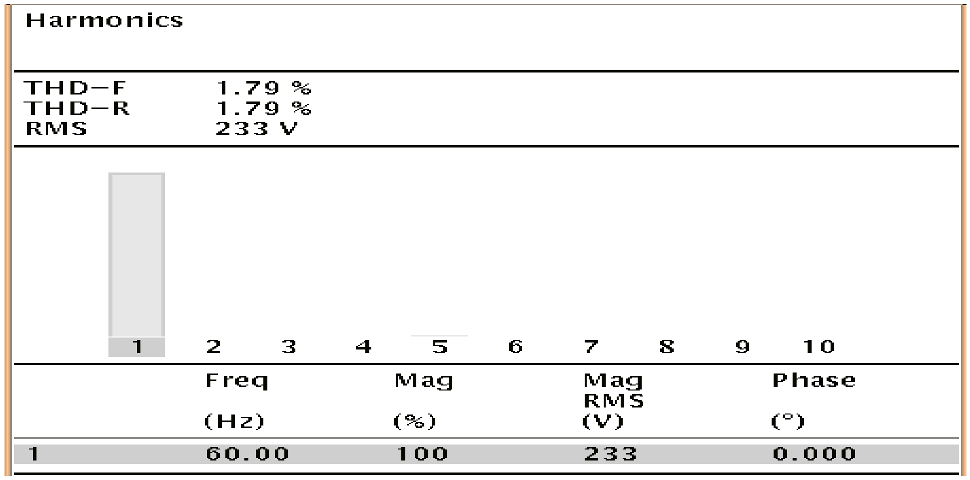

Figure 5.4 Harmonic Spectrums Before Connecting the AF.

According to Fig. 5.4, the obtained value for the THD is 1.79%. Practically, the THD value fluctuates from 1.68% to 1.85%. Since the THD is less than the standard IEEE limits, then it can be assumed that the performance of the PDS will be acceptable.

5.3.2 Original Voltage from Utility with AF

The second case that was considered during the evaluation was to measure the THD when the AF is connected to the PDS, but before being turned on. This has been done to verify the effect of the active filter itself. The filter absorbs around 6 ampere, which will affect the study because the load is small, and cannot exceed 4.8 ampere. The obtained signal voltage under this condition is illustrated in Figure 5.5.

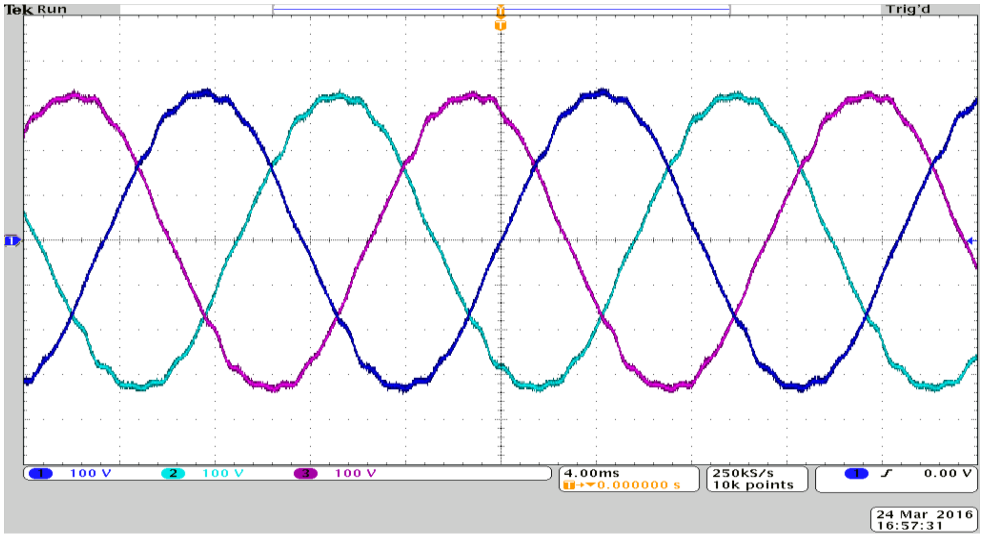

Figure 5.5 Original Voltage Obtained from Utility after Connecting AF

According to Fig.5.5, more distortion occurred with the original voltage signal. The spectrum values were measured under these conditions and the obtained results was as shown in Figure 5.6.

Harmonics

THD−F	2.34 %
THD−R	2.34 %
RMS	233 V

	Freq (Hz)	Mag (%)	Mag RMS (V)	Phase (°)
1	60.00	100	233	0.000
2	120.0	13.8m	32.3m	779.6m
3	180.0	660m	1.54	94.00
4	240.0	18.1m	42.3m	−109.2
5	300.0	1.25	2.92	125.5
6	360.0	36.7m	85.7m	−59.24
7	420.0	378m	882m	157.8
8	480.0	38.3m	89.4m	87.49
9	540.0	478m	1.12	−131.4
10	600.0	10.8m	25.1m	−121.6

Figure 5.6 Harmonic Spectrum Values After Connecting AF.

According to Figure 5.6, connecting the AF increases the THD from 1.79% to 2.34%; this means that the AF circuit increases the THD in the system despite not being turned on yet. Around 0.55 % increase with THD is the contribution of the AF in the System THD.

5.3.3 Effect of Electrical Loading on THD

In this case, the THD is measured with and without AF while varying the load. The goal in this case is to evaluate the behavior of the THD while increasing the load. For all given cases, the source voltage, filter current, source current and load current are estimated. The first load value was selected to be equal to 1.5A. The obtained THD value without AF is as shown in Figure 5.7.

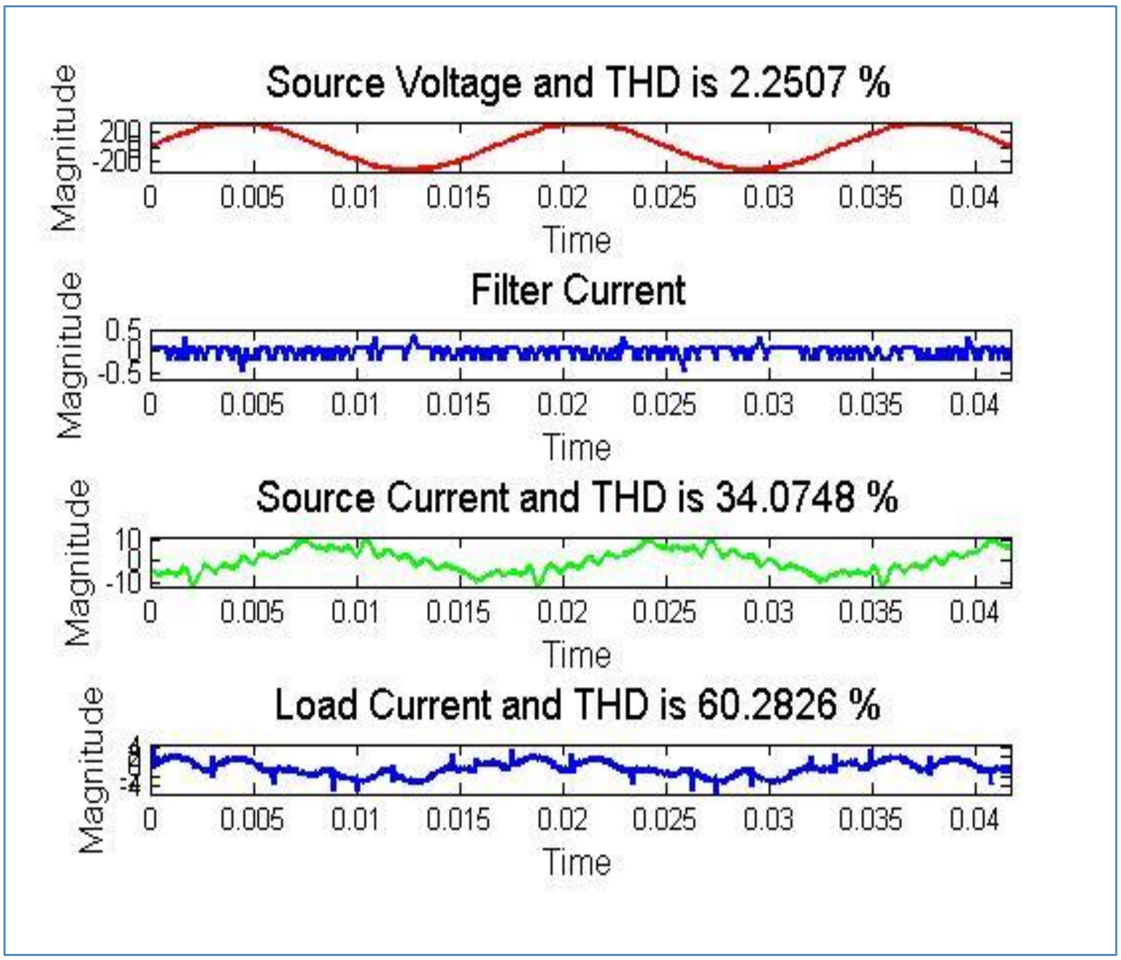

Figure 5.7 Result of 1.5A Load without AF

According to Figure 5.7, 1.5A load results in 2.2507 % THD for the source voltage, 34.07 % for the source current and 60.28 % for the load current. It is clear that the filter current is equal to zero since it is still switched off. After turning on the filter, the obtained results for this load value are as shown in Figure 5.8.

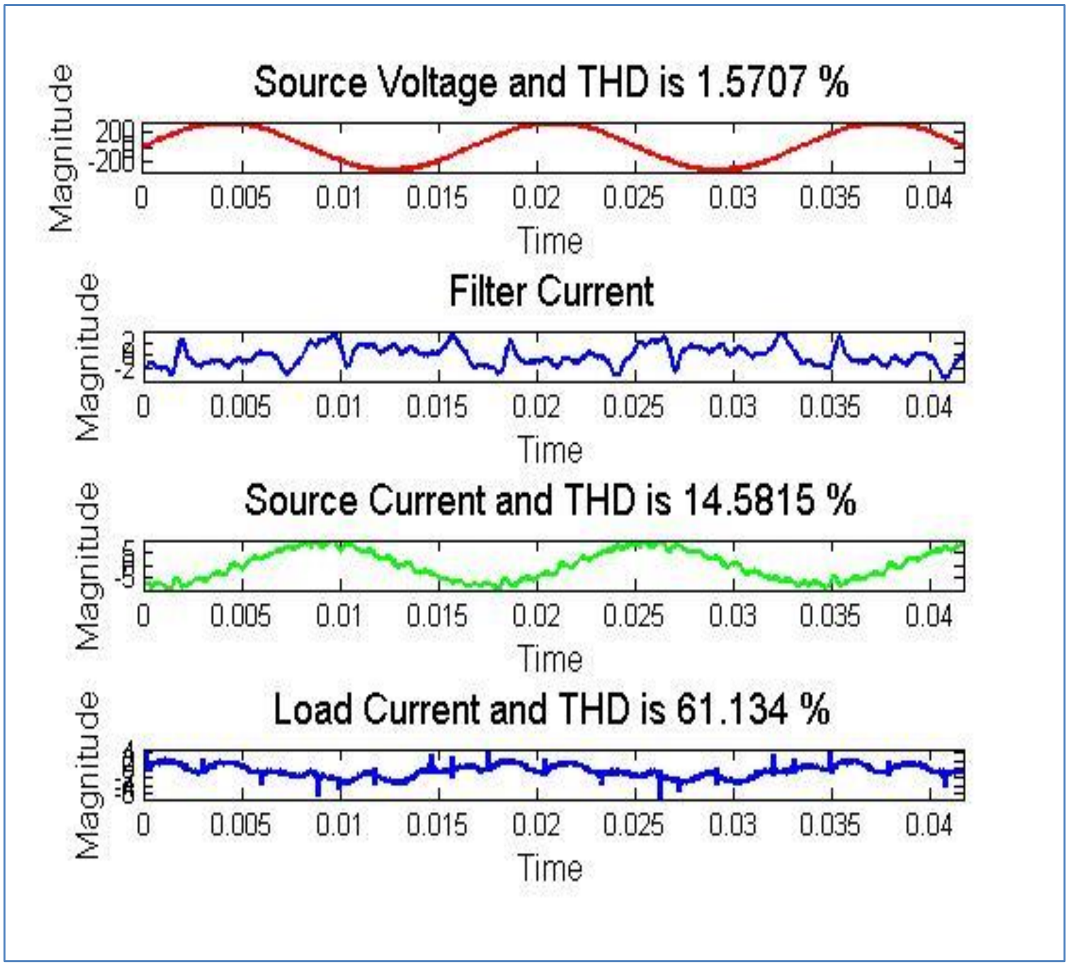

Figure 5.8 Results of 1.5A Load With AF.

Clearly, the THD value decreases to 1.5707 % compared to 2.25 % without using the AF. This means that the AF is effective enough in reducing the THD occurring within the system. The second load value that has been selected throughout the evaluation in this stage is 2.5A. The load was then increased to 3.5A and the THD was also measured. Table 5.4 summarizes the results for different loads with and without AF.

Table 5.0.4 THD Results While Varying the Load With and Without AF

Load (A)	1.5 A	2.5 A	3.5 A
Without Filter	**THD %**		
V_s	2.25	2.35	2.24
I_s	34.08	44.77	57.19
I_L	60.28	42.32	35
With Filter	**THD %**		
V_s	1.57	1.67	1.62
I_s	14.58	18.55	21.95
I_L	61.13	41.51	35.08

According to Table 5.4, increasing the load will results in more THD in the power distribution system. Furthermore, employing the AF was effective in reducing the THD within voltage and current signals. The results illustrate how increasing the load results in more THD value on the source side and decrease at load side. This reduction in the THD on the load side can be considered as harmonic cancelation for this load module (uncontrolled rectifier). Furthermore, both the simulation and experimental results confirmed the effectiveness of the AF in reducing the harmonics.

5.3.4 Effect of Varying the Firing Angle

In this stage, the Thyristor firing angle will be varied between$75°$ and $90°$, and the THD values will be measured and recorded. The selected range of the firing angle was small due to the limitation of the DC drive. Table 5.5 summarizes the obtained THD values for different firing angles.

Table 5.0.5 THD While Varying the Thyristor Firing Angle

THD %		
Firing angle in electrical degree	Current source (I_s)	Voltage Source (V_s)
75^o	34.08	2.25
78^o	38	2.4
80^o	37.3	2.35
82^o	38.37	2.34
86^o	35.94	2.28
90^o	35.48	2.25

As shown in Table 5.5, there was only small fluctuation within the obtained THD values while varying the firing angle. This means that the limitation of the available range, and because of using only one very small load compared to the system, it was difficult to precisely estimate the effect of Thyristor firing angle on THD experimentally.

CHAPTER 6

CONCLUSION AND FUTURE WORKS

6.1 Conclusion

Much significance has been recently given to PDS since it is now applied and adopted in most practical fields for different applications. Ensuring the best achievable performance in these systems is considered an essential concern that has been given a great deal of importance by the researchers and designers throughout the last years. All research performed has the aim of improving the performance of PDS so that the users are satisfied with the provided level of service in terms of different criteria. A common and known phenomenon usually occurred within these systems; the harmonic distortion, which in turns results in bad effects in the overall system performance. Furthermore, these harmonics also cause faults, reduction in the system service life, increase in the system loss, reduction in the power factor and effectiveness of the electric consumption use and increase in the economic loss.

In this thesis, a comprehensive literature review was established. Also, it aimed to estimate and investigate the effect of electrical loading on the THD in PDS for different load types. A PDS module was implemented and simulated in MATLAB/SIMULINK program. An active filter module was also applied in order to reduce the THD in the PDS for one type of load. Different harmonic cancelation cases for the loads, and the sequence of loads running were considered during the investigation. The real performance of PDS was also implemented and discussed via performing the laboratory experiments. The analysis confirmed the compatibility of simulation and experimental results and illustrated the effect of electrical loading conditions on the THD for the PDS. The results also confirmed the effectiveness of the active filter in reducing the THD to be within the acceptable range according to IEEE standards.

The main conclusion of this thesis can be stated as:

- Investigate the harmonic effects for different types of loads in cases of loading and the sequence of loading.
- THD values during the loading depend on the load itself. Some types of loads increased the value of THD when inserting more load of similar types (ARC), and the other is the opposite (controlled and uncontrolled rectifier) can be consider as harmonic cancelation.
- The sequence of running the loads on the system will not affect the final value of THD when all the loads are running.
- The THD is affected by firing angle of the Thyristor rectifier, which reaches its maximum when the firing angle is 60°. From this it is suggested to run the controlled rectifier between approximately $0^{\circ} – 50^{\circ}$.
- A good agreement has been observed between the experimental results and the simulation results for measurement of loading impact and mitigation of harmonics.

6.2 Future Work

As a future work, The cost which saved or lost by changing the level of harmonic during the loading need to be investigated. Also, apply other compensation methods on same system to evaluate their effectiveness in reducing the THD distortion. Moreover, filter capacity can be investigated after harmonic increased or decreased during the loading. For the laboratory work, needs to avoid some limitations in the power quality laboratory, for example:

- Number of DC drives to be able to connect many loads and the study contributes better results
- The size of DC load, since the motor used rated is 4.8A which is less than current absorbed by the filter.
- Offering a filter which can work with programmable AC source (Chroma 61511) since the available filter is not working with it.

References

[1] Ozerdem, O.C., Al-Barrawi, A., Biricik, C., “Measurement and Comparison Analysis of Harmonic Losses In Three Phase Transformers,” *International Journal on Technical and Physical Problems of Engineering (IJTPE),* vol. 5, no. 1, pp. 114-118, March 2013**.**

[2] Chattopadhyay, S., M. Mitra, and S. Sengupta, Electric Power Quality. Springer Science & Business Media, 2011.

[3] Singh, B. A. Chandra, and K. Al-Haddad, Power Quality: Problems and Mitigation Techniques. John Wiley & Sons, 2015.

[4] “IEEE Recommended Practice and Requirements for Harmonic Control in Electric Power Systems.” pp. 1–29, 2014.

[5] K. Deng, J. Cao, P. Guo and X. Xu, “Energy Saving Analysis of Harmonic Suppression in a Distribution Network” In Proc. ICNDC, pp. 121 – 125, 2013.

[6] S. Khalid, Bharti Dwivedi, "Power Quality Issues problems Standards and their Effects in Industry with Corrective Means", International Journal of Advances in Engineering and Technology, vol. 1, no. 2, pp. 1-11, May 2011.

[7] Blajszczak, G. and Antos, P., “Power Quality Park - Idea and Feasibility Study,” *Proc. Of Electric Power Quality and Supply Reliability Conference (PQ),* 16-18 June, pp. 17–22, 2010.

[8] Ryckaert, W.R.A, Chijselen, J.A.L, Desmet, J.J.M, Van den Bossche, A.P.M, Melkebeek, J.A.A and Van deSype, D.M., “The Location Of A Resistive Shunt Harmonic Impeding Along A Distribution Feeder And Its Influence On Harmonic Propagation,” *Electrical Engineering*, vol. 87, pp. 315-326, 2010.

[9] Stevanović, D., and Petković, P., “The Losses At Power Grid Caused By Small Nonlinear Loads,” *Serbian Journal of Electrical Engineering*, vol. 10, no. 1, pp. 209-217, 2013.

[10] A. Gupta and R. Singh, "Computation of Transformer Losses Under the Effects of Non-Sinusoidal Currents," *Advanced Computing: An International Journal (ACIJ),* Vol. 2, No. 6, pp. 91-104, Nov. 2011.

[11] Lalotra, J., Sharma, A., Khan, S., Lehana, P., “To Analysis The Effect Of RLC Load On Harmonic Distortion Of IGBT Based Voltage Stabilization,”

International Journal of Innovative Research in Science, Engineering and Technology, vol. 2, no. 8, pp. 3650-3656, August 2013.

[12] Eduful, G., Jackson E.A., and Cole J.E., “Harmonic Emission Limits and Selecting PCC Location Based on the Type of Distribution System,” *Proceedings of the World Congress on Engineering 2014* Vol I, WCE, London, U.K., 2014.

[13] Mahar, M.A., Uqaili. M.A., and Larik, A.S., “Harmonic Analysis of Ac-Dc Topologies and Their Impacts on Power Systems.” *Mehran University Research Journal of Engineering & Technology*, vol. 30, pp. 173-178, 2011.

[14] Ingale, R., “Harmonic Analysis Using FFT and STFT,” *International Journal of Signal Processing, Image Processing and Pattern Recognition*, vol. 7, no. 4. pp. 345-362, 2014.

[15] Rauma, K., Electrical Resonances and Harmonics in a Wind Power Plant. Master of Science Thesis in Technology. Aalto University School of Electrical Engineering, Espoo, Finland 17th February 2012.

[16] Power Quality Technical Application Guide. Online source, available at www.gentec.ca/stock/fra/power-quality-technical-applicationguide.pdf

[17] Harmonic Management. Online source, available at www.schneider-electric.com.au/.../EIG-Mharmonic-management.pdf

[18] Effects of harmonics - Economic impact. Online source, available at http://www.electricalinstallation.org/enwiki/Effects_of_harmonics_-_Economic_impact

[19] Kusumalatha, Y., Saibabu, Ch., and Obulesu, Y.P., “Minimization of Harmonic Distortion of Industrial Motor Drives with Active Power Filter in Paper Mill - a Case Study,” *Proceedings of The International Multi Conference of Engineers*, vol. 30, March 2012.

[20] Mishra, G. and Gopalakrishna, S., “Design Of Passive High Pass Filter For Shunt Active Power Filter Application,” in *2013 International Conference on Circuits, Power and Computing Technologies (ICCPCT)*, pp. 17–21, March 2013.

[21] Shu, Z., Xie S., Li ″Z Q., “Single-Phase Back-To-Back Converter for Active Power Balancing, Reactive Power Compensation, and Harmonic Filtering in Traction Power System,” *IEEE Trans. on Power Electronics*, vol. 26, no. 2, pp. 334-343, 2011.

[22] Gol, M., Salor O., Alboyac B., Mutluer B., Cadırc I., Ermis M., "A New Field Data-Based EAF Model for Power Quality Studies," *IEEE Trans. On Industry Applications*, vol. 46, no. 3, pp. 1230-1242, 2010.

[23] Lee, T.L., Hu, S.H., "Discrete Frequency-Tuning Active Filter to Suppress Harmonic Resonances of Closed-Loop Distribution Power Systems," *IEEE Trans. on Power Electronics*, vol. 26, no. 1, pp. 137-148, 2011.

[24] Chang, G.W., Liu Y.J., Dinavahi V., Su H.J., "On Real-Time Simulation for Harmonic and Flicker Assessment of an Industrial System With Bulk Nonlinear Loads," *IEEE Trans. on Industrial Electronics,* vol. 57, no. 9, pp. 2998-3009, 2010.

[25] Shuai, Z., Luo A., Zhu W., Fan R., Zhou K., "Study on a Novel Hybrid Active Power Filter Applied to a High-Voltage Grid," *IEEE Trans. on Power Delivery*, vol. 24, no. 4, pp. 2344-2352, 2009.

[26] Akagi, H., Kondo R., "A Transformerless Hybrid Active Filter Using a ThreeLevel Pulsewidth Modulation (PWM) Converter for a Medium-Voltage Motor Drive," *IEEE Trans. on Power Electronics*, vol. 25, no. 6, pp. 1365-1374, 2010.

[27] Lee, K., Blasko V., Jahns T.M., Lipo T.A., "Input Harmonic Estimation and Control Methods in Active Rectifiers," *IEEE Trans. on Power Delivery*, vol. 25, no. 2, pp. 953-960, 2010.

[28] Pragale, R., Dionise T.J., Shipp D.D., "Harmonic Analysis and Multistage Filter Design for a Large Bleach Production Facility," *IEEE Trans. On Industry Applications*, vol. 47, no. 3, pp. 1201-1209, 2011.

[29] Singh, B., Singh S., Chender S.P.H., "Harmonics Mitigation in LCI-Fed Synchronous Motor Drives," *IEEE Trans. on Energy Conversion*, vol. 25, no. 2, pp. 369-380, 2010.

[30] Yong, J., Chen L., Chen S., "Modeling of Home Appliances for Power Distribution System Harmonic Analysis," *IEEE Trans. on Power Delivery,* vol. 25, no. 4, pp. 3147-3155, 2010.

[31] Zhao, W., Luo A., Shen Z.J., Wu C., "Injection-Type Hybrid Active Power Filter in High-Power Grid with Background Harmonic Voltage," *IET Power Electronics,* vol. 4, no. 1, pp. 63–71, 2011.

[32] Akagi, H., Isozaki K., “A Hybrid Active Filter for a Three-Phase 12-Pulse Diode Rectifier Used as the Front End of a Medium-Voltage Motor Drive,” *IEEE Trans. on Power Electronics*, vol. 24, no. 1, pp. 69-77, 2012.

[33] Farooq, H., Zhou, C., Farrag, M.E., “Analyzing the Harmonic Distortion in a Distribution System Caused by the Non-Linear Residential Loads, International Journal of Smart Grid and Clean Energy,” vol 2, no. 1, pp. 46-51, 2013.

[34] Attia, H.A., El-Metwally, M., and Fahmy, O.S., “Harmonic Distortion Effects and Mitigation in Distribution Systems,” *Journal of American Science,* vol. 6, no. 10, pp. 173-183, 2010.

[35] Lalotra, J., Khan, S., Sharma, S., and Lehana, P., “Investigation of the Effect of Inductive Load on Harmonic Distortion of IGBT based Power System”, *International Journal of Engineering and Advanced Technology (IJEAT),* vol. 2, no. 5, pp. 423-426 une 2013.

[36] Bhattacharyya, S., Cobben, J.F.G., and Kling, W.L., “Harmonic Current Pollution in a Low Voltage Network”, In Proc. IEEE PES General Meeting, 2010.

[37] K. D. McBee, M. G. Simões, "Evaluating the long-term impact of a continuously increasing harmonic demand on feeder level voltage distortion", IEEE Trans. Industrial Applicat., vol. 50, no. 3, pp. 2142-2149, May–Jun. 2014.

[38] Kaushik, A. and Varanasi, J., “Harmonic Voltage Distortions in Power Systems due to Non Linear Loads”, *International Journal of Applied Power Engineering (IJAPE)*, vol. 3, no. 1, pp. 67-74, April 2014.

[39] A. Lagar , G. N. Popa , C. M. Dinis , “ The influence of home nonlinear electric equipment operating modes on power quality ”, WSEAS Trans. on Syst., vol. 13, pp. 357 – 367, 2014.

[40] Ghorbani, M.J., and Mokhtari, H., “Impact of Harmonics on Power Quality and Losses in Power Distribution Systems”, *International Journal of Electrical and Computer Engineering,* vol. 5, no. 1, pp. 166-174, 2015.

[41] M. S. Witherden, R. Rayudu, R. Rigo-Mariani, "The influence of nonlinear loads on the power quality of the New Zealand low voltage electrical power distribution network", 20th Australasian Universities Power Engineering Conference (AUPEC), pp. 1-6, 2010.

[42] Kocatepe, C., Yumurtacı, R., Arıkan, O., Baysal, M., Kekezoğlu, B., Altuğ Bozkurt, A., and C. Fadıl Kumru, C.F., Chapter Seven: Harmonic Effects of

Power System Loads: An Experimental Study, Power Quality Issues, pp. 1750-2000, 2013.

[43] Khandakji, K.A., “Effect of Loading of VSI-Fed Three-Phase Induction Motor on the Line Current THD,” *Jordan Journal of Electrical Engineering JJEE,* vol. 2, no. 1, pp. 53-60, 2016.

[44] Olikara, K., “Power Quality Issues, Impacts, and Mitigation for Industrial Customers,” Rockwell automation, 2015.

[45] Collin, A.J., Djokic, S.Z., Cresswell, C.E., Blanco, A.M., Meyer, J., “Cancellation of Harmonics Between Groups of Modern Compact Fluorescent Lamps,” *International Symposium on Power Electronics, Electrical Drives, Automation and Motion*, pp. 1170-1175, 2014.

[46] Meyer, J., Scegner, P., and Heidenreich K., ”Harmonic Summation Effects Of Modern Lamp Technologies And Small Electronic Household Equipment,” presented at CIRED, Frankfurt, Germany, Jun. 2011.

[47] Collin, A.J.,”Advanced Load Modelling For Power System Studies, Ph.D. thesis, Inst. for Energy Syst ., Univ. Edinburgh, Edinburgh, UK, 2013.

[48] A. J. Collin, C. E. Cresswell and S. Z. Djokic, "Harmonic Cancellation of Modern Switch-Mode Power Supply Load," presented at 14th IEEE International Conference on Harmonics and Quality of Power, ICHQP, Bergamo, Italy, Sept. 26 - 29, 2010.

[49] Collin, A. J. and Djokić S.Z., “Voltage Disturbances and Inrush Current of DC Power Supplies,” presented at *The International Conference of Renewable Energy and Power Quality (ICREPQ),* Granada, vol. 1, no. 8, pp. 869-875, March 23-25, 2010.

[50] Mazin, H. E., Gallant, J., “A Probabilistic Analysis on the Harmonic Cancellation Characteristics of the Scott Transformer,” *J. Electromagnetic Analysis & Applications*, vol. 2, pp. 18-24, 2010.

[51] Harrasi, A., Zobaa, A.F., “A Cost Effective Harmonic Cancellation Method For High Frequency Silicon Carbide MOSFET Based Single Phase Inverter, *IEEE Power and Energy Technology Systems Journal*, 2016.

[52] K Dartawan, L. Hui, R Austria et al., "Harmonics issues that limit solar photovoltaic generation on distribution circuits[C]", World Renewable Energy Forum & Colorado Renewable Energy Society (CRES) Annual Conference, pp. 2292-2298, 2012.

[53] IEEE Recommended Practices and Requirements for Harmonic Control in Electrical Power Systems, IEEE Std 519TM 2014.

[54] Heydt, G.T., Electric power quality. Stars in a circle publications, 1994.

[55] Schoene, J., and EnerNex, Evaluation of the Impact on Non Linear Power On Wiring Requirements for Commercial Buildings, Final Report, Quincy, MA, USA, The Fire Protection Research Foundation, 2011.

[56] F. Barrero, Martinez S., Yeves F., and Martinez P. M., “Active Power Filters For Line Conditioning: A Critical Evaluation,” *IEEE Trans. Power Deliv.*, vol. 15, no. 1, pp. 319–325, 2000.

[57] EL-Kholy E.E., EL-Sabbe A., El-Hefnawy A., and Mharous H.M., “Three-Phase Active Power Filter Based On Current Controlled Voltage Source Inverter,” *Int. J. Electr. Power Energy Syst.*, vol. 28, no. 8, pp. 537–547, Oct. 2006.

[58] Mesbahi N., Ouari A., Ould Abdeslam D., Djamah T., and Omeiri A., “Direct Power Control Of Shunt Active Filter Using High Selectivity Filter (HSF) Under Distorted Or Unbalanced Conditions,” *Electr. Power Syst. Res.*, vol. 108, pp. 113–123, Mar. 2014.

[59] Kmail, M., “Investigation Of Shunt Active Power Filter For Power Quality Improvment,” NEAR EAST, 2012.

[60] Abellan A., Benavent J.M., Garcera G., and Cerver D., “Fixed Frequency Current Controller Applied To Shunt Active Filters With UPF Control In Four-Wire Power Systems,” in *IEEE 2002 28th Annual Conference of the Industrial Electronics Society. IECON 02*, vol. 1, pp. 780–785, 2002.

[61] Hussien Z.F., Atan N., and Abidin I.Z., “Shunt Active Power Filter For Harmonic Compensation Of Nonlinear Loads,” in *Proceedings. National Power Engineering Conference, 2003. PECon 2003*., pp. 117–120, 2003.

[62] Agarwal, P,. and Gupta H.O., “Modeling Of Frequency Domain Control Of Shunt Active Power Filter Using MATLAB Simulink and Power System Blockset,” in *2005 International Conference on Electrical Machines and Systems,* vol. 2, pp. 1124–1129, 2005.

[63] Fathi S.H., Pishvaei M., and Gharehpetian G.B., “A Frequency Domain Method for Instantaneous Determination of Reference Current in Shunt Active Filter,” in *TENCON 2006 - 2006 IEEE Region 10 Conference*, pp. 1–4, 2006.

[64] Liu, H., Liu, G., and Shen, Y., "A Novel Harmonics Detection Method Based on Wavelet Algorithm for Active Power Filter," in *2006 6th World Congress on Intelligent Control and Automation*, vol. 2, pp. 7617–7621, 2006.

[65] Forghani, M., and Afsharnia S., "Online Wavelet Transform-Based Control Strategy for UPQC Control System," *IEEE Trans. Power Deliv.*, vol. 22, no. 1, pp. 481–491, Jan. 2007.

[66] Lee T.-S., Tzeng K.-S., and Chang C.-J., "A Repetitive Control Approach For Three-Phase Shunt Active Power Filters With Real-Time Wavelet Transform," in *2009 International Conference on Power Electronics and Drive Systems (PEDS)*, pp. 376–380, 2009.

[67] Kamble S.Y., Mate S.N., and Waware M.M., "Online Wavelet Based Control Algorithm For Shunt Active Power Filter operation," in *2013 IEEE International Conference on Control Applications (CCA)*, pp. 1153–1158, 2013.

[68] Ijaz, M., "Harmonic Detection and Mitigation in Power Systems Using Wavelet Packet Transform", King Fahd University of Petroleum & Minerals Dhahran-31261, Saudi Arabia, Master thesis, May, 2015.

[69] Akagi H., Kanazawa Y., and Nabae A., "Instantaneous Reactive Power Compensators Comprising Switching Devices without Energy Storage Components," *IEEE Trans. Ind. Appl*., vol. IA-20, no. 3, pp. 625–630, May 1984.

[70] Noguchi T., Tomiki H., Kondo S., and Takahashi I., "Direct Power Control Of PWM Converter Without Power-Source Voltage Sensors," *IEEE Trans. Ind. Appl*., vol. 34, no. 3, pp. 473–479, 1998.

[71] Benhabib M. C., and Saadate S., "New Control Approach For Four-Wire Active Power Filter Based On The Use Of Synchronous Reference Frame," *Electr. Power Syst. Res.*, vol. 73, no. 3, pp. 353–362, Mar. 2005.

[72] Soares V., Verdelho P., and Marques G.D., "An Instantaneous Active And Reactive Current Component Method For Active Filters," *IEEE Trans. Power Electron*., vol. 15, no. 4, pp. 660–669, Jul. 2000.

[73] Kale M.. and Ozdemir E., "A Novel Adaptive Hysteresis Band Current Controller For Shunt Active Power Filter," in *Proceedings of 2003 IEEE Conference on Control Applications, 2003. CCA*, vol. 2, pp. 1118–1123, 2003.

[74] Panda G., Dash S. K., and Sahoo N., "Comparative Performance Analysis Of Shunt Active Power Filter And Hybrid Active Power Filter Using FPGA-Based

Hysteresis Current Controller," in *2012 IEEE 5th India International Conference on Power Electronics (IICPE)*, pp. 1–6, 2012.

[75] Panda A.K., Suresh M., and Suresh Y., "Real-time Implementation Of Adaptive Fuzzy Hysteresis-Band Current Control Technique For Shunt Active Power Filter," *IET Power Electron.*, vol. 5, no. 7, pp. 1188–1195, Aug. 2012.

[76] Chauhan, S.K., and Tekwani, P.N., "Current Error Space Phasor Based Hysteresis Controller For Two-Level And Three-Level Converters Used In Shunt Active Power Filters," in *IECON 2013 - 39th Annual Conference of the IEEE Industrial Electronics Society*, pp. 8522–8527, 2013.

[77] Swain S., Panda P.C., and Subudhi B.D., "Three Phase Shunt Active Power Filter Using A New Weighted Adaptive Hysteresis Band Current Controller," in *2014 International Conference on Circuits, Power and Computing Technologies [ICCPCT-2014]*, pp. 781–786, 2014.

[78] Komurcugil H., "Double-Band Hysteresis Current-Controlled Single-Phase Shunt Active Filter For Switching Frequency Mitigation," *Int. J. Electr. Power Energy Syst.*, vol. 69, pp. 131–140, Jul. 2015.

[79] Gautam, S., and Gupta, R., "Three-Level Inverter Based Shunt Active Power Filter Using Generalized Hysteresis Current Control Method," in *2010 International Conference on Power, Control and Embedded Systems*, pp. 1–6, 2010.

[80] Ribeiro R.L. de A., Rocha T. de O.A., de Sousa R.M., dos Santos E.C., and Lima A.M.N., "A Robust DC-Link Voltage Control Strategy to Enhance the Performance of Shunt Active Power Filters Without Harmonic Detection Schemes," *IEEE Trans. Ind. Electron.*, vol. 62, no. 2, pp. 803–813, Feb. 2015.

[81] Rahmani S., Mendalek N., and Al-Haddad K., "Experimental Design of a Nonlinear Control Technique for Three-Phase Shunt Active Power Filter," *IEEE Trans. Ind. Electron.*, vol. 57, no. 10, pp. 3364–3375, Oct. 2010.

[82] Chen W., Chen W., Ma X., Chen J., Wang Z., and Han Y., "An Adaptive Noise Canceling Theory Based Single-Phase Shunt Active Power Filter," in *Proceedings of Power Conversion Conference - PCC '97*, vol. 1, pp. 191–196, 1997.

[83] Zaro, F.R., "Efficient Techniques for Detection and Mitigation of Power Quality Events," King Fahd University of Petroleum and Minerals University, Dhahran, Saudi Arabi, 2013.

[84] H. AKAGI, "Modern active filters and traditional passive filters", Bulletin of The Polish Academy of Sciences Technical Sciences Vol. 54, No. 3, 2006.

[85] DCS800 Industrial DC drives.Available at http://new.abb.com/ drives/dc/dcs800-s

[86] Power Quality Filters PQFI-PQFM-PQFS. Available at http://new.abb.com/ high-voltage/capacitors/lv/power-quality-filters.

[87] Mixed domain oscilloscope MDO4000B series (Tektronix). Available at http://www.tek.com/ datasheet/mdo4000/mdo4000b-series-datasheet-0

APPENDIX A

System Configuration

The data of used system as shown in MATLAB R2010a demo:

Source voltage:

25 KV, 100 MVA, 60Hz

Feeder 1:

21 Km, 60 Hz, 0.1153 Ω/Km, 1.048e-3 H/Km, 11.33e-9F/Km.

Feeder 2:

2 Km, 0.2306 Ω/Km, 2.096e-3 H/Km.

Step down transformer:

Nominal Power=6 MVA

Primary line voltage= 25 KV

Primary resistance= 0.00083334 PU

Primary inductance= 0.05 PU

Secondary line voltage= 600V

Secondary resistance= 0.00083333 PU

Secondary inductance= 0 PU

Magnetizing resistance= 500 PU

Magnetizing reactance= 500 PU

APPENDIX B

Data of four Modules of load

Arc Load:

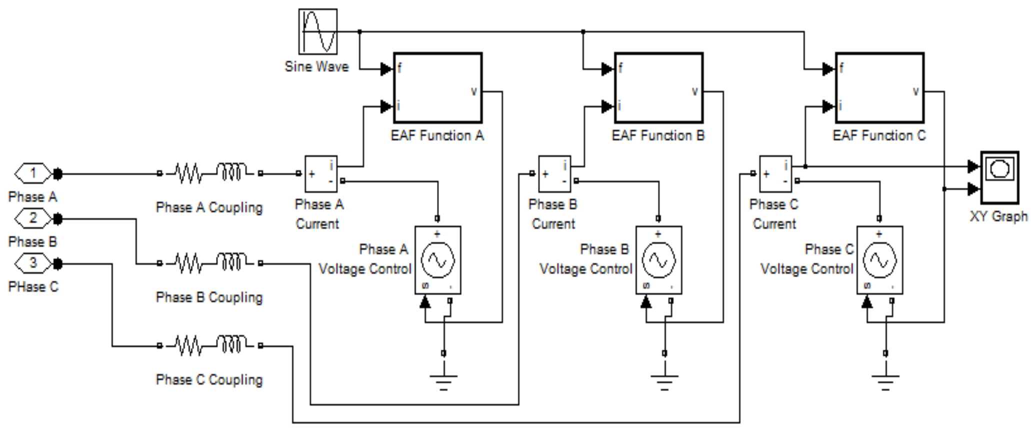

Figure B.1 Arc Load MATLAB Module

1- Number of Arc for (25% Full load)=6 unit

2- Number of Arc for (50% Full load) =12 unit

Data of 1 unit:

V=566 v, C=1.68e6, D=20.65e3, m=0.2, Vat0=289.75

Controlled Rectifier Load:

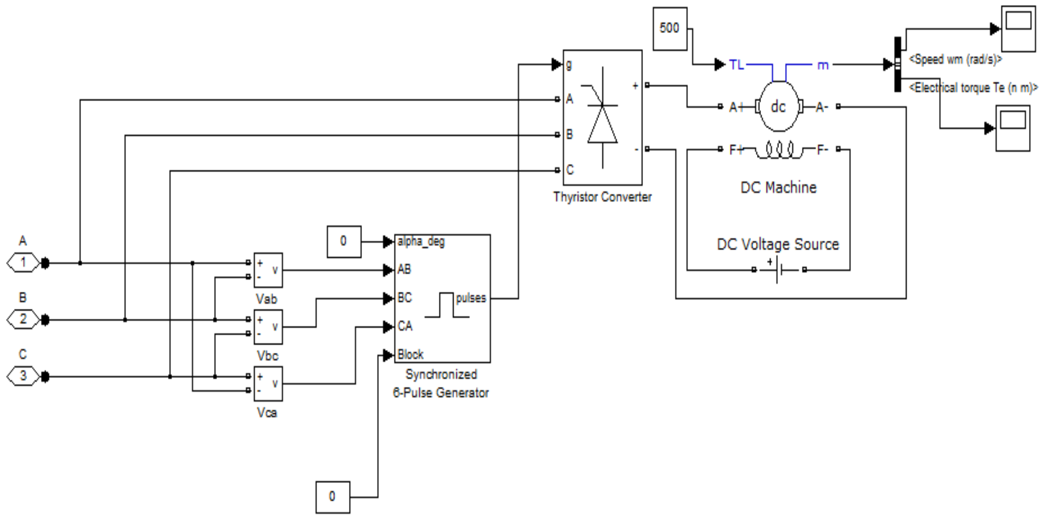

Figure B.2 Controlled Rectifier MATLAB Module

1- Number of rectifier for (25% Full load)=3 unit
2- Number of rectifier for (50% Full load) =6 unit

Data of 1 unit:

250 HP, 500 V,Speed=1750 rpm, Field voltage=300 V, Ra=0.06727 Ω, La=0.001882 H, Lf=3.166 H, Rf=0.2641Ω

Inertia= 1.019 Kg.m^2, Viscous friction coefficient =0.02516, rating torque=1020 N.m, Loading torque=500N.m

Diode rectifier load:

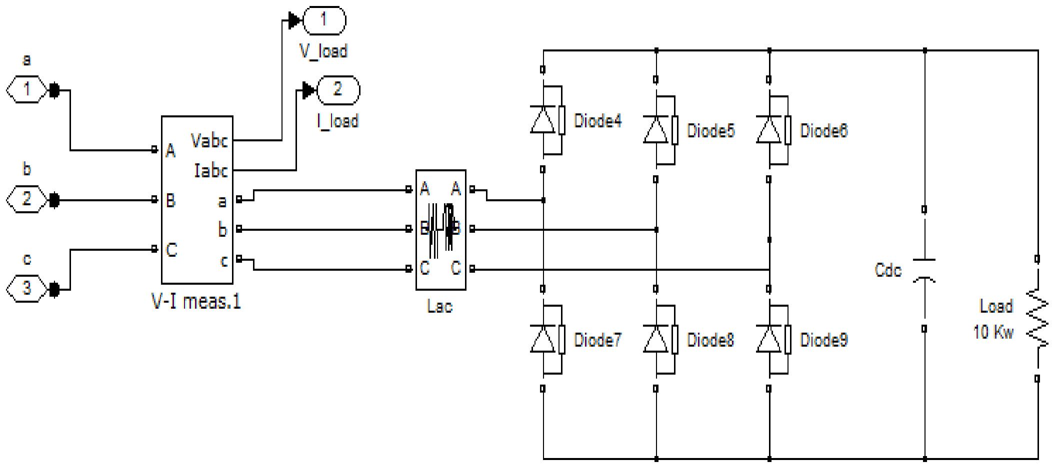

Figure B.3 Diode Rectifier Load MATLAB Module

1- Number of Diode rectifier unit for (25% Full load)=27 unit
2- Number of Arc for (50% Full load) =54 unit

Data of 1 unit:

Load resistance=10 ohm, Line to line voltage =600 volt, 55 KVA rating.

VFD load:

200 HP=149 Kw, Rs= 0.02475 Ω, Ls= 0.000284 H, Rr= 0.0133 Ω, Lr= 0.000284 H, Lm= 0.01425 H, J= 2.6 Kg.m^2, N=1785 rpm, F= 60 Hz, Vs=575 (V), rating torque=800 N.m, Loading torque=500N.m

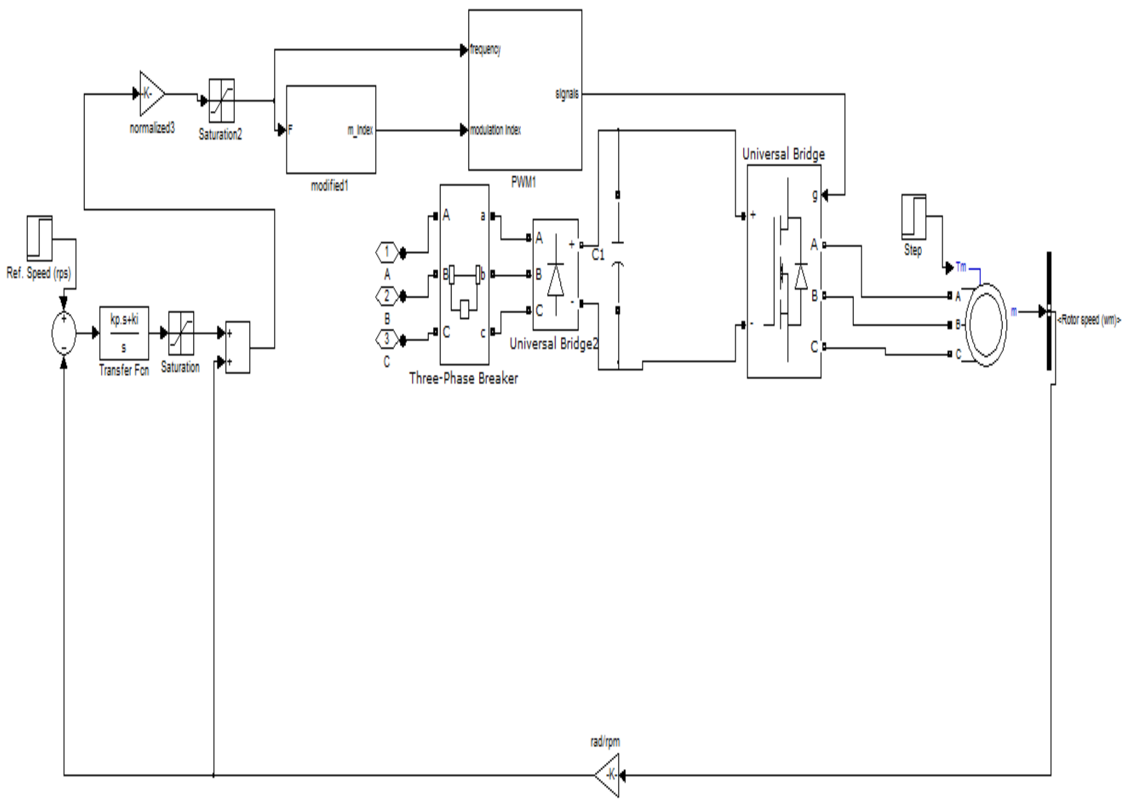

Figure B.4 VFD Load MATLAB Module

Vitae

Name	: Bandar S Alsharif
Nationality	: Saudi
Date of Birth	:3/20/1987
Email	: bandar7772@gmail.com
Address	: ALKALEEJ District, NAWRAS Street, House 141, Jubail Industrial City, Saudi Arabia

Academic Background : **Master of Science (M.Sc)**

Electrical Engineering

King Fahd University of Petroleum and Minerals

May 2016.

Bachelor of Science (B.Sc)

Electrical Engineering

King Fahd University of Petroleum and Minerals

September 2009.